UNIVERSIDAD
NACIONAL
DE COLOMBIA

Plastificante Biobasado obtenido a partir de corrientes residuales agroindustriales

Laura Nathalia Nájera Losada

Universidad Nacional de Colombia

Facultad de Ingeniería, Departamento de Ingeniería Química y Ambiental

Bogotá, Colombia

2023

UNIVERSIDAD
NACIONAL
DE COLOMBIA

Biobased plasticizer from agro-industrial residual streams

Laura Nathalia Nájera Losada

National University of Colombia

Faculty of Engineering, Department of Chemical and Environmental Engineering

Bogotá, Colombia

2023

Biobased plasticizer from agro-industrial residual streams

Laura Nathalia Nájera Losada

Thesis or research work presented as a partial requirement for the degree of:

Master of Chemical Engineering

Director:

Ph.D., Chemical Engineer Alvaro Orjuela Londoño

Co-director:

Ph.D., Chemical Engineer Paulo Cesar Narvaez

Line of research:

Oleochemical processes

Research Group of Chemical and Biochemical processes

National University of Colombia

Faculty of Engineering

Bogotá, Colombia

2023

To my mom, the bravest and strongest woman I have ever known.

To my family, my driving force and inspiration to live every day of my life.

And to Tom,

Acknowledgments

Firstly, I would like to express my sincere gratitude to Professor Alvaro Orjuela. His guidance has been a key factor in achieving each of the objectives of this project. I have a deep admiration for his work, which has influenced my professional and personal life.

I would also like to thank my thesis co-director Paulo Cesar Narvaez, whose wide knowledge and experience provided me with strong support to move forward in each of the stages of the project, and I would like to express my gratitude and appreciation to professors Juan Guillermo Cadavid and Julio Cesar Vargas for their advice, generosity, and thoughtfulness.

I also want to express my thanks to the staff of the chemical engineering laboratory Ricardo, Oscar, Edgar, and Jaime for their incredible recursiveness and constant support in handling equipment and materials, and to each member of the research group for their support and company during the long days in the laboratory.

I would also like to thank Professors Nestor Montañez and Rafael Balart for welcoming me to the Universidad Politécnica de Valencia and making me part of their amazing team.

Finally, I would like to thank my family who has always given me their unconditional support and has been present at every step I have taken. I would also like to express my gratitude to Adrián Rodriguez, Jhosue Hernandez, and all my friends, who have given me their support, company, and motivation even in the most difficult moments, and to all those who have directly or indirectly contributed to the completion of this project.

Abstract

Biobased plasticizer from agro-industrial residual streams

Soybean Oil Deodorizer Distillate (SODD) is a valuable agro-industrial waste stream that can be used as feedstock for a wide range of oleochemicals. In this regard, this work evaluates the production of biobased green plasticizers from SODD. A potential oleochemical plasticizer was selected through a computer-aided product design method that performed a screening of potential candidate molecules by assessing different criteria associated to their plasticizing performance. The selected criteria were compatibility, efficiency, permanence, toxicity, and cost, which were predicted for the potential molecule candidates using group contribution methods and empirical correlations. As a result of the screening method, epoxidized isobutyl esters were found to be the most promising plasticizers for polymers such as PVC. Subsequently, isobutyl fatty ester epoxides were produced experimentally using a two-step reaction process: esterification and epoxidation. Additionally, a kinetic model of the epoxidation of isobutyl esters was obtained and the influence of reaction conditions on selectivity, efficiency, and yield was studied. As a result, the best operating conditions for the synthesis of epoxidized isobutyl fatty esters were determined. Finally, the performance of the assessed epoxides as plasticizers for PVC was evaluated in terms of mechanical, optical, rheological, and barrier properties. These epoxides exhibited exceptional mechanical performance and thermal stability compared to traditional petrochemical plasticizers (i.e. phthalates). However, in terms of overall performance, they cannot be considered as general-purpose plasticizers and are expected to be used in specific applications.

Keywords: Esterification, fatty acids, Soybean oil deodorizer distillate, Isobutanol, Epoxidation, Epoxidized isobutyl esters, Kinetics, Plasticizer, PVC.

Resumen

Plastificante biobasado obtenido a partir de corrientes residuales agroindustriales

El destilado del desodorizado de aceite de soya (SODD) es un residuo agroindustrial que se puede utilizar como materia prima para obtener un amplio espectro de productos oleoquímicos. En esta dirección, se realizó inicialmente la selección de un derivado oleoquímico con potencial plastificante mediante un método de diseño de producto asistido por computador. Este método permitió realizar una selección entre moléculas potencialmente útiles mediante la evaluación de diferentes criterios asociados con su desempeño como plastificante. Los criterios seleccionados fueron compatibilidad, eficiencia, permanencia, toxicidad y costo. Estos criterios se predijeron para las moléculas candidatas utilizando métodos de contribución de grupo y correlaciones empíricas. Como resultado del método de selección, se encontró que los ésteres de isobutilo epoxidados pueden ser plastificantes promisorios para polímeros como el PVC. Posteriormente, los epóxidos de ésteres grasos de isobutilo se produjeron experimentalmente utilizando un proceso de reacción de dos pasos: esterificación y epoxidación. Además, se obtuvo un modelo cinético de epoxidación de ésteres de isobutilo y se estudió la influencia de las condiciones de reacción sobre la selectividad, la eficiencia y el rendimiento. Como resultado, se obtuvieron las mejores condiciones de operación para la síntesis de ésteres grasos de isobutilo epoxidados. Finalmente, se evaluó el desempeño de los epóxidos isobutílicos como plastificantes para PVC en términos de propiedades mecánicas, ópticas, reológicas y de barrera. Estos epóxidos mostraron un rendimiento mecánico y una estabilidad térmica excepcional en comparación con los plastificantes petroquímicos tradicionales (es decir, los ftalatos). No obstante, en cuanto a su desempeño general, no pueden ser considerados como plastificantes de uso general y se espera que puedan ser utilizados en aplicaciones específicas.

Palabras claves: Esterificación, ácidos grasos, destilado desodorizado de aceite de soya, isobutanol, epoxidación, ésteres de isobutilo epoxidados, cinética, plastificante, PVC.

Content

Figures

Pág.

Tables

Pág.

List of symbols and abbreviations

Symbols

Symbol	Term
δ_D	Dispersion forces
δ_P	Polar forces
δ_H	Hydrogen bonding forces
δ_t	Total solubility parameter
Φ	Polarity parameter
$\mathrm{A_p}$	Carbon atoms in aliphatic chains
$\mathrm{P_o}$	Polar groups
D_P^*	Overestimated diffusion coefficient
M_r	Migrant substance
A_p	Polymer specific constant
Tc	Crystallization temperature
Tm	Melting temperature

Abbreviations

Abbreviation	Term
DOP	Dioctyl phthalate
DINP	Diisonononyl phthalate
DNOP	Din-octyl phthalate
DOTP	Dioctyl terephthalate
DIDP	Diisodecyl phthalate
DBP	Dibutyl phthalate
BBP	Benzyl butyl phthalate
MDES	Methyl diepoxystearate
EDES	Ethyl diepoxystearate
PDES	Propyl diepoxystearate
IPDES	Isopropyl diepoxystearate
BDES	Butyl diepoxystearate
IBDES	Isobutyl diepoxystearate
IADES	Isoamyl diepoxystearate

ODES	2-octyl diepoxystearate
EEGDL	Epoxidized ethylene glycol dilinoleate
EPGDL	Epoxidized 1,2-propanediol dilinoleate
EPRGDL	Epoxidized 1,3-propanediol dilinoleate
EBGDL	Epoxidized 1,3-butanediol dilinoleate
ESBO	Epoxidized soybean oil
EC	Esterification cost
EPC	Epoxidation cost
OA	Oleic Acid
LA	Linoleic Acid
SODD	Soybean Oil Deodorized Distillate
IBO	Isobutil Oleate
IBL	Isobutil Linoleate
ISD	Distilled Isobutyl Soyate
ISO	Isobutyl Soyate
EIO	Epoxidized Isobutil Oleate
EIL	Epoxidized Isobutil Linoleate
EID	Epoxidized Isobutyl soyate Distillate
EIS	Epoxidized Isobutil Soyate
Tc	Crystallization temperature
Tn	Melting temperature
$\boldsymbol{A_1}$	Preexponential factor ($L^2\,mol^{-2}\,min^{-1}$)
$\boldsymbol{A_{-1}}$	Preexponential factor ($L^2\,mol^{-2}\,min^{-1}$)
$\boldsymbol{A_2}$	Preexponential factor ($L\,mol^{-1}\,min^{-1}$)
$\boldsymbol{A_3}$	Preexponential factor ($L^2\,mol^{-2}\,min^{-1}$)
$\boldsymbol{A_4}$	Preexponential factor ($L^2\,mol^{-2}\,min^{-1}$)
$\boldsymbol{E_{a_1}}$	Activation energy ($J\,mol^{-1}$)
$\boldsymbol{E_{a_{-1}}}$	Activation energy ($J\,mol^{-1}$)
$\boldsymbol{E_{a_2}}$	Activation energy ($J\,mol^{-1}$)
$\boldsymbol{E_{a_3}}$	Activation energy ($J\,mol^{-1}$)
$\boldsymbol{E_{a_3}}$	Activation energy ($J\,mol^{-1}$)
$\boldsymbol{k_1}$	Kinetic constant ($L^2\,mol^{-2}\,min^{-1}$)
$\boldsymbol{k_{-1}}$	Kinetic constant ($L^2\,mol^{-2}\,min^{-1}$)
$\boldsymbol{k_2}$	Kinetic constant ($L\,mol^{-1}\,min^{-1}$)
$\boldsymbol{k_3}$	Kinetic constant ($L^2\,mol^{-2}\,min^{-1}$)
$\boldsymbol{k_4}$	Kinetic constant ($L^2\,mol^{-2}\,min^{-1}$)
$\boldsymbol{\dot{F}_i}$	g/min
$\boldsymbol{V^i}$	Volume of the phase $\boldsymbol{i}$ (L)
$\boldsymbol{H^+}$	Hydronium ions
$\boldsymbol{KAA}$	Acetic acid partition coefficient adimensional
$\boldsymbol{KPAA}$	Peracetic acid partition coefficient adimensional
$\boldsymbol{k_t a}$	Global mass transfer coefficient (min^{-1})
AA	Acetic acid
C=C	Instauration concentration

Introduction

The incentive for implementing circular economy models has boosted the development of processes and products around the exploitation of agro-industrial waste, especially those related to the food production and consumption chain. In this sense, the manufacture of chemical products from food waste is considered an alternative to reduce the impacts in both sectors. The use of biobased waste streams and residues as raw materials can reduce life cycle impacts and generate renewable, biodegradable, and biocompatible products. Using biobased raw materials is possible to obtain a variety of direct and functional substitutes for a wide number of products from fossil resources. Particularly, one of the sectors requiring a rapid shift towards renewable raw materials is the polymer industry. The high global consumption of these materials and the predominant use of monomers and additives from petroleum resources make imperative the development of biobased raw materials as an alternative to polymers and industrial plastics.

Among the different additives in commercial polymer processing, plasticizers play a primary role. Plasticizers are chemical compounds that not only facilitate the transformation and processing of polymers but also improve their physicochemical properties (i.e. flexibility, plasticity, softness, etc.) [1]. Although plasticizers are used in different polymer formulations, the market is mainly driven by their use in PVC products [1],[2]. In general, the traditional PVC plasticizers are esters of polycarboxylic acids (phthalates, terephthalates, adipates, sebacates, etc.) with a molecular weight ranging from 390 to 450 g/mol [2], [3].

To mitigate some of the environmental impacts generated during the production, shelf life, and post-consumption of the plasticized materials, some biobased compounds have been proposed as effective functional substitutes for traditional petrochemical plasticizers.

Recently, non-phthalate plasticizers such as epoxidized soybean oil, castor oil, linseed oil, tall oil derivatives, isosorbide esters, acetyl citrates, and cardanol derivatives, among others, have been obtained from different biobased feedstocks and sustainable routes. Some of these compounds have been derived from vegetable oils and other oleochemical feedstocks. These oleochemical derivatives have great potential to replace traditional petrochemical plasticizers in a wide variety of applications. Some oleochemical-derived products (e.g. epoxidized soybean oil) already have a significant share in the plasticizers market, being the second most consumed class of plasticizers after petrochemical additives [3]. Nonetheless, to avoid the food-water-energy nexus associated with the consumption of first-generation chemicals, there is a need to explore the use of waste oleochemicals as a potential feedstock for commercial plasticizers.

In this direction, this work is focused on the transformation of oleochemical waste into valuable derivatives with plasticizing potential. First, using a computer-aided method, target molecules with plasticizing potential were identified from the oleochemical feedstocks. This stage involved the identification of the main performance properties of commercial plasticizers and the derivation of predictive models to estimate these properties based on the molecular structure of the potential compounds. The models were based on group contribution methods and empirical correlations. In addition, the selection method evaluated only renewable feedstocks (mainly biobased alcohols and waste streams) aiming to produce plasticizers through a sustainable biobased route and promote the sustainable production of new plasticizers with low environmental impacts. The selection among the candidates was done by minimizing the difference between the predicted performance properties of the assessed oleochemical molecules and those of the most typical general-purpose plasticizer, dioctyl phthalate (DOP).

Once identified, a second stage of research was focused on the synthesis of the identified biobased plasticizer using traditional chemicals and waste oleochemical stream, namely Soybean Oil Deodorizer Distillate (SODD). The biobased plasticizer was produced through a two-step approach via esterification and epoxidation, and a kinetic model of the second step was experimentally developed. The model was used to determine the best operating conditions for a bench-scale experiment to obtain a suitable amount of plasticizer for further evaluation as a polymer additive. Finally, the performance of the obtained oleochemical compounds was assessed in the plasticization of PVC films. Such films were produced by a solvent casting method, and a variety of physicochemical performance properties were

evaluated in comparison with films prepared using the most traditional petrochemical plasticizer (i.e. DOP). It is envisioned that the proposed methodology could be employed in the design of biobased products for various applications and could foster the development of more waste-based products for the chemical industry. Besides, it is expected that the obtained models can aid in the development of scale-up studies for further sustainability assessment of the proposed technologies.

1. Reuse of oleochemicals waste streams into the polymer industry

Resource depletion, pollution, and increasing environmental impacts, especially those associated to greenhouse gas emissions, have promoted the incorporation of global policies (e.g., The Kyoto Protocol and the Paris Agreement) to promote the dematerialization of economic activities. These policies have drawn attention to the unsustainable dependence on fossil resources, leading to a paradigm shift from linear economic development based on waste generation to biobased circular economy models that enable closing the production cycle of materials. In this direction, generated waste has been recognized as a potential feedstock for different industrial processes to reduce the consumption of virgin raw materials and mitigate economic, social, and environmental impacts. In this context, the harnessing and reuse of waste lipids from food chains and residual streams from the oleochemical industry have become major research topics in recent years. Harnessing of second-generation feedstocks from the oleochemical industry would enable to reduce of pressure on the fossil sources, water, and arable land used in the production of vegetable oils, and reduce the amount of edible oils diverted from food and feeding purposes [4].

The exploitation of waste lipids from the vegetable oil chain is of particular importance for Colombia, where palm oil production is a key agro-industrial sector. Currently, global vegetable oil consumption amounts to 228 Mt, with palm oil accounting for 31% of the total consumption in the food and biofuels sectors. Other major vegetable oils in the global market are soybean (25%), canola (11%), and sunflower (8%) [5]. Although major local production corresponds to palm oil, other vegetable oils are highly used in food applications mainly for their characteristic properties. For instance, in some cases, a liquid product (e.g.

table oil) is required, while in other cases, a spreadable grease is more desirable (e.g. butter-like product). These properties are highly dependent on the fatty acid distribution in the triacylglycerides of the oils. Table 1-1 presents the typical composition of common vegetable oils and the average content of unsaturated fatty acid chains in their constituent triacylglycerides [6].

Table 1-1. Fatty acid composition of common vegetable oils.

	Fatty acid	Castor	Corn	Linseed	Olive	Palm	Soybean	Canola
Number of double bonds		3.0	4.5	6.6	2.8	1.7	4.6	3.9
Palmitic acid	C16:0	1.5	10.9	5.5	13.7	42.8	11	4.1
Stearic acid	C18:0	0.5	2.0	3.5	2.5	4.2	4.0	1.8
Oleic acid	C18:1	5.0	25.4	19.1	71.1	40.5	23.4	60.9
Linoleic acid	C18:2	4.0	59.6	15.3	10.0	10.1	53.3	21.0
Linolenic acid	C18:3	0.5	1.2	56.6	0.6	--	7.8	8.8

1.1 High-free fatty acid waste streams

Oleochemical waste streams are lipid effluents composed mainly of free fatty acids (FFAs), glycerides, and soaps, that are obtained as residues or by-products of the oleochemical industry, as well as post-consumption residues [7]. Large-volume waste streams include trap greases, deodorizer distillates, bleaching earth, mill effluents, used cooking oils, wastewater sludges, rancid oils, acidified soapstocks, and acidified oils, among others [7],[8]. Some of these side streams come from the physical or chemical refining of vegetable oils, which involves stages of saponification, degumming, distillation, and steam refining of free fatty acids. Since the residual streams are derived from the treatment and processing of vegetable oils, these streams exhibit lipid profiles similar to that of the original oils or fatty materials. Table 1-2 presents the typical content of free fatty acids (FFAs) in common residual acid streams.

Table 1-2. FFAs content in residual oleochemical streams

Feedstock	FFAs content (% wt.)	Reference
Trap greases	50-100	[9]
Finished greases	9-26	[10]

Restaurant waste grease	1-42	[9]
Municipal Sludge	>65	[10]
Animal Fat	5-30	[9]
Used cocking oil	3-80	[11], [12]
Waste oil	47	[10]
Vegetable Oil Deodorizer Distillate	20-82	[13]

Streams with a high content of free fatty acids, also known as acid oleochemical streams, have attracted great interest on account of their low cost and high availability as raw materials for oleochemical processes. A residual stream with high industrial potential for further valorization is the Soybean Oil Deodorizer Distillate (SODD). Soybean oil is extracted from soybeans and has a particular composition of fatty acids that is valued for industrial use due to its high content of unsaturations and low acidity in the range of 0.5-2.1%. Table 1-3 presents a typical distribution of FFA in the triacylglycerides of commercial soybean oils [14]. Currently, the global consumption of soybean oil is estimated in 56 Mt [5]. It is also the second most consumed oil after palm oil with a market share of around 22% of the total fat and oils [14].

Table 1-3. Composition of commercial soybean fatty acids.

Type of commercial Oils	**Fatty acid composition (% wt.)**				
	Palmitic 16:0	**Stearic 18:0**	**Oleic 18:1**	**Linoleic 18:2**	**Linolenic 18:3**
Commodity	11	4	23	54	8
Low saturated	3	2	30	59	6
High palmitic	24	5	19	45	7
High stearic	10	24	40	20	6
High saturated	23	19	9	40	10
High oleic	8	2	83	3	4
Low linolenate	12	6	37	43	2

The SODD is obtained during the physical refining of crude soybean oil when compounds that provide color, odor, and acidity are removed by high-vacuum distillation. In this stage, FFAs are vaporized and separated selectively from the oil. The obtained stream, also known as deodorizer distillate, has a high content of FFAs (>70%). The remaining content corresponds to acylglycerols and unsaponifiable matter (5-10%) [5],[15]. The acylglycerols fraction includes Triglycerides (TAGs), Diglycerides (DAGs), and Monoglycerides (MAGs)

[13]. In addition to these components, SODD also contains ketones, peroxides, lecithin, hydrocarbons, and olefins [14]. Table 1-4 presents a typical composition of the soybean oil deodorizer distillate along with some physicochemical properties [16],[17]. As shown, the high double bond content in SODD leads to an iodine value in the range of 109 - 114 cg I_2/g. This high unsaturation content enables a wide range of chemical transformations to obtain a diverse portfolio of high-value-added products. Valuable compounds present as non-saponifiable matter, which is rich in phytosterols and tocopherols, have attracted great interest. These compounds have many applications in the food, pharmaceutical, cosmetic, and nutraceutical industries [16]. FFAs and acylglycerols from SODD can be exploited by a variety of chemical of physical processes such as hydrolysis, esterification, transesterification, distillation, crystallization, adsorption, and liquid-liquid extraction.

Table 1-4. Composition of soybean oil deodorizer distillate

Parameter	Value
Acidity (% wt.)	23-54
Peroxide value (mequiv O_2/kg)	8-120
Iodine value (cg I_2/g)	109-114
Saponification value (mg KOH/g)	133-166
Acylglycerols (% wt.)	28-65
Unsaponifiable matter (% wt.)	11-35
Tocopherols (% wt.)	2
Phytosterols (% wt.)	6-7

Besides industrially derived oleochemical waste streams (i.e. SODD), acid oils such as used cooking oils (UCOs) represent a major fraction of the residual lipids currently used as second-generation feedstocks. UCOs are produced as residues in the frying and cooking process of food, and they have a FFAs content of about 3-80% [11], [12]. In Colombia, the generation of UCOs is higher than 225 kt/year, which is equivalent to a per capita production of 5 kg/person/year [8]. This output gives an idea of the potential use of this type of waste as an industrial raw material.

Currently, most of the acid oleochemical streams are used for biodiesel production, and to a lesser extent for the manufacture of soaps, as well as animal feed. However, an incentive to develop higher value-added products is necessary to ensure sustainability in the long-term harnessing second-generation oleochemicals [7]. To achieve this goal, it is necessary to develop and improve different pretreatment and purification processes to remove

impurities and generate a less heterogeneous feedstock. This would enable to fulfillment of technical specifications of commercial industrial oleochemicals. Likewise, it is required the identification of products with industrial scale-up potential that match their demand with the availability and physicochemical characteristics of the residual materials. The biobased polymers industry represents a potential niche for introducing waste lipids as second-generation feedstock. On one side, there is a need to implement low-cost alternatives to replace fossil-derived polymers and additives. On the other hand, consumers are increasingly aware of after-life impacts, so biodegradable, biocompatible, and biobased materials are highly welcome in the polymers industry. Among the variety of biobased polymers and additives that can be produced from oleochemical sources, epoxidized vegetable oils and esters are of particular interest.

Epoxides are useful intermediates to obtain a wide variety of chemical products such as polyols, amino alcohols, acetylated esters, diamines, and others. They have many applications as plasticizers in the polymer sector, where a high content of oxirane is advantageous [6]. Epoxides of vegetable oils have a wide market in the plasticizer segment, where they are commonly used as additives in films, wires, rubbers, cables, flooring, coating, etc. Plasticizers are widely used as additives in flexible plastics for many final products from the automotive industry to different medical applications. These additives improve the flexibility, plasticity, workability, and elongation of polymers, and they are mainly employed in the manufacture of polyvinyl chloride products (PVC) [18]. The large growth in the plasticizers market has been driven to a great extent by an increase in the use of flexible PVC, the third most consumed polymer in the industry. The manufacture of PVC products consumes between 80-90% of the global plasticizer production, which reached 8.4 Mt in 2017, and it is estimated to reach 9.75 Mt by 2024 [2],[19]. As plasticized plastics are used in many non-sensitive applications (e.g. gaskets, mats, building materials, etc.), such products can incorporate biobased additives obtained from residual oleochemical streams.

It is important to point out that epoxidation takes place on the unsaturations of the organic chains to form a cyclic ether group called oxirane ring. Therefore, high content of unsaturated chains (e.g. oleic, linoleic, linolenic acids) is necessary for the epoxidation of FFAs. While the waste stream derived from the palm oil industry could be used for epoxidation, those from the soybean oil refining would be most suitable for further epoxidation as soybean oil has a high content of unsaturated fatty acid chains. Then, it

would be expected that SODD would be a suitable raw material for the manufacture of second-generation epoxides for the polymers industry. Advantageously, the traditional epoxidation process could be easily adaptable to the local infrastructure as the process is usually carried out in agitated tanks, at low temperatures using homogeneous acid catalysts. In addition, the hydrogen peroxide commonly used as oxidizing agent in the epoxidation process can also be used as a bleaching agent for oleochemical waste, improving the sensory characteristics of derived oleochemicals.

1.2 Plasticizers

In recent years, more than 30.000 substances with plasticizing characteristics have been investigated, of which just 1200 have industrial applicability and only 100 have a significant market share [20],[21]. These substances are predominantly esters owing to their polarity and good compatibility with the PVC matrix [4],[22]. Due to their unique properties and high performance, the most used plasticizers in the PVC industry are esters derived from phthalic anhydride. In particular, the most widely used commercial plasticizer is bis(2-ethylhexyl) phthalate (DEHP) also known as dioctyl phthalate (DOP). Other phthalates widely employed are diisononyl phthalate (DINP), diisodecyl phthalate (DIDP), and din-octyl phthalate (DNOP) [23]. These petrochemical compounds are used as primary plasticizers and often account for about 50% of the PVC matrix [24]. According to the application of the polymer, the plasticizer is added in the range of 15-60 % wt. with typical values between 35 to 40 % wt. for most flexible applications [25]. Figure 1-1, presents the structure of some of these compounds.

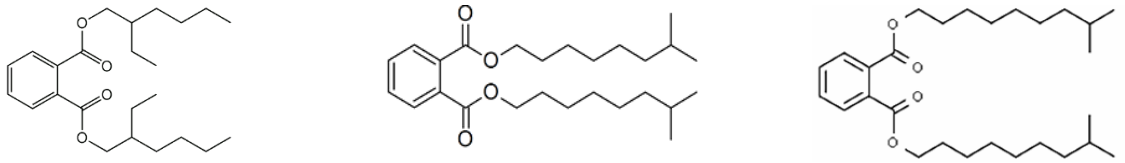

a) Dioctyl phthalate (DOP) b) Diisononylphthalate (DINP) c) Diisodecyl phthalate (DIDP)

Figure 1-1. Phthalates of industrial use

However, since the early introduction of phthalates in the market, they have been under scrutiny due to their toxicity and problems associated to leaching, migration, and evaporation during their use or final disposal. Migrated plasticizers from plastics in consumer products may come in contact with humans (food and beverage packaging,

medical devices, toys, etc.) representing a health risk from chronic exposure [26]. This is concerning because petrochemical phthalates are considered potential carcinogens and endocrine disruptors to reproductive health [27]. Additionally, these compounds are an environmental problem because they are hardly degradable [28]. The European Union and the USA have tightened measures to limit the use of phthalates. Since 2018 and 2019, the use of specific phthalates has been restricted to a maximum of 0.1% of the total plastic content, especially in critical applications such as infant care and teething products. These phthalates include DOP, dibutyl phthalate (DBP), benzyl butyl phthalate (BBP), diisononyl phthalate (DINP), and diisobutyl phthalate (DIBP) [29], [30]. Consequently, in recent years the market share of phthalates has progressively decreased. In 2014, the total consumption of phthalates accounted for 70% of the total volume of plasticizers [31]; however their consumption gradually decreased to 65% by 2017, and in 2020 their industrial use reached only 55% of global plasticizer consumption [31],[32]. As a result, many traditional phthalates have been replaced by compounds of similar structures such as di 2-ethylhexyl terephthalate or dioctyl terephthalate (DOTP). Alternative plasticizers have been introduced into this segment including citric acid esters, acetyl citrates, phosphoric acid esters, polyesters, cyclohexane esters, epoxides, adipates, dicarboxylic acid esters, benzoates, sebacates, terephthalates, trimellitates, and cardanol esters [2],[31],[33]. Among this group, adipates have the largest market share, accounting for 39.8% of the total in 2020 [34].

According to global market trends, the demand for plasticizers is expected to increase to 9.75 Mt in 2024 with a growth rate of 3 to 3.5%. Within this group, the non-phthalic plasticizers would have the fastest growth [2]. On the other hand, the market of biobased plasticizers accounted for 2,1 Mt in 2019 and is expected to reach 3.1 Mt by 2030 [35],[36]. These types of products have several advantages owing to their renewable, biodegradable, and safe nature [37]. Within this group, ESBO is the most consumed biobased plasticizer accounting for 37% of the total demand of biobased plasticizers [38]. An incentive for the use of biobased molecules is to reduce the potential negative impacts mentioned above on the environment and public health [2],[33].

1.3 Plasticizers derived from vegetable oils

Whereas most plasticizers are esters of phthalic and terephthalic acid, the industry is now searching for more environmentally friendly, bio-based, and ortho-phthalate-free alternatives. Biobased plasticizers that are commonly used are derived from vegetable oils such as soybean oil, castor oil, linseed oil, palm olein, and sunflower oil. Moreover, by-products and waste streams of the oleochemical sector such as tall oil, cardanol, and used cooking oil are also used for this purpose. Common feedstocks used for plasticizer production are presented in Figure 1-2. Some of the green additives that have fulfilled the technical requirements for the polymer segment are epoxidized vegetable oils, epoxidized fatty acid esters, polyalcohol esters (e.g. pentaerythritol, glycerin, isosorbide esters), and acetyl esters, among others [33], [39]. These compounds are used as secondary plasticizers because of their high thermal and light UV stability, but limited compatibility, and exudation from the PVC matrix [2]. Therefore, an effective functional replacement of petrochemical phthalates should exhibit low toxicity, good miscibility with the polymer, extraction resistance, and also low cost [40].

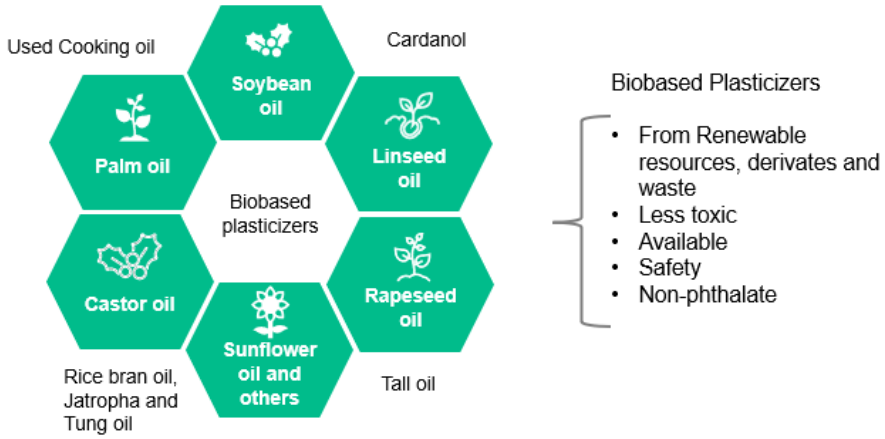

Figure 1-2. Vegetable oils used in plasticizers production.

To enhance compatibility and affinity with the polar groups of PVC, vegetable oils require transformation and functionalization processes [2]. Fatty materials can be transformed into high-polarity functional compounds through various methods such as epoxidation,

transesterification, esterification, hydrolysis, epoxidation-hydroxylation, acetylation, ethoxylation, oligomerization, and acrylation [6]. The functionalization of oleochemicals derivates is mainly performed on the double bonds of the fatty acid chains. In the case of functionalization through epoxidation, oxirane groups can be used as an intermediate for synthesis. Considering their high reactivity, oxirane groups can be easily converted into tailor-made specific derivates for the polymer sector. Figure 1-3, presents a scheme of the main non-phthalate plasticizers and those obtained from renewable resources.

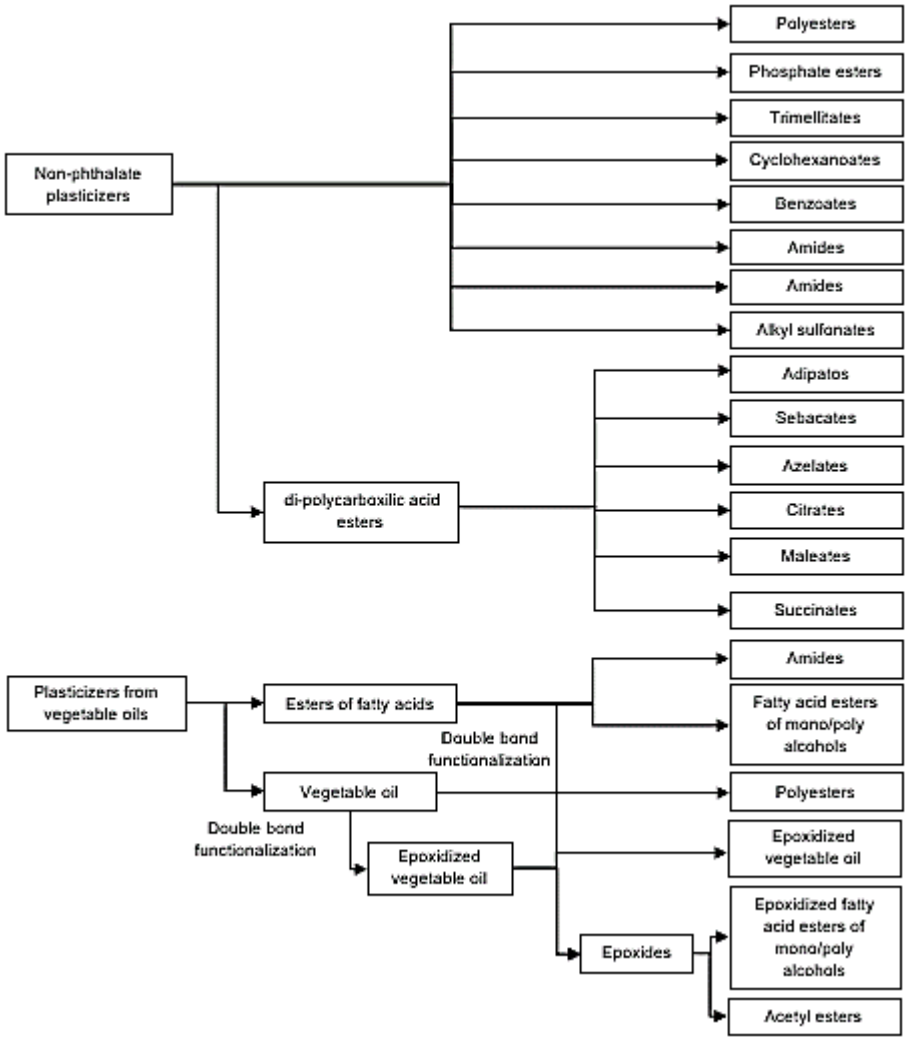

Figure 1-3. Derived oleochemicals in plasticizers applications

1.3.1 Fatty acid esters of mono and polyalcohols

In the case of trans-esterification reactions between glycerides and alcohols, a wide variety of short-chain alcohols (e.g., methanol, ethanol, butanol, and isobutanol) or medium alkyl

chain alcohols (e.g., isoamyl alcohol) are commonly used. Likewise, large alkyl chain alcohols such as octanol, decanol, and dodecanol are also employed in the production of oleochemical plasticizers. These alcohols can be obtained through biological or enzymatic processes from natural resources [2]. Within the group of polyalcohol esters, glycerol esters (i.e., mono-, di- and try-acyl glycerides) have shown a high plasticizing capacity for PVC and good thermomechanical performance in plasticized materials. Glycerol esters are obtained from the esterification of glycerol and short-chain carboxylic acids (e.g., butanoic, propanoic, benzoic acid, etc.). Triacetin, the triglyceride of acetic acid, and epoxidized and acetylated monoglycerides are also commonly used as plasticizers [41],[42]. Finally, isosorbide esters have shown a similar plasticizing effect to common phthalates (DOTP and DIOP) in mixtures of PLA and PVC polymers [43],[44]. Isosorbide esters are produced by esterification of isosorbide, a dehydration product from D-sorbitol, with long-chain carboxylic acids [44].

1.3.2 Epoxidized Plasticizers

Epoxidized plasticizers represent a family of compounds obtained by epoxidation of vegetable oils, such us soybean oil (ESBO), linseed oil (ELSO), and fatty acid esters. During the epoxidation process, peroxy acids are used as reaction intermediates to introduce an oxirane ring into the double bonds of the fatty acid chain. As a result, oxygen is incorporated into the molecule, which enhances its polarity and compatibility with PVC. Epoxidized oils have been used as a secondary plasticizer typically at a level of 5 to 15% wt. in the PVC resins owing to their thermal and UV stability. Epoxy compounds are effective acid scavengers for the hydrochloric acid released during PVC degradation. This fact slows down polymer degradation and reduces color formation. On the other hand, these compounds exhibit limited compatibility with PVC because of their high molecular weight and viscosity, inducing exudation of the additive [27],[24]. Figure 1-4 and Figure 1-5 represent typical structures of epoxide compounds.

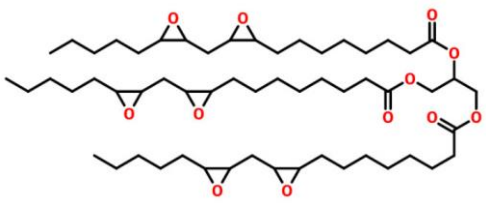

Figure 1-4. Epoxidized Soybean oil

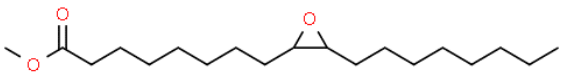

Figure 1-5. Methyl 9,10 epoxy stearate

In addition to epoxidized oils, epoxidized polyol esters are widely used as green additives. These esters are highly compatible plasticizers that can be produced by esterification or transesterification of fatty chains and mono or polyalcohols (e.g. methanol, pentaerythritol, propylene glycol, ethylene glycol, and sucrose) followed by the epoxidation of the esters. The presence of fatty chains greatly improves the thermal and mechanical characteristics of PVC, while the epoxy groups reduce the glass transition temperature. However, only some of these substances have shown lower or marginal migration compared to the DOP standard [24]. Recently, epoxidized glycidol esters from epichlorohydrin have been investigated as an alternative plasticizer. In the first step, fatty acids react with epichlorohydrin catalyzed by benzyl triethyl ammonium chloride, then the double bonds are epoxidized by the conventional method. The resulting additive contains terminal and internal epoxy functionality that enhances its performance and provides improved thermal stability, reduced color formation upon heating, and marginal volatile and migration losses. [28],[45].

Plasticizers that have structural similarities to petrochemical additives, particularly DOP, have been produced by using branched alcohols such as 2-ethylhexyl alcohol. This results in improved mechanical and thermal performance, but with low migration resistance [4]. On one side, epoxidized vegetable oils have limited compatibility with PVC owing to their high molecular weights. On the other hand, epoxy esters, exhibit high migration from the PVC matrix. To enhance the properties of plasticizers and overcome those hindrances, molecules with more than one functional group (e.g. acetoxy, methoxy, amines, thiirane, aziridine among others) have been developed [42],[46],[47]. Esters functionalization by epoxidation of unsaturated chains, followed by ring-opening reactions yields plasticizers with good compatibility, high efficiency, and mechanical properties similar to commercial plasticizers [46]. Once the oxirane ring is formed, it can react with a hydroxylation agent such as carboxylic acids, water, alcohols, and polyols. In this case, branched molecules are obtained with hydroxyl groups in their structure. Afterward, the hydroxyl groups are acetylated with acetic anhydride. In a recent study [48], bio-based plasticizers were obtained from waste cooking oil and terephthalic acid, adipic acid, and benzoic acid using this reaction sequence. In that study, the green plasticizer derived from terephthalic acid exhibited comparable performance with DOP. Figure 1-6, outlines the functionalization by epoxidation, hydroxylation, and acetylation.

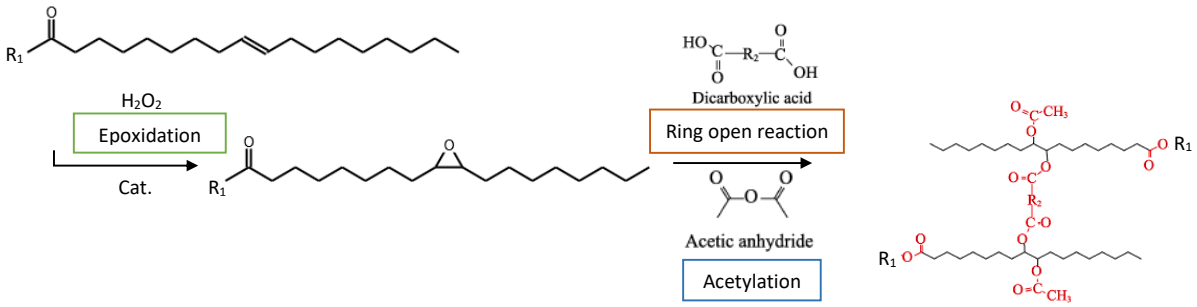

Figure 1-6. Functionalization of esters by epoxidation, hydroxylation, and acetylation. Adapted from [48].

Besides epoxidation, the double bonds of the unsaturated fraction of vegetable oils can be functionalized via Diels-Alder reactions. In this case, the oil reacts with maleic or acetic anhydride to obtain a Diels-Alder adduct, which can be converted into a triester by opening the ring with different alcohols [40]. In addition to these transformations, sustainable additives have been developed using amino-methylation or Mannich reactions. These derivates have high migration resistance and thermal stability [49].

To overcome some of the current limitations of biobased plasticizers, it is imperative to develop compounds with better properties to decrease their extraction and volatility from the plastic products, and thus, promote their use as general-purpose plasticizers. The incorporation of residual streams will close the production cycle of the oleochemical industry, reducing the consumption of raw materials, and mitigating economic, social, and environmental impacts. The available residual oleochemical raw materials (i.e., deodorizer distillate) can be transformed by different routes to generate versatile, high value added materials with the potential to replace petrochemical plasticizers.

1.3.3 The market of biobased plasticizers

Recently the global consumption of ESBO has reached up to 328 kt/year [50], which represents about 4% of the total plasticizer market. ESBO price has a significant impact on the price of bio plasticizers, alongside succinic acid and castor oil, since they are key raw materials for their production [38]. Figure 1-7 shows some historical market prices of ESBO and SBO [51]. As observed, ESBO had a market price ranging from 910 to 1600 USD/t for

the period 2019 to 2020 [52],[50]. Soybean oil, the main raw material for its production accounts for the highest share of the production cost. Because of this, and the large number of purification steps that are required, the use of biobased plasticizers is still limited, being less cost-effective than the traditional petrochemical additives [52],[53],[54]. For instance, the price of DOP for the same period ranges between 1080 to 1130 USD/t [55]. In this sense, waste streams such as soybean deodorizer distillate, with a market price of around 300 to 500 USD/t, are advantageous as a starting material due to their availability and low cost [46],[50],[56].

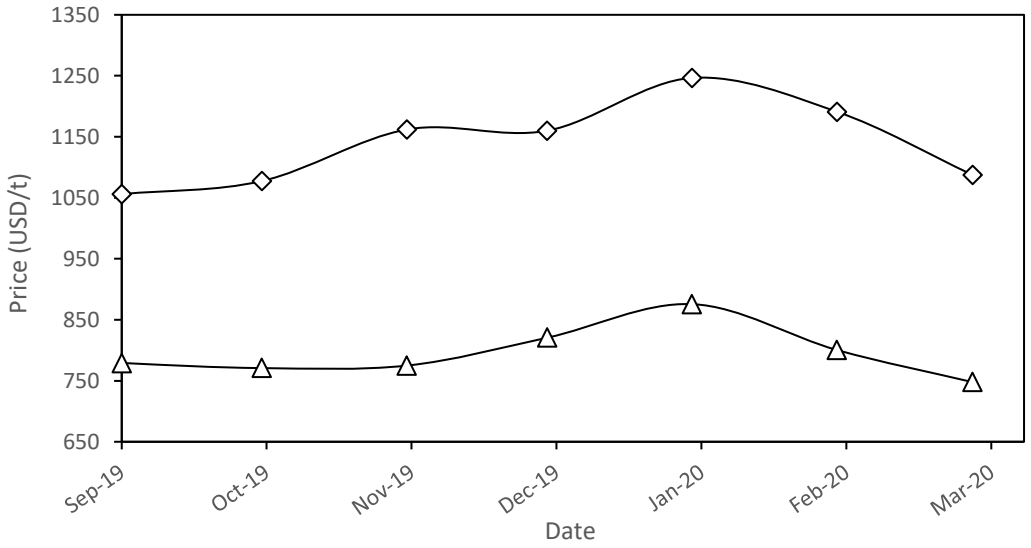

Figure 1-7. Price of epoxidized soybean oil and soybean oil

Despite ESBO is the main oleochemical plasticizer, there is a wide range of biobased plasticizers available in the market. Table 1-5, presents some of the commercial plasticizers mainly derived from soybean oil, linseed oil, and epoxidized esters [40], [57],[58].

Table 1-5. Some commercial plasticizers derived from vegetable oils

Manufacturer	Country	Trade name	Plasticizer
Acme-Hardesty	USA	Jenkinol® 680	Epoxidized Soybean Oil
Arkema	USA	Vikoflex® 7170	Epoxidized Soybean Oil
		Vikoflex® 7190	Epoxidized Linseed Oil
		Vikoflex® 5075	Epoxy propylene glycol di-oleate
		Vikoflex® 4050	Octyl epoxy ester

Baerlocher	USA	Baerostab H2000 IN	Epoxidized Soybean Oil
Chang Chung Petrochemical	Taiwan	ESBO	Epoxidized Soybean Oil
Chemodex	Germany	HiOmega Linseed	Epoxidized Linseed Oil
Danisco	Denmark	Grinsted® Soft N Safe	Acetylated monoglyceride from hydrogenated castor oil
Hallstar	USA	Hallgreen	Epoxidized esters of soybean oil, castor oil, and linseed oil
Hebei Jingu Palsticizer	China	HY-B, HY, S, Z	Epoxidized Soybean Oil and Epoxidized methyl esters
Makwell Plasticizers	India	Makplast	Epoxidized Soybean Oil
Nexoleum	Brazil	Nexo E1	Methyl Epoxy Soyate
New Japan Chemical	Japan	Sanso Cizer	Epoxidized Linseed Oil
Novance/Oleon	France	Radia	Pentaerythritol and 2-ethyl hexyll esters
Petrom	Brazil	PLS Green 5 PLS Green 8 PLS Green 9	Isoamyl epoxy-stearate 2-ethyl hexyl epoxy-stearate Isononyl epoxi-stearate
PolyOne	USA	Reflex100 Reflex300	Esters of fatty acids
The Chemical Company	USA	Chemflexx (ESBO) Natureflexx (ELSO)	Epoxidized Soybean Oil Epoxidized Linseed Oil
Traquisa	Spain	Plasticizer E Plastificante 401	Epoxidized Soybean Oil Epoxidized ethyl hexyl esters C14-C22
Unipox S.A.	Argentina	Soya EP Gira EP	Epoxidized Soybean Oil Epoxidized Sunflower Oil
Varteco	Peru	Kalflex – Varflex	Epoxidized Soybean Oil
Valtris	USA	Lankroflex™ ED6 Lankroflex™ E2307 Lankroflex™ L	Octyl epoxi estearate Epoxidized Linseed Oil Epoxidized Linseed Oil
Zhejiang Jiaao Enprotech Stock	China	ESBO	Epoxidized Soybean Oil

Epoxidized derivates are also used as intermediates to produce other high-value compounds such as lubricants, stabilizers, polyols, coatings, polyurethanes, cosmetics, alkanolamines, carboxylic compounds, and glycols among others [59],[60]. In Colombia, epoxides are mainly used as feedstock for epoxy resins, epoxy adhesives, plasticizers, and for polyurethane manufacture. Figure 1-8, shows the consumption of these compounds for the period 2010 to 2018. The consumption of plasticizers for 2019 reached 24.6 kt, mostly for the manufacture of PVC, which represents a national consumption of 170 kt [57],[61].

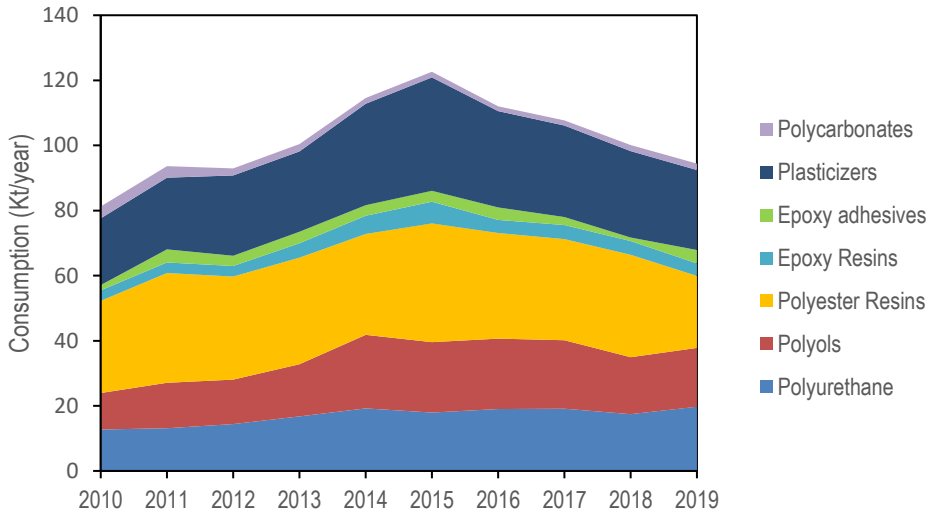

Figure 1-8. Consumption of products derived from epoxidized compounds. Polycarbonates (■), Plasticizers (■), Epoxy adhesives (■), Epoxy resins (■), Polyester Resins (■), Polyols (■) and Polyurethane (■)

1.4 Properties of plasticizers

Plasticizers improve the mechanical properties of polymers such as the elastic module, tensile strength, hardness, density, viscosity, and glass transition temperature [62],[63]. The selection of a specific plasticizer molecule should consider its properties and the functionality of the final polymer. In this sense, the additive must offer a balance between the desired characteristics including low volatility, low glass transition temperature, high plasticizing efficiency, resistance to solvent extraction, good mechanical properties, low diffusion rates, high permanence as well as low cost [27],[64]. Figure 1-9 presents a scheme of the plasticizing effect of DOP in PVC and the possible interaction forces [65]. Polar groups such as the carboxylic moiety and the aromatic ring of DOP interact with chlorine atoms of PVC. These interactions reconfigure the polymer matrix, retaining the plasticizer, increasing the volume, and reducing polymer-polymer interactions [66].

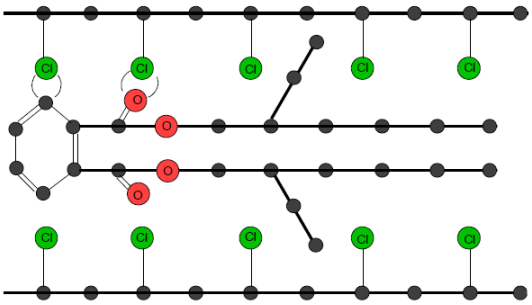

Figure 1-9. PVC plasticized with DEHP.

The design of plasticizers has been a central point of research in recent years. The need for predicting the interaction forces between plasticizers and polymers and the final properties of the additive has led to the implementation of semi-empirical equations and predictive methods. However, one of the hindrances in this area is the scarcity of experimental data on physicochemical properties required in the early stages of the plasticizer evaluation. In the case of epoxidized esters, there is not only limited information about their physicochemical properties but also their production process, especially for epoxides of superior alcohols. In this direction, predictive tools such as equations of state, molecular dynamics simulation, group contribution methods, and empirical equations among others, are useful to predict the performance of such molecules. For instance, different group contribution methods can be applied to predict a specific parameter based on the molecular structure of the polymer segment, the position of the atoms in the molecule, and the repetition of the functional groups [67].

1.5 Production process

The main routes to produce epoxidized esters involve an initial Fisher esterification or transesterification, followed by the epoxidation of the double bonds. The reverse sequence (epoxidation followed by esterification) is not usually done because the oxirane ring is very reactive and unstable, inducing ring-opening reactions in the presence of alcohols in acid medium.

1.5.1 Esterification

Fatty acid esters are widely produced by esterification and transesterification reactions. However, when the oleochemical feedstock contains high acidity, direct esterification of fatty acids with suitable alcohols is usually employed (Eq. 1-1)

$$RCOOH + R_1OH \rightleftharpoons RCOOR_1 + H_2O \quad (1\text{-}1)$$

Esterification is usually carried out in a homogeneous phase, catalyzed by organic acids such as H_2SO_4, HF, H_3PO_4, p-toluene sulfonic acid (p-TsOH), methanesulfonic acid, trichloroacetic acid, sulfonic acids, among others. The reaction takes place over a wide range of temperatures (60°C-150°C) depending on the alcohol used in the process [68]. Among different options, sulfuric and methanesulfonic acids have shown higher conversions of fatty acids [69]. Table 1-6 shows the main advantages and limitations of acid catalysts used in homogeneous esterification. In addition to homogeneous catalysts, the esterification reaction is also catalyzed by acidic heterogeneous catalysts such as ion exchange resins, zeolite, oxides, hydrotalcite, among others [10].

Table 1-6. Acid catalysts employed in the homogeneous esterification of fatty acids.

Catalyst	Process	Remarks	Ref.
H_2SO_4	Esterification of palm fatty acids	Zero soap formation High catalytic activity More waste due to the neutralization stage Product darkening	[10]
Methanesulfonic acid	Esterification of palm fatty acids	High catalytic activity	[69]
p-toluene sulfonic acid	Esterification of Soybean oil fatty acids	High catalytic activity	[70]
H_3PO_4	Esterification of palm fatty acids	Low catalytic activity Product darkening	[69]

Esterification is an equilibrium reaction that limits the complete conversion of fatty acids [71]. Therefore, the equilibrium is generally shifted towards the products using a molar excess oil to alcohol of 1:5 – 1:20 and a catalyst loading of 0.5-2% wt. to ensure complete conversion. Higher catalyst loadings can induce product darkening indicating oxidation processes [68],[72],[73]. Once all the fatty material is esterified, a two-phase mixture is formed as water and ester/alcohol are immiscible, then they are separated through decantation. Subsequently, the ester layer is neutralized and washed until neutral pH. To

achieve low acid values and shift the equilibrium of the reaction, a multi-stage esterification process is also employed [73]. In a previous study [71], esterification of soybean oil with high acidity content (20%) was carried out at 60°C using a methanol: oil molar ratio of 10:1 and 5% H_2SO_4. Once the reaction reached the equilibrium the phases were separated, and the ester phase reacted with an additional load of catalyst and alcohol in a ratio of 6:1 to 35:1. This process was repeated until the acid value reaches less than 1% wt.

Transformation of feedstocks with a high content of glycerides and fatty acids usually involves a double reaction process. First, a pre-esterification of fatty acids with low molecular weight alcohol is performed, afterwards, an alkali-catalyzed transesterification takes place with the desired alcohol [74]. At the end of the esterification process, an acid value less than 2mg KOH/g is required to perform the subsequent alkaline transesterification [71]. Besides the abovementioned strategy for reducing acidity before transesterification, it is also possible to distill, saponify or even remove FFAs by solvent extraction using a suitable solvent like methanol, ethanol, or glycerol [75]. Finally, it is important to recall that secondary reactions such as hydrolysis and saponification can take place during the esterification. These reactions can produce higher content of free fatty acid or soaps that can trigger emulsification, which might hinder the liquid-liquid separation process.

1.5.2 Epoxidation

Epoxides are ethers with a cyclic ring in their structure. In the epoxidation process, an oxirane ring is formed by the incorporation of an oxygen atom into the double bonds of the lipid raw material [68]. In this process and especially for plasticizer applications, the high content of saturated fatty acids such as palmitic acid and stearic acid is undesired because these groups are not susceptible to epoxidation, and consequently they have a poor affinity to the polymer matrix, inducing the migration of the additive from the plastic [68], [76]. There are four routes for the production of epoxides: (i) epoxidation of alkene groups with peroxyacids ii) epoxidation of alkene groups with organic and inorganic peroxides iii) halohydrin formation and iv) ozonolysis with molecular oxygen [77]. The epoxidation of alkenes is usually catalyzed by homogeneous acids such as H_2SO_4 HNO_3, H_3PO_4, and HCl. However, H_2SO_4 is the most widely used catalyst due to its efficiency, effectiveness, and low cost [78].

Heterogeneous and biologic catalysts such as ion exchange resins (Amberlite IR-120) and enzymes are also widely explored for the epoxidation process [6]. Although these catalysts produce low degradation rates, their industrial application is limited due to the recovery and separation processes required [6],[57],[79]. Table 1-7 summarized the most typical operating conditions when using different catalysts for the epoxidation of alkenes.

Table 1-7. Epoxidation conditions using different catalysts.

Catalyst	Raw Material	T (°C)	t (h)	C=C/CA/H_2O_2	OO* (% wt.)	Conversion (%)	Selectivity (%)	Ref.
Ion exchange resins	Methyl ester of castor oil	60	10	1:0.5:1.5	4.86	96.04	--	[80]
	Soybean oil	60	5	1:0.5:1.5	6.50	92-95	97	[81]
Enzymes	Soybean oil	50	4	1:0.05:2.0	6.91	98.9		[82]
Silicates	Soybean oil	80	10	--	6.0	80.0	96	[83]

* OO – Oxirane oxygen content

- Prileschajew epoxidation

The Prileschajew reaction is the most widely used route at the industrial scale for producing epoxidized vegetable oils and other derivates. This route is commonly used because it can be carried out in typical stirred reactors, requires mild conditions, is well-known, and has low operating costs. During this reaction, the double bonds in fatty acids are partially oxidized by transferring oxygen from a carrier such as the peroxycarboxylic group. This process is known as the peroxyacid oxidation of unsaturation. For safety reasons, a peroxyacid generated in situ from a carboxylic acid is often used instead of using a peroxyacid group as a reagent. The epoxidation is a strongly exothermic reaction, releasing about 250 kJ per mol. Therefore controlled dosing of the reagents is required [57], [84].

The epoxidation reaction takes place in two stages: the formation of the peroxyacid, which is considered the limiting step of the reaction, and the formation of the epoxide by the reaction of the peroxyacid and the double bonds present in the oleochemical substrate [68]. Peroxyacid is formed by the reaction of a carboxylic acid, usually acetic or formic acid with hydrogen peroxide. When formic acid is used the reaction is autocatalytic, but when the process is carried out using acetic acid, sulfuric acid is employed as a catalyst [4]. Previous studies have shown that acetic acid is preferred as an oxygen carrier compared to formic acid because it results in lower formation of undesired products [85]. Due to the chemical nature of reactants and products, there are two different phases involved in the reaction.

The aqueous phase has the hydrogen peroxide and the catalyst, and the oil phase contains the double bonds of the fatty chains. Acetic acid and peracetic acid have partial miscibility in both phases and they can be transferred between them.

The following is a description of the epoxidation process and its relation to the mass transfer phenomena between the phases. Firstly, acetic acid reacts with hydrogen peroxide in the aqueous phase to produce peracetic acid.

$$H_3CCOOH + H_2O_2 \rightleftharpoons H_3CCOOOH + H_2O \quad (1\text{-}2)$$

Once peracetic acid is transferred from the aqueous phase to the oil phase, it reacts with double bonds to form the epoxide, releasing acetic acid [60], [68].

$$H_3CCOOOH + R_1CH = CHR_2 \rightarrow R_1CHOCHR_2 + H_3CCOOH \quad (1\text{-}3)$$

Finally, the acetic acid is transferred from the oil phase to the aqueous phase to regenerate another molecule of peracetic acid. This cycle lets a simultaneous or in situ formation of the peroxyacid.

Epoxides are very reactive groups and may undergo secondary reactions of ring-opening and oligomerization. These reactions are triggered by high temperatures, low pH, and the presence of water and acid in the reaction medium. Ring-opening can generate undesired products such as acetates, diacetates, alcohols, and polyols [6],[57][86],[87]. Polymerization reactions, such as those presented in Figure 1-10 can also occur. They are undesired because these increase the viscosity of the epoxide, reaching values of 2000 mPa s [88]. This viscosity is 10-fold higher than reported for epoxidized soybean oil which is around 210 Pa s [81].

According to previous works, the rate of ring opening generated by peracetic acid and acetic acid is faster than the effect caused by water and hydrogen peroxide. It has been reported that the ratio between the cleavage kinetic constants by peracetic acid and acetic acid (k_{PAA}/k_{AA}) at 70°C is 18 [89]. However, the concentration of peracetic acid in the medium is low because it reacts as soon as it is produced, and therefore its nucleophilic attack is expected to be negligible. This fact is supported by the low reaction rate of peracetic acid formation $9.81 \cdot 10^{-3}$ ($L^2 \cdot mol^{-2} min^{-1}$) at 333K [90], which is the controlling step of the reaction [90]. Consequently, it is expected that the degradation of the oxirane is mainly caused by the carboxylic acid attack [89].

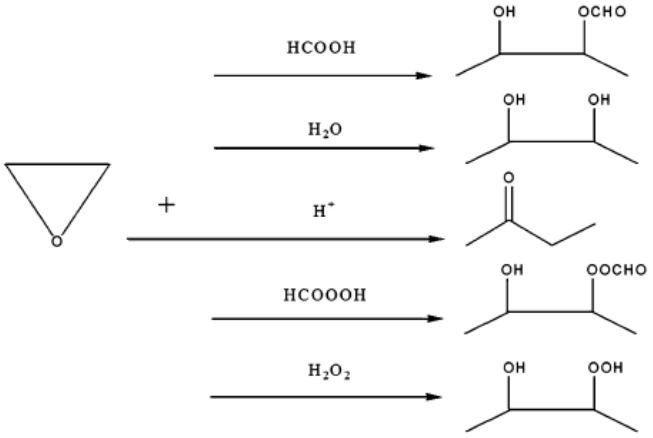

Figure 1-10. Secondary ring-opening reactions occurring during epoxidation.

In terms of cleavage by hydration, a previous study investigated the excision of oxirane by water at different pH and temperatures [89]. According to their findings, a significant hydration rate was observed when epoxidation was performed under harsh conditions (70°C and pH:1) and a high interfacial contact area between the liquid phases. The degradation of oxirane by hydrogen peroxide is not very effective as it has low solubility in the oil phase due to its polar nature. As a result, the oxirane cleavage by hydrogen peroxide can be negligible [89]. Therefore, it can be assumed that the main degradation reactions are caused by water and acetic acid. Besides ring-opening reactions, the ester can undergo hydrolysis in the presence of water during the epoxidation process which can increase the acid value.

To assess the progress of the reaction during epoxidation, the change in iodine value (i.e. conversion of double bonds) and the oxirane content (i.e. oxidation yield) over time are monitored. This can be done using titrimetric methods as well as spectroscopic techniques such as FTIR and NIR [81], [91]. The effect of the reaction conditions is evaluated based on the conversion, yield, and selectivity, which are defined as follows:

Double bonds conversion:

$$DBC\ (\%) = \left(\frac{II_0 - II}{II_0}\right) * 100 \qquad (1\text{-}4)$$

In equation (1-4) II_0 is the initial iodine value or iodine index of the sample, and II is the time changing iodine value along the reaction. The iodine value is a surrogate of the unsaturation content in the material and a method for its determination is presented in Annex A.

Yield to oxirane oxygen:

$$RC\ (\%) = \frac{OO\ exp}{OO\ máx} * 100 \quad (1\text{-}5)$$

Equation (1-5) enables to calculate the epoxide yield based on the oxirane oxygen (OO) content of samples from experiments and the theoretical maximum oxirane oxygen (OO max) according to the nature of the feedstock.

Maximum theoretical content of oxirane oxygen

$$OO\ \max = \left[\frac{\left(\frac{II}{2A_i}\right)}{100 + \left(\frac{II}{2A_i}\right) * A_0}\right] * A_0 * 100 \quad (1\text{-}6)$$

In Equation (1-6) II is the iodine value, Ai and Ao are the atomic weights of iodine (126.9 g/mol) and oxygen (16.0 g/mol), respectively.

As the reaction can derive inside ring-opening reaction products, the corresponding selectivity towards epoxides is calculated with Equation (1-7).

Selectivity:

$$Selectivity = \frac{RC}{DBC} * 100 \quad (1\text{-}7)$$

- Variables in the epoxidation reaction

The control of the operating conditions during epoxidation is important to achieve high double bond conversion, as well as high selectivity towards oxirane [79]. The effect and the relationship among the different variables have been a central point of research. Among the variables that have a higher effect on the conversion, it is worth mentioning the molar

ratio of the reagents, the catalyst loading, temperature, degree of agitation, and reaction time [72], [79]. According to the L'Chatelier principle, the formation of the products is favored by an excess of reactants. In this case, it is necessary to add a molar excess of hydrogen peroxide to promote peroxyacid formation. Preliminary studies indicate that a molar ratio of 1.5 - 3 of H_2O_2 to unsaturation content maximizes the oxirane oxygen yield [79]. However, higher molar ratios promote side reactions that hinder achieving high oxirane content [72]. Furthermore, the concentration of hydrogen peroxide, typically 30-60% (w/w), has a decisive effect on the kinetics [79], [92]. The yield of epoxide is also correlated to the amount of carboxylic acid in the medium. According to the literature, a typical molar ratio to double bonds is 0.5-1:1, higher ratios can promote oxirane losses [93]. Additionally, the epoxidation is usually carried out at 40-85°C, but, owing to the strong exothermic character of the reaction, strict temperature control is required to operate under isothermal conditions and achieve high yields [79].

Higher conversions are achieved by increasing the temperature, however, temperatures above 80°C strengthen the rate of hydrolysis and ring-opening reactions. Furthermore, extreme temperatures above 96°C promote the decomposition of hydrogen peroxide decreasing the epoxide content [28], [72]. In terms of yield, using lower temperatures close to 40°C and higher reaction times enhances the selectivity of oxirane [79]. In addition, it is important to consider the effect of reaction time on epoxidation and side reactions. Long reaction times (>9h) can intensify oxirane cleavage reactions, decreasing the oxirane content [79]. Concerning mass transfer rates, a higher degree of agitation produces larger interfacial areas in the immiscible liquid phases, enabling faster epoxidation of double bonds. However, a very high stirring rate can trigger ring-opening and decrease selectivity. Therefore, it is usual to use a stirring rate in the range of 350 - 1500 rpm [79]. Furthermore, to reduce side reactions, epoxidation used to be carried out in an inert solvent such as an aromatic, aliphatic, or halogenated hydrocarbon such as benzene, hexane, or toluene [84]. Modern processes are designed with solvent-free routes reducing economic and environmental impacts [94].

The formation of the peracetic acid is usually catalyzed by sulfuric acid H_2SO_4. Typically, a catalyst concentration ranging from 1-1.5% w/w based on the mass of the oil is commonly used [76]. A recent study [85] investigated the effect of H_2SO_4 loading (1% to 3% of the aqueous phase) on the epoxidation kinetics. In this study, an optimum concentration of oxirane was obtained at 2% loading, higher concentrations increase the oxirane cleavage.

Table 1-8 summarizes the operation conditions reported in previous works for the conventional epoxidation process using acetic acid and formic acid. Finally, it is necessary to study the combined effect of the variables on the kinetic to obtain the highest yield towards oxirane oxygen content.

1.5.3 Purification

The purification of the epoxidized ester is normally performed by neutralization and washing stages to remove the remaining acidity of the aqueous phase. Additionally, a bleaching treatment is usually carried out to meet the technical color specification of the epoxidized derivative. In this process, the immiscible phases obtained in the epoxidation are separated; the aqueous layer is discarded, and the oil phase is neutralized using a saturated solution of sodium bicarbonate $NaHCO_3$. The epoxidized ester is then washed with water and NaCl solution until a neutral pH is achieved. Finally, the epoxide is dried over sodium sulfate and distilled under a vacuum to remove the remaining moisture. [76], [79], [92]. It is also possible to carry out the purification process using liquid-liquid extraction with ethyl acetate to remove some impurities and the remaining moisture [81]. To obtain a translucent epoxide that meets the specification of a commercial plasticizer, a bleaching process is conducted using diatomaceous earth, clays, or Magnesol to remove colored compounds [24], [46].

1.5.4 Epoxidation kinetics

Several kinetic models have been proposed for the epoxidation of unsaturations in vegetable oils and fatty acid methyl esters (FAMEs). In general, three types of models have been used to describe the epoxidation rates, namely pseudo-homogeneous, two-phase, and macro-kinetic models [95]. The corresponding equations of such models are summarized in Table 1-9.

Table 1-8. Operating conditions and main results obtained during conventional in situ epoxidation processes of different oleochemical feedstocks.

Raw material	CA	T (°C)	t (h)	H_2O_2 (%wt)	Agitation (rpm)	Cat.	Cat. (% wt.)	Molar ratio C=C:CA:H_2O_2	OO (% wt.)	Conversion C=C (%)	Selectivity (%)	Ref.
Methyl ester of soybean oil	AF	50	11	40	400	--	--	1:0.5:2.0	6.97	97[a]	97[b]	[96]
Methyl ester of soybean oil	AF	40	11.5	59	350	--	--	1:0.5:2.0	6.2	97	86	[79]
Methyl ester of Jatropha	AF	70	4.6	30	1500	--	--	1:1:3.1	5.6	--	--	[92]
Methyl ester of Jatropha	AA	69	6.0	30	1500	H_2SO_4	1.5	1:0.6:3.5	--	74	--	[97]
2-hetylhexyl ester of used cooking oil	AF	66	7	50	600	--	--	1:0.35:2.41	5.2	99	93	[4]
Rapeseed oil	AA	65	6	30	--	H_2SO_4	2.9	1:0.7:4.0	3.2	91	73	[98]
Karanja oil	AA	85	3.5	30	1500	H_2SO_4	1.4	1:0.5:1.5	4.2	85	94	[77]
Cottonseed oil	AA	60	4	50	2400	H_2SO_4	0.8	1:0.5:2.0	6.1	91	79	[85]
Soybean oil	AA	90	~3.0	31	400	H_2SO_4	1.5	1:0.4:1.2	4.5	--	--	[84]
Soybean oil	AA	80	2.3	50	100-2000	H_2SO_4	2.0	1:0.2:1.3	6.4	--	--	[99]
Used cooking oil	AA	50	3	50	400	H_2SO_4	2.0	1:0.2:1.5	3.1	--	--	[60]
Used cooking oil	AA	50	5	50	500-800	H_2SO_4	1.0	1:0.15:0.4	3.2	59.4	86	[57]

CA: Carboxylic acid, Cat: (%w/w) respect to oil mass, molar ratio (C=C:CA:H_2O_2) based on ethylenic unsaturation content,
(a),(b) calculated value assuming II:129.4 g I_2/100g y OO theoretical: 7.4% wt.

Table 1-9. Kinetic models used to describe the homogeneous catalytic epoxidation of vegetable oils and derivates.

Oil	CA, Catalyst	Reactions	Rate	Remarks	Ref.
Soybean oil (SBO)	AA, H_2SO_4	$AA + H_2O_2 \overset{k_1}{\rightleftharpoons} PAA + H_2O$ $C = C + PAA \overset{k_2}{\underset{k_3}{\rightleftharpoons}} EP + AA$	$\frac{dC_{EP}}{dt} = k(C_{HP_o} - C_{EP}) * C_{AA_o}$	*Macro-kinetic model *The concentration of peracetic acid is constant *Negligible degradation of oxirane.	[77]
Palm oil methyl esters	AA, H_2SO_4		$r = k(C_{HP_o} - C_{EP}) * C_{AA_o}$ $r_{Deg} = -k\ C_{EP} * C_{AA}^2$	**Macro-kinetic model *Degradation of oxirane by acetic acid	[100]
Soybean FAME	FA	$FA + H_2O_2 \overset{k_1}{\rightleftharpoons} PFA + H_2O$ $C = C + PFA \overset{k_2}{\underset{k_3}{\rightleftharpoons}} EP + FA$ $EP + FA \overset{k_4}{\rightarrow} Deg_1$ $EP + PFA \overset{k_5}{\rightarrow} Deg_2$	$\frac{dC_{HP}}{dt} = -k_1 C_{FA} C_{HP} + k_2 C_{PFA} C_{WT}$ $\frac{dC_{FA}}{dt} = \left(\frac{1 - \phi_{org} * (1 - m_{FA})}{m_{FA}}\right)^{-1} * (-k_1 C_{FA} C_{HP} + k_2 C_{PFA} C_{WT})\phi_{aq} - k_4 {C_{FA}}^2 C_{EP} * \phi_{org}$ $\frac{dC_{PFA}}{dt} = \left(\frac{1 - \phi_{org} * (1 - m_{PFA})}{m_{PFA}}\right)^{-1} * (k_1 C_{FA} C_{HP} - k_2 C_{PFA} C_{WT})\phi_{aq} - k_5 {C_{PFA}}^2 C_{EP} * \phi_{org}$ $\frac{dC_{WT}}{dt} = k_1 C_{FA} C_{HP} - k_2 C_{PFA} C_{WT}$ $\frac{dC_{DB}}{dt} = -k_3 C_{PFA} C_{DB}$ $\frac{dC_{EP}}{dt} = k_3 C_{PFA} C_{DB} - k_4 C_{EP} {C_{FA}}^2 - k_5 C_{EP} {C_{PFA}}^2$	*Two phase reaction model *Epoxide degradation by carboxylic and percarboxylic acid	[79]
Soybean FAME	FA	$FA + H_2O_2 \overset{k_1}{\rightleftharpoons} PFA + H_2O$ $PFA \overset{k_2}{\underset{k_3}{\rightleftharpoons}} H_2O + CO_2 \uparrow$ $PFA + C = C \overset{k_4}{\rightarrow} EP + FA$ $EP + X \overset{k_5}{\rightarrow} Y$	$\frac{dC_{HP}}{dt} = -k_1 C_{FA} C_{HP} + k_2 C_{PFA} C_{WT}$ $\frac{dC_{PFA}}{dt} = k_1 C_{FA} C_{HP} - k_2 C_{PFA} C_{WT} - k_3 C_{PFA} - k_4 C_{PFA} C_{DB}$ $\frac{dC_{DB}}{dt} = -k_4 C_{PFA} C_{DB}$ $\frac{dC_{EP}}{dt} = k_4 C_{PFA} C_{DB} - k_5 C_{EP}$ $\frac{dC_{FA}}{dt} = -k_1 C_{FA} C_{HP} + k_2 C_{PFA} C_{WT} + k_4 C_{PFA} C_{DB}$	*Pseudo homogeneous model *PFA consumption by hydrolysis, decomposition, and epoxidation	[95]

1.6 Commercial biobased plasticizers

When developing a process to produce an established industrial product, it is important to ensure that the required specifications and commercial standards are met to facilitate its introduction in the market. In this regard, some technical specifications of epoxidized soybean and linseed oils have been compiled in the Colombian standard NTC 2366 [101]. Nonetheless, it is important to recall that the epoxide content and the properties of the epoxidized esters largely depend on the alcohol used in the esterification or transesterification process, as well as the length of the fatty acid chain. Some properties of commercial epoxy derivates are summarized in Table 1-10 [102], [103].

Table 1-10. Some physicochemical properties of commercial epoxides from oleochemical derivates

Parameter	Epoxidized soybean oil	Epoxidized methyl soyate	Epoxidized butyl soyate	Isoamyl epoxy stearate
Commercial name	Vikoflex® 7170	Vikoflex® 7010	Vikoflex® 7040	Provion, PLS Green 5
Oxirane Oxygen (%)	6.8 mín.	7.0 mín.	6.3 mín.	5.4 min
Acid value (mg KOH/g)	0.5 máx.	2.0 máx.	2.0 máx.	2.0 máx.
Relative density (25°C)	0.993	0.954	0.936	0.934
Color APHA	150 máx.	175 máx.	175 máx.	--
Viscosity CSt (25°C)	420	80	80	33
Iodine value (gI2/100g)	2.0 máx.	3.0 máx.	3.0 máx.	--

2. Selection of the alcohol used for plasticizer production.

The production of plasticizers from soybean fatty acids involves two processes. Firstly, the esterification of the fatty acids using alcohol, and secondly the epoxidation of the double bonds. The selection of suitable alcohols for the process is important not only for ensuring good performance as a plasticizer, but also to facilitate the incorporation of bio-based derivatives to produce sustainable additives for the polymer segment. This chapter proposes a method for screening and selecting biobased alcohols and diols to produce green and sustainable plasticizers derived from vegetable oils. The method evaluates five criteria in the performance of the plasticized PVC: compatibility, efficiency, permanence, toxicity, and cost. Prediction of the properties required to assess such criteria was calculated through group contribution methods and empirical correlations. In this sense, this chapter developed a computational-aided plasticizer product design with an emphasis on epoxidized fatty ester structures.

2.1 Biobased alcohols

In a biorefinery, renewable feedstocks are transformed into intermediate products which serve as building blocks to produce high-value-added products. Currently, the market of biobased chemicals, including biobased alcohols and polyols accounts for 90 Mt/yr. [104]. Recently, the chemical industry has increasingly incorporated biobased materials as feedstocks for a variety of processes. In particular, the use of biobased alcohols and polyols in the production of commercial esters and polyesters has been highly promoted. Many of

these bioderived alcohols have been produced from biobased synthesis gas, sugars, glycerol, and vegetable oils, among other sources.

In the case of those from biobased synthesis gas, low-weight alcohols such as methanol and ethanol can be produced by further conversion of this gas via thermo-catalytic processes. Syngas is a mixture composed mainly of hydrogen (H_2), carbon monoxide (CO), nitrogen (N_2), and methane (CH_4) produced by the gasification of biomass at high temperatures (800-1500°C) [105]. Regarding those produced from sugars, they are mainly produced by fermentation processes; alcohols and diols like ethanol, propanol, isopropanol, butanol, isobutanol, and 1,4 butanediol can be sustainably produced. From these alcohols, and particularly from ethanol, it is also possible to produce ethylene glycol. The recent interest in the production of ethylene glycol through this route has led the industry to a production capacity of 175 kt/yr that is used for the manufacture of biobased plastic products such as polyethylene terephthalate (PET) [104]. Similarly, butanol, isoamyl alcohol, and amyl alcohol can be obtained and refined from side streams during ethanolic fermentation [104]. Finally, from the building block of glycerol and vegetable oils, is possible to obtain derivatives such as 1,3 propanediol, 1,2 propanediol, and propylene glycol. The latter is already implemented at the industrial scale with a capacity of around 120 kt/year [104],[106]. In addition, through a cracking process of ricinoleic acid, it is possible to obtain branched alcohol such as 2-octanol [107]. Besides these routes, other alcohols can be produced by Guebert reactions enabling to transform short-chain, linear, biobased alcohols into long-chain branched alcohols.

After a literature and market review, it was possible to identify some of the currently available biobased alcohols that can potentially be used as feedstocks for the large-scale synthesis of fatty esters. From the identified bioderived chemicals, the following linear and branched alcohols, diols, and triols were selected as potential feedstocks for the esterification process: methanol, ethanol, propanol, isopropanol, butanol, isobutanol, isoamyl alcohol, 2-octanol, ethylene glycol, 1,2 propanediol, 1,3 propanediol, 1,4 butanediol, and glycerol.

2.2 Classification of Epoxidized Esters

This section describes the compounds that have been considered for the selection of suitable biobased plasticizer molecules to be produced from waste oleochemical streams.

Soybean oil deodorizer distillate (SODD) will be used as a feedstock, which is mainly composed of linoleic acid (50-57%). This fatty acid was used as a model molecule of the acid chain in the potential oleochemical plasticizer to be assessed. In this case, epoxidized linoleates of different mono, di, and trioles are considered, and Table 2-1 presents the alcohols and epoxides involved in their synthesis.

Table 2-1. Potential bioderived epoxidized esters from different alcohols intended to be used for plasticization applications.

Abbreviated Term	Name	Structure	Type	Alcohol (R)
MDES	Methyl diepoxystearate	Linear	Monoester	Methanol
EDES	Ethyl diepoxystearate	Linear	Monoester	Ethanol
PDES	Propyl diepoxystearate	Linear	Monoester	Propanol
IPDES	Isopropyl diepoxystearate	Branched	Monoester	Isopropanol
BDES	Butyl diepoxystearate	Linear	Monoester	Butanol
IBDES	Isobutyl diepoxystearate	Branched	Monoester	Isobutanol
IADES	Isoamyl diepoxystearate	Branched	Monoester	Isoamyl alcohol
ODES	2-octyl diepoxystearate	Branched	Monoester	2-octanol
		Epoxidized Monoester		
		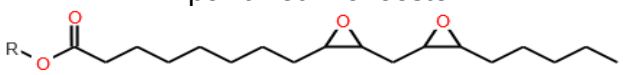		
EEGDL	Epoxidized ethylene glycol dilinoleate	Linear	Diester	Ethylene glycol
EPGDL	Epoxidized 1,2-propanediol dilinoleate	Branched	Diester	1,2 propanediol
EPRGDL	Epoxidized 1,3-propanediol dilinoleate	Linear	Diester	1,3 propanediol
EBGDL	Epoxidized 1,3-butanediol dilinoleate	Branched	Diester	1,4 butanediol
		Epoxidized Diester		
		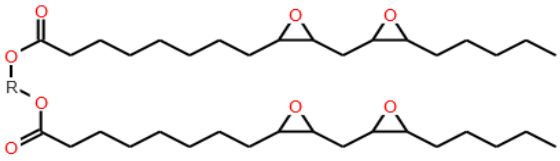		
ESBO	Epoxidized soybean oil	Linear	Triester	Glycerol
		Epoxidized Triester		
		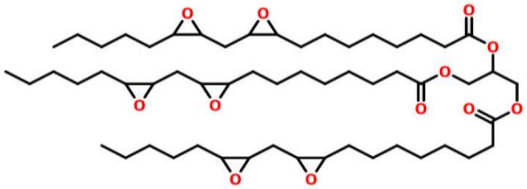		

2.3 Selection criteria and methods

As observed in Table 2-1, the number of biobased epoxidized fatty esters to be assessed as potential plasticizers is large. Therefore, a preliminary screening process is necessary to select the most promising ones to reduce resource consumption, such as materials, energy, time, and funds during their synthesis and experimental assessment. The selection process should prioritize molecules with a balanced set of physicochemical and plasticizing performance properties. The most important performance properties that can be used as selection criteria for a plasticizer are compatibility, efficiency, permanency, low toxicity, and low cost. These properties are related to low volatility, high extraction resistance in a solvent medium, low viscosity, low glass transition temperature, and softness. In general, these characteristics are a good indicator that a plasticizer is compatible, efficient, and permanent in the polymer structure [108]. Additionally, low environmental impacts are expected for new plasticizers. In this sense, toxicity is introduced as a selection criterion to develop an environment-friendly plasticizer. This seeks to mitigate the potential impact of traditional additives in sensitive applications (e.g., toys, childcare products, medical devices, and food packaging). Finally, cost is also considered as a selection criterion when seeking a competitive plasticizer that can be an alternative to traditional plasticizers. Figure 2-1 summarizes the selection criteria for the identification of epoxidized fatty esters.

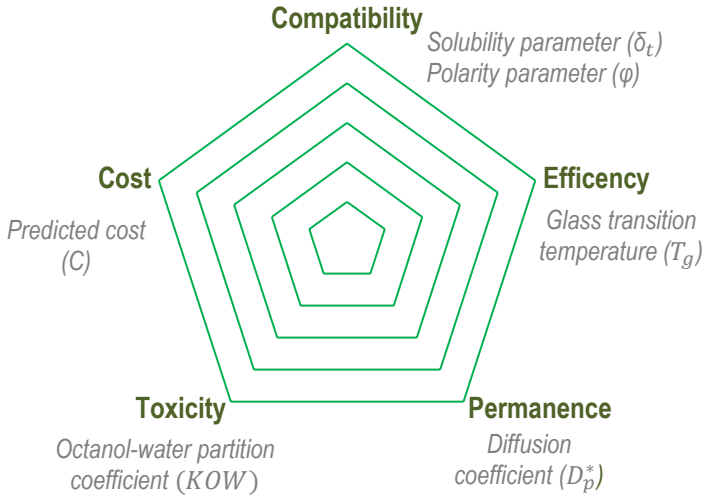

Figure 2-1. Selection criteria used to screen and rank potential biobased plasticizers derived from oleochemical waste streams.

For the potential green plasticizer molecules listed in Table 2-1, and in the absence of data from the literature, the assessment criteria presented in Figure 2-1 were quantified using group contribution methods and empirical equations. Nonetheless, to validate the accuracy of the predicting models, they were utilized to forecast the corresponding properties of the most used commercial phthalate plasticizers. The predicted properties were then compared with the reported values to identify the most suitable model for each criterion and property. Among the commercial plasticizers used for the selection of predictive methods, DOP was selected as the reference target compound since it produces highly elastic, low volatility, and well-gelling compounds, and it is the most widely used general-purpose plasticizer [3],[23], [109]. In addition, Table 2-2 presents other conventional plasticizers utilized for comparative evaluation.

Table 2-2. Common commercial phthalate plasticizers for PVC used in the assessment of predictive models of physicochemical properties.

Plasticizer	Structure	Carbons	Name	Applications
DEHP/DOP	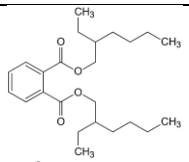	C8	Di-2-ethylhexyl phthalate	General-purpose plasticizer Application in medical devices
DNOP	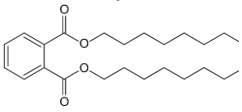	C8	Di-isooctyl phthalate	General-purpose plasticizer Application in medical devices
DEHT/DOTP	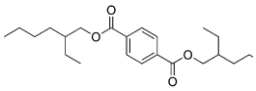	C8	Di-octyl terephthalate	General-purpose plasticizer Application in medical devices, wires, food packing, and toys
DINP	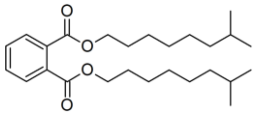	C9	Di-isononyl phthalate	General-purpose plasticizer. Application in wires and toys
DIDP	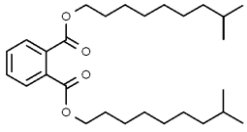	C10	Di-isodecyl phthalate	General-purpose plasticizer. Application in wires and toys
DBP	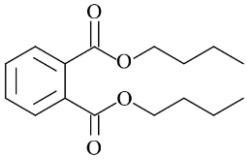	C4	Di-butyl phthalate	Specialty phthalate esters. Application in flooring
BBP	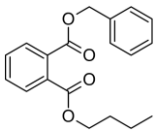	C4-7	Butyl benzyl phthalate	Specialty phthalate esters. Application in flooring

2.3.1Compatibility

Compatibility is the ability of a plasticizer to form a homogeneous system with a polymer, and this property depends on the chemical structure, the polarity, and the molecular weight of the plasticizer [40]. To obtain a compatible plasticizer with the polymeric matrix, it must be soluble in the polymer and polar enough to reduce the interaction between polymer-polymer molecules. The solubility and affinity of the additive for the PVC matrix can be predicted by using the solubility parameter (δ) as a surrogate. This parameter is defined as the square root of the cohesive energy density ($Ecoh$) and is commonly used to describe solvent-polymer interactions [67].

$$\delta_{(298\ K)} = \sqrt{\frac{Ecoh}{V}} \tag{2-1}$$

$$(J/cm^3)^{1/2}, (MJ/m^3)^{1/2}, (MPa)^{1/2}$$

In Equation $(2\text{-}1)$, $Ecoh$ is cohesive energy density and V is the molar volume. The thermodynamic solubility criterion is based on the free energy of mixing (ΔG_M). According to it, two substances are soluble when the value of free energy of mixing is negative ($\Delta G_M < 0$) [67].

$$\Delta G_M = \Delta H_M - T\Delta S_M \tag{2-2}$$

In Equation $(2\text{-}2)$, ΔH_M is the enthalpy of mixing and ΔS_M is the entropy of mixing. Hildebrand proposed a relation between the solubility parameter and the enthalpy of mixing:

$$\Delta H_M = \varphi_p \varphi_a V_M (\delta_P - \delta_S)^2 \tag{2-3}$$

In Equation $(2\text{-}3)$, P refers to polymer, S plasticizer, φ volume fraction of the components and V_M is the volume of mixing.

The cohesive energy $Ecoh$ relates to the effect of the interaction forces between the two substances.

$$E_{coh} = E_d + E_p + E_h \tag{2-4}$$

In Equation (2-4), E_d is the contribution of dispersion forces, E_p is the contribution of polar forces and E_h is the contribution of hydrogen bonding. Using this definition, the solubility parameter is equivalent to:

$$\delta^2 = ({\delta_D}^2 + {\delta_P}^2 + {\delta_h}^2) \quad (2\text{-}5)$$

In Equation (2-5), δ_d represents dispersion forces, δ_p polar forces, and δ_h hydrogen bonds. Then using this definition, the equation (2-3), can be written as:

$$\Delta h_M = \varphi_p \varphi_a * \left[(\delta d_P - \delta d_S)^2 + \left(\delta p_p - \delta p_S\right)^2 + (\delta h_P - \delta h_S)^2\right] \quad (2\text{-}6)$$

There are several methods to estimate the solubility parameter of a plasticizer in a polymer. The most relevant methods were developed by Small, Van Krevelen, Hoy, Fedors, Dunkel, Di Benedetto, Hansen, and Stefanis [67],[110],[111]. In particular, Hoy developed a method to predict the solubility parameter of amorphous polymers of high molecular weight by considering the molar volume, molar attraction (Ft), and a polar component (Fp) [67].

According to the concept that "like dissolves like", the solubility parameters of the solvent and the polymer should be as similar as possible to ensure solubility and compatibility. Setting the value of the polymer solubility parameter (δp) as the center of a sphere with coordinates ($\delta d,\ \delta p,\ \delta h$). Solubility increases as the distance between the solubility parameter of the plasticizer (δ_a) and the center decreases ($\Delta\delta$). To ensure solubility, the parameter $\Delta\delta$ that is computed with Equation (2-4) should be small, normally lower than 5 $Mpa^{1/2}$ [67].

$$\Delta\delta = \sqrt{(\delta d_P - \delta d_S)^2 + (\delta p_P - \delta p_S)^2 + (\delta h_P - \delta h_S)^2} \quad (2\text{-}7)$$

The computed solubility parameters for PVC and phthalate plasticizers, as well as their reported parameters are listed in Table 2-3 [112].

In Figure 2-2, the results are outlined in triangular coordinates defined in Equation (2-4).

$$d = \frac{\delta d}{\delta d + \delta h + \delta p};\ h = \frac{\delta h}{\delta d + \delta h + \delta p};\ p = \frac{\delta p}{\delta d + \delta h + \delta p} \quad (2\text{-}8)$$

As observed, significant discrepancies were observed between the estimated and the reported values for the parameter (δh), indicating that Hoy's method is not accurate in predicting the contribution of hydrogen bonds. However, most of the parameters for different compounds were well-predicted and were similar to those reported in the literature. The calculated error was approximately 9.5%, which is consistent with the claimed accuracy of the method (~ 10%) [63].

Table 2-3. Solubility parameters for PVC and phthalate plasticizers calculated with Hoy's group contribution methods and reported values from the literature.

Substance	δd $Mpa^{1/2}$	δp $Mpa^{1/2}$	δh $Mpa^{1/2}$	δt $Mpa^{1/2}$	Error δt (%)	Ref.
PVC	15.4	11.3	6.9	20.3	--	This work
	18.4	6.6	8.0	21.1	3.7	[112]
	19.2	9.2	7.2	22.5	9.5	[113]
	18.6	8.8	5.8	21.4	4.9	[114]
	18.2	7.5	8.3	21.4	4.8	[115]
DEHP/DOP	16.6	8.2	4.8	19.1	--	This work
	16.6	7.0	3.1	18.3	4.7	[112]
	16.0	8.0	3.1	18.2	5.4	[116]
DNOP	16.7	8.2	5.5	19.5	--	This work
	16.6	7.0	3.1	18.3	6.5	[112]
DINP	16.7	7.9	4.6	19.0	--	This work
	16.6	6.6	2.9	18.1	5.3	[112]
DIDP	16.8	7.6	4.4	19.0	--	This work
	16.6	6.2	2.6	17.9	6.0	[112]
DBP	16.1	10.0	6.9	20.2	--	This work
	17.8	8.6	4.1	20.2	0.1	[112]
BBP	15.9	10.8	7.8	20.7	--	This work
	19.0	11.2	3.1	22.4	7.4	[112]

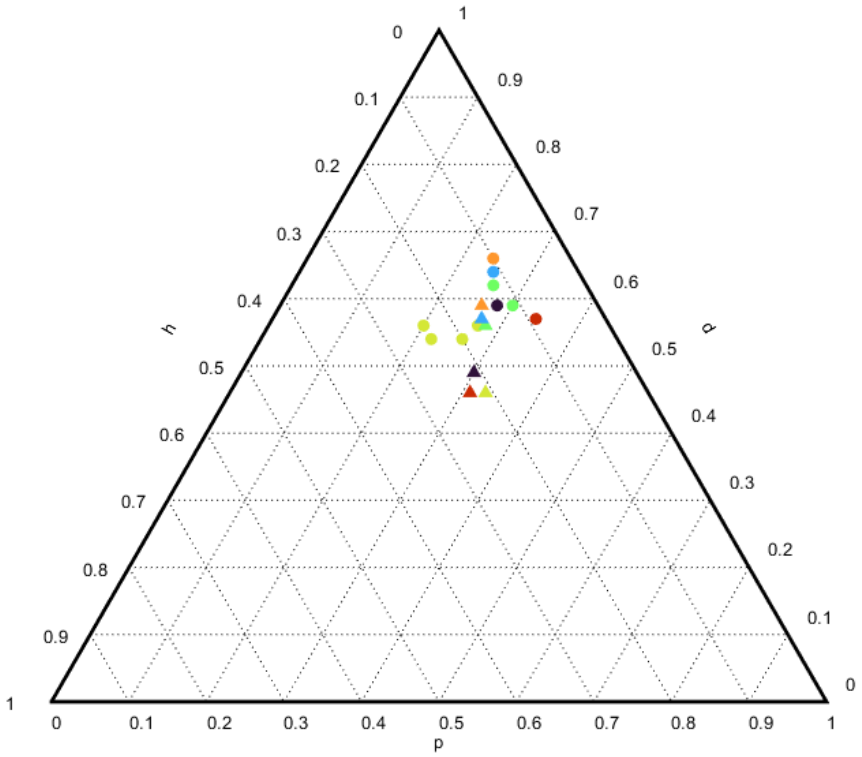

Figure 2-2. The solubility parameter of common plasticizers.
PVC (▲), DOP(▲), DINP(▲), DIDP(▲), DBP (▲) BBP(▲), reported in the literature (●)

In addition to the solubility parameter, a plasticizer-polymer system is considered compatible if they have approximately the same polarity. The polarity parameter (Φ) proposed by Van Veersen and Meulenberg compares the polarity of different molecules based on the balance between polar and non-polar groups along the chain [109].

$$\Phi = \frac{\mathrm{M}(\mathrm{A_p}/\ \mathrm{P_o})}{1000} \qquad (2\text{-}9)$$

In Equation $(2\text{-}9)$, M is the molar mass of the plasticizer, A_p is the number of carbon atoms without considering the carbons present in aromatic rings and carboxylic groups, and P_o is the number of polar groups. Low polarity parameters indicate high PVC compatibility [3]. Conversely, polar polymers are expected to plasticize with polar substances. Efficient plasticization is not achieved if the intermolecular forces between the plasticizer molecules are stronger than the interactions between the plasticizer and the polymer [117].

2.3.2 Permanence

Three main mechanisms control plasticizer retention, volatility, migration, and extractability. Volatile losses occur when the additive is evaporated from the polymer surface to the surrounding air. Migration occurs when the plasticizer is transferred from the polymer surface to any adjacent material and extractability occurs when the additive is dissolved into organic liquids. All of these mechanisms result in plasticizer depletion [3]. In this work, permanence is evaluated by estimating the migration of the additive. Migration is the mass transfer of substances from plastic material to an external matrix in contact with it. This property is determined by the mobility of the polymer according to Fick's law, which is a function of concentration, time, and temperature [118],[119].

The migration process begins with the diffusion of the plasticizer from the polymer to the surface. Then the migrant plasticizer is transferred across the polymer interface to the external phase and finally, it is assimilated into the external phase. Otto Piringer proposed a semi-empirical model to predict the migration from plastic packings into food simulants [118]. The model predicts an overestimation of the diffusion coefficient ($D \leq D_p$) of the plasticized materials by employing three parameters: a polymer specific constant (A_p), the molar mass of the migrant substance (M_r), and the absolute temperature (T). This approach is valid for temperatures below 70°C, molecular masses between 370 and 419 g/mol, and plasticizer concentration of 30%. This model follows an Arrhenius-type equation. Using this simplified approach, higher diffusion rates (D_p) are associated with a higher migration through the polymer [118].

$$D_p = D_o * exp^{\frac{-E_A}{RT}} \tag{2-10}$$

$$D_p = D_o * \exp(A_p - 0.1351 * {M_r}^{2/3} + 0.003 * M_r - \frac{10454}{T}) \tag{2-11}$$

$$A_p = -1 + 0.52 * (\%Plastificante) \tag{2-12}$$

In Equation (2-10) and Equation (2-11), D_p is the diffusion coefficient, D_o is the preexponential factor ($D_o = 10^4\ cm^2/s$), R is the ideal gas constant and A_p is a polymer's specific constant. The parameter A_p was previously evaluated for PVC polymers and can be assumed as 14.48, which is valid when a concentration of 67phr at 20°C is used [25].

2.3.3Efficiency

The efficiency of a plasticizer is defined as the amount of additive required to impart a certain level of flexibility and mechanical properties to the polymer. In plasticized polymers, the forces between macromolecules are reduced compared to unplasticized materials due to increased mobility of the polymer and greater free volume between chains [3]. In this regard, the plasticization efficiency is related to the depression on the glass transition temperature (Tg) [120]. Below this point, polymers behave as a crystalline vitreous state [120]. Generally, a lower glass transition temperatures for an additive indicates greater efficiency, which means that less additive is required to achieve a certain level of softness in the final polymer.

Several authors have developed group contribution methods for estimating glass transition temperature based on the chemical structure [110],[121]. However, these methods mostly apply to polymers. Therefore, the glass transition temperature of epoxidized esters was estimated through a group contribution method previously reported [122], which can differentiate between the glass transition temperature of polymers and additives. In the case of polymers, like PVC, it is estimated based on the groups in the main (i) and side chains (j) of the polymer repeating unit. For additives, this parameter is calculated with the regressed constants for side chains (j). The method of Equation (2-13) was developed through mathematical regression of Tg of different polymers and additives such as DOP, DIDP, and DEHP.

$$T_g = \frac{1}{M} * \left[\sum_i \left(T_g M\right)_i + \sum_j \left(T_g M\right)_j \right] \qquad (2\text{-}13)$$

In Equation (2-13), Tg and M correspond to the glass transition temperature and the molecular weight of the repeating unit for polymers or the whole molecular structure for additives. The glass transition temperature of pure plasticizers can be considered as a “pseudo melting” transition at low temperatures [123]. This point is also described as the temperature at which a liquid transitions to a glassy state, becoming more viscous and less able to flow or vice versa [124].

The glass transition temperatures estimated for PVC and phthalate plasticizers using this group contribution method, along with the corresponding values reported in the literature are presented in Table 2-4. As observed, predictions for phthalate plasticizers present low

relative errors in comparison with those observed for PVC. Nonetheless, the main goal to use this method is to predict the corresponding glass transition temperatures of the assessed oleochemical plasticizers.

Table 2-4. Glass transition temperature (Tg) of PVC and phthalate plasticizers

Material	Estimated Tg (°C)	Reported Tg (°C)	Error (%)	Ref.
PVC	68.8	82.8	16.9	[125]
DEHP/DOP	-86.7	-90.2	3.9	[122]
DNOP	-87.0	-87.2	0.2	[122]
DINP	-86.6	-82.7	4.7	[123]
DIDP	-86.5	-85.7	0.9	[123]
DBP	-87.8	-82.9	5.9	[123]

2.3.4 Toxicity

Environmental and health concerns about the potential impacts of the use of plasticizers have increased in the last few years. Since plasticizers are not chemically bound to the polymer, they can migrate from the polymer to the medium in contact with it. Due to their organic and hydrophobic nature, as well as their low volatility at room temperature, plasticizers tend to migrate into lipids, which can lead to an increase in the bio-concentration factor and generate impacts on ecosystems [126]. Then, the octanol-water partition coefficient (Kow), which determines the affinity of these substances for lipids, can be an indirect indicator of the potential toxicity of plasticizers.

Group contribution methods to estimate the octanol-water partition coefficient (Kow) have been implemented in commercial software. In this work, the octanol-water partition coefficient is estimated using the KOWWIN method available in EPIsuite™ software [127]. This contribution method divides the molecule into atoms or fragments, and the parameter associated with each fragment is determined empirically. Also, the method uses correction factors based on the molecular structure.

Table 2-5 shows the estimated values of log Kow using EPIsuite™ and the reported values for PVC and some phthalate plasticizers.

Table 2-5. Octanol water partition coefficient (log Kow) for PVC and phthalate plasticizers

Material	log Kow	log Kow exp.	Error (%)	Ref.
PVC	1.58	1.46	8.2	[128]
DEHP/DOP	8.39	7.6	10.4	[128]

DNOP	8.54	8.1	5.4	[128]
DINP	9.37	10.71	12.5	[129]
DIDP	10.36	10.36	0.00	[129]
DBP	4.61	4.5	2.44	[128]
BBP	4.84	4.73	2.33	[128]

From a general perspective, the estimation method enables a good prediction of the log Kow, with errors below 12.5%. This level of accuracy is considered adequate for a completely predictive model. As expected, low molecular weight plasticizers such as DBP and BBP presented lower log Kow values. However, these compounds are more volatile and can migrate easier than high molecular-weight additives.

2.3.5 Cost

One of the most important features of plasticizers is their price since they have a large impact on the final cost of the plastic material. In this regard, it is important to identify the most cost-competitive biobased plasticizers against phthalates. The price of common plasticizers is defined by available market prices. In the case of some of the assessed plasticizers from Table 2-1, they are not produced in large volumes and thus their market prices are unavailable. Therefore, a method was developed to estimate their cost based on the raw materials used to produce these substances. With this purpose, the total cost was predicted by estimating the cost of esterification (EC) and epoxidation (EPC).

The cost of esterification (*EC*) was calculated based on the prices of the biobased alcohols and fatty acids, which are listed in Annex B, Table B-1. The epoxidation cost (*EPC*) was estimated by calculating the epoxidation cost of one double bond in soybean oil. Using this information, along with the theoretical iodine value of each epoxide, it was possible to estimate the epoxidation cost for the different biobased green plasticizers. To do so, it was necessary to consider the prices of soybean oil and epoxidized soybean oil as a reference.

$$Total\ cost\ (USD/t) = EC + EPC \tag{2-14}$$

$$EPC\ (USD/t) = \frac{(CESBO - CSO\ ) * II_i * M}{II_{SO}} \tag{2-15}$$

In Equation (2-14) and Equation (2-15), CESBO and CSO are the prices of epoxidized soybean oil and soybean oil respectively $\left(\frac{USD}{t}\right)$, II_i and II_{SO} are the iodine value of assessed epoxidized esters (i) and soybean oil respectively$\left(\frac{gI_2}{100g}\right)$ and M is the mass of the ester.

Table 2-6 summarizes the theoretical effect of the alkyl chain length and the degree of branching of the alcohol in each criterion. Here, H and L refer to high and low effects.

Table 2-6. Effect of the selected alcohol on the performance of the plasticizer ester in PVC applications

Parameter	Alkyl chain length of alcohol	Branching of alcohol
Compatibility (H)	↓	↓
Efficiency (H)	↓	↓
Permanence (H)	↑	↑
Toxicity (L)	↓	=
Cost (L)	↓	=

2.3.6 Objective function for plasticizer selection

Epoxidized esters were compared using the score of the objective function described in Equation (2-16), which is based on the selected criteria of Figure 2-1. The corresponding parameters in this objective function and their normalization are presented in Table 2-7.

$$F = 0.2 * (0.5 * \delta_R + 0.5 * \Phi_R) + 0.3 * \mathrm{Tg}_R + 0.1 * \mathrm{D'p}_R + 0.2 * \mathrm{Log\,Kow}_R + 0.2 * \mathrm{C}_R \quad (2\text{-}16)$$

Table 2-7. Parameters evaluated in the objective function.

Parameter	Description	Indicator	Formula
δ_R	Solubility parameter	Compatibility	$\left\lvert\frac{\Delta\delta_{PVC-a}}{\Delta\delta_{PVC-DOP}} - 1\right\rvert$
Φ_R	Polarity	Compatibility	$\left\lvert\frac{\Phi_a}{\Phi_{DOP}} - 1\right\rvert$
Co_R	Compatibility	Compatibility	$0.5\,\delta_R + 0.5\Phi_R$
Tg_R	Efficiency	Efficiency	$\left\lvert\frac{Tg_a}{Tg_{DOP}} - 1\right\rvert$
$\mathrm{D'p}_R$	Diffusion coefficient	Permanence	$\frac{D'p_a}{\max(D'p_a)}$
$\mathrm{Log\,Kow}_R$	Octanol-water partition coefficient	Toxicity	$\frac{Log\ Kow_a}{\max(Log\ Kow_a)}$
C_R	Cost	Cost	$\left\lvert\frac{Cost_a}{Cost_{DOP}} - 1\right\rvert$

The objective function was weighted for each dimension. Each weighting factor was assigned seeking a high plasticizing efficiency through the parameters of compatibility and Tg. A lower weighting factor was given to the diffusion parameter considering that all plasticizers have a high molecular weight (> 326.5 g/mol). In the case of the compatibility criterion (Co_R), the weighting factor was equally divided between solubility (δ_R) and polarity parameter (Φ_R).

2.4 Election of the biobased plasticizer

Table 2-8 summarizes the results for the solubility parameter and molar volume of each molecule calculated using Hoy's method, along with the corresponding experimental volumes reported in SciFinder [130].

Table 2-8. Results of solubility parameter using Hoy's group contribution method for common phthalates and the epoxidized esters

Material		(MPa)$^{1/2}$					(cm^3/mol)		
		δ_d	δ_p	δ_h	δ_t	$\Delta\delta$	$V_{cal.}$	$V_{exp.}$	% $Error$
PVC		15.4	11.3	6.9	20.3	--	44.6	45.2	1.3
Common Phthalates	DBP	16.1	10.0	6.9	20.2	1.4	252.3	266.0	5.4
	BBP	15.9	10.8	7.8	20.7	1.0	274.2	284.0	3.6
	DOP	16.6	8.2	4.8	19.1	3.9	376.7	396.1	5.1
	DNOP	16.7	8.2	5.5	19.5	3.6	376.7	399.3	6.0
	DOTP	16.7	8.2	5.1	19.3	3.8	376.7	396.1	5.1
	DINP	16.7	7.9	4.6	19.0	4.3	407.8	430.2	5.5
	DIDP	16.8	7.6	4.4	19.0	4.6	438.9	462.4	5.3
Epoxidized esters	MDES	17.7	7.0	6.7	20.2	4.8	304.5	342.2	11.0
	EDES	17.7	6.9	6.5	20.1	5.0	320.1	--	--
	PDES	17.7	6.7	6.3	20.0	5.1	335.6	--	--
	IPDES	17.6	6.7	6.0	19.8	5.2	335.7	--	--
	BDES	17.7	6.6	6.2	19.9	5.3	351.2	393.8	11%
	IBDES	17.7	6.6	5.8	19.7	5.3	351.2	393.8	11%
	IADES	17.7	6.4	5.7	19.6	5.5	366.8	409.6	10%
	ODES	17.7	6.0	5.3	19.5	5.9	413.4	459.6	10%
Epoxidized diesters	EEGDL	17.8	7.1	7.2	20.5	4.8	597.1	--	--
	EPGDL	17.8	7.0	6.9	20.3	4.8	612.6	--	--
	EPRDL	17.8	7.0	7.1	20.4	4.9	612.6	--	--
	EBGDL	17.8	6.9	7.0	20.3	4.9	628.2	--	--
Epoxidized triester	ESBO	17.8	7.13	7.22	20.5	4.8	889.6	978.3	9%

According to these values, the volume error is around 11%, which is very close to the accuracy reported for the Hoy's method (~10%) [67]. As observed, the solubility parameter decreases as the molar mass of the plasticizer increases, indicating less polarity. In terms of the interaction forces δ_d varies slightly increasing the alkyl chain, while δ_p and δ_h showed notable differences. Figure 2-4 graphically presents a solubility space of coordinates δ_d, δ_p, δ_h, and a sphere of solubility assuming a radio of 5 $(MPa)^{1/2}$ [67]. The evaluated phthalates exhibited similar solubility parameters to PVC, especially DBP and BBP. On the other hand, some epoxidized esters, diesters, and ESBO are very close to the solubility limit. The smallest molecules in the group of epoxidized monoesters such as epoxidized esters of methanol and ethanol exhibited solubility parameters closer to PVC. As expected, the size of the molecule and the number of polar groups have a significant effect on the solubility. This tendency is also correlated with the content of oxirane.

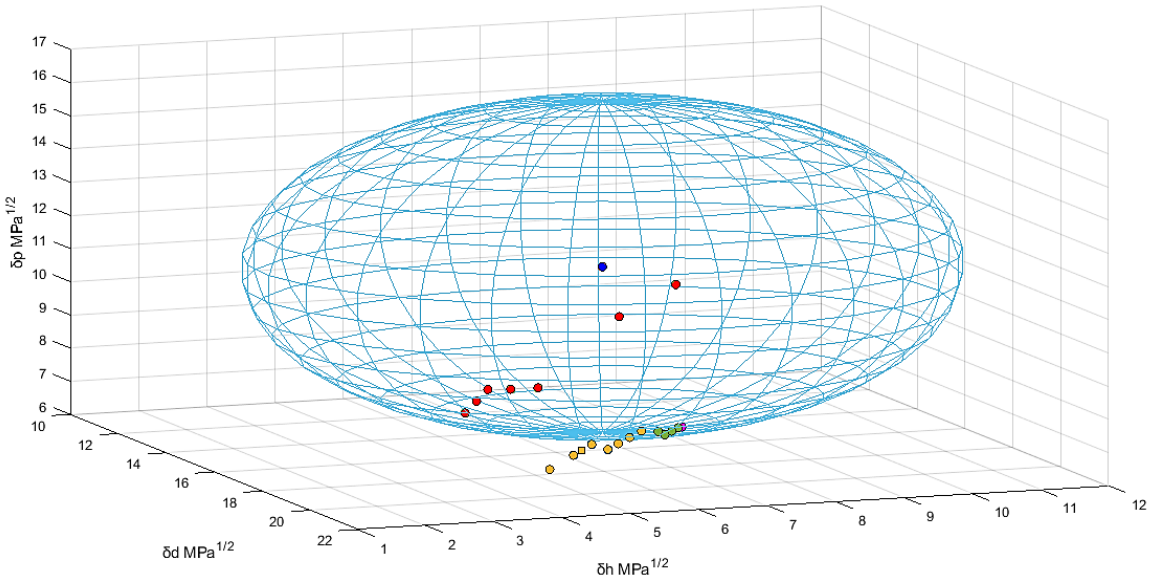

Figure 2-3. Results of solubility parameter with Hoys group contribution method. PVC (●), common phthalates (●), epoxidized esters (●) epoxidized diesters (●), and ESBO (●)

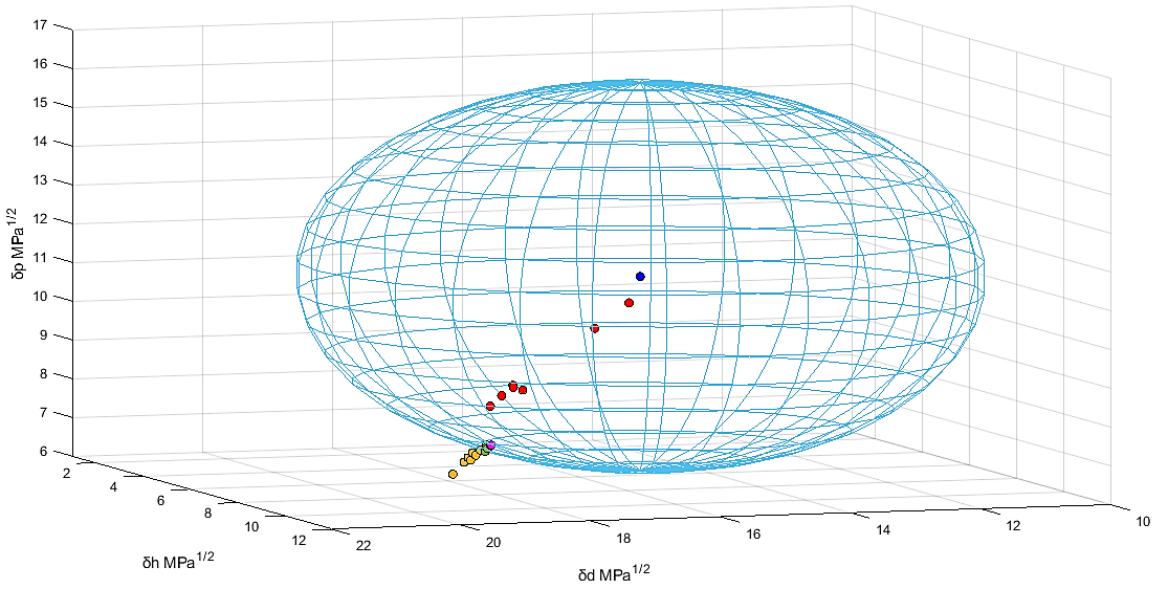

Figure 2-4. Results of solubility parameter with Hoys group contribution method. PVC (●), common phthalates (●), epoxidized esters (●) epoxidized diesters (●), and ESBO (●)

The theoretical oxirane content was estimated using Equation (1-6) and the iodine value was calculated for each molecule considering the increase in the molecular weight. Oxirane oxygen decreases by increasing the alkyl chain length of the alcohol. This tendency is presented in Table 2-9. The polar nature of the epoxidized esters improves the compatibility, due to the incorporation of epoxide and carboxylic groups. This is evident by comparing the solubility of some of these molecules in PVC. In this sense, previous studies have found that epoxidized methyl oleate exhibited the highest solubility (73 g/100g PVC at 80°C) compared to the values reached by epoxidized esters of (1-propyl oleate, 2-propyl oleate, 1-butyl oleate, and isobutyl oleate). Likewise, the same study compared the solubility of epoxidized methyl oleate and epoxidized methyl linoleate (244 g/100g PVC). In this case, the solubility of epoxidized methyl linoleate is higher due to a higher oxirane content [131],[132].

Table 2-9. Theoretical oxirane oxygen of epoxidized esters

Plasticizer	Iodine value (mg I_2/100g)	(%) Oxirane Oxygen
MDES	130.47	7.6
EDES	124.54	7.3
PDES	119.13	7.0
IPDES	119.13	7.0

BDES	114.16	6.7
IBDES	114.16	6.7
IADES	109.60	6.5
ODES	97.86	5.8
EEGDL	134.57	7.8
EPGDL	131.35	7.6
EPRDL	131.35	7.6
EBGDL	128.28	7.5
ESBO	137.99	7.9

*****Theoretical oxirane oxygen of epoxidized esters was calculated by assuming the lipidic profile of the soybean oil as follows:C16: 11.5%, C18:0: 3.6%, C18:1: 24.1, C18:2:54.8% C18:3: 5.9%.

The results of the objective function for the group of assessed epoxidized plasticizers of mono-esters, di-esters, and tri-ester are summarized in Table 2-10. In addition, the results obtained for phthalates are displayed for comparison purposes. The complete set of results of the selection criteria is summarized in Annex B. The lowest value for the objective function represents the best performance as a plasticizer.

Table 2-10. Calculated objective function used to screen among potential PVC plasticizers from different epoxidized fatty esters.

Material	Plasticizer	δ_R	Φ_R	Co_R	Tg_R	$D'p_R$	$Log\ Kow_R$	C_R	Total
Common Phthalates	DOP	0.00	0.00	0.00	0.00	0.33	0.57	0.00	0.146
	DNOP	0.07	0.00	0.04	0.00	0.33	0.58	0.13	0.182
	DOTP	0.02	0.00	0.01	0.04	0.33	0.57	0.16	0.191
	DINP	0.10	0.21	0.15	0.00	0.25	0.63	0.01	0.185
	DIDP	0.19	0.43	0.31	0.00	0.20	0.70	0.14	0.250
	DBP	0.64	0.64	0.64	0.01	1.00	0.31	0.05	0.302
	BBP	0.74	0.75	0.74	0.25	0.70	0.33	0.62	0.481
Epoxidized esters	MDES	0.23	0.51	0.37	0.36	0.61	0.35	0.13	0.338
	EDES	0.28	0.46	0.37	0.34	0.53	0.38	0.12	0.329
	PDES	0.32	0.39	0.36	0.33	0.46	0.42	0.16	0.332
	IPDES	0.32	0.39	0.36	0.33	0.46	0.41	0.16	0.332
	BDES	0.36	0.33	0.35	0.32	0.40	0.45	0.14	0.323
	IBDES	***0.37***	***0.33***	***0.35***	***0.32***	***0.40***	***0.44***	***0.12***	***0.319***
	IADES	0.41	0.27	0.34	0.31	0.35	0.48	0.25	0.340
	ODES	0.52	0.05	0.29	0.28	0.24	0.58	0.26	0.331
Epoxidized diesters	EEGDL	0.23	0.03	0.13	0.53	0.04	0.68	0.16	0.357
	EPGDL	0.24	0.03	0.14	0.52	0.03	0.71	0.25	0.378
	EPRDL	0.25	0.03	0.14	0.52	0.03	0.71	0.25	0.379
	EBGDL	0.27	0.09	0.18	0.51	0.03	0.74	0.25	0.391

Epoxidized triester	ESBO	0.23	0.46	0.34	0.59	0.00	1.00	0.62	0.569

According to the results obtained, epoxidized mono-, di- and tri-esters (i.e. ESBO) of fatty acids have good compatibility with PVC due to their polarity and solubility. Also, these molecules exhibit low diffusion coefficients (ranging from $1{\cdot}10^{-9}$ to $1{\cdot}10^{-10}$ cm/s at 20°C) resulting in lower migration rates. Nonetheless, monoesters exhibited lower glass transition temperatures to enhance plasticization. Comparatively, epoxidized diesters and ESBO obtained higher values for the octanol-water partition coefficient indicating a higher tendency for bioconcentration. Finally, the estimated cost of the assessed molecules increased with their molecular weight considering that superior alcohols are usually more expensive.

Considering all these aspects, the selection was narrowed to the epoxidized mono-esters of linoleic acid, as they presented a better performance than diesters or tri-esters (ESBO). The performance of the epoxidized mono-esters for each assessed criterion of the objective function is presented in Figure 2-5. In this figure, PDES and BDES were omitted since they exhibited similar results as those of the branched molecule (see Table 2-10).

Regarding the efficiency criterion, the epoxidized mono-esters did not achieve the same glass transition temperature as that obtained by common phthalates. Additionally, only a slight difference in the glass transition temperature was found for branched and linear structures of the same molecular weight, being slightly lower for linear structures. In this regard, Tg results are only satisfactory as a rough screening test. In terms of permanence, the diffusion coefficient of the additives in the polymer decreases, while the size of the alcohol increases. In the case of epoxidized monoesters, the calculated diffusion coefficients were like those of phthalates. Linear and branched molecules obtained the same values using the migration approach, as in the case of Tg.

The results of the toxicity criterion showed that higher Kow values were obtained as the length of the alkyl chain increased. This trend was also obtained in the solubility parameter δ_t. Notably, epoxidized esters of mono alcohols obtained lower Kow values than the reference phthalates. Finally, regarding cost estimation, large molecules as the epoxidized esters of 2-octyl (ODES) and isoamyl alcohol (IADES) were the most expensive and therefore the least competitive against traditional phthalates in the group of epoxidized monoesters.

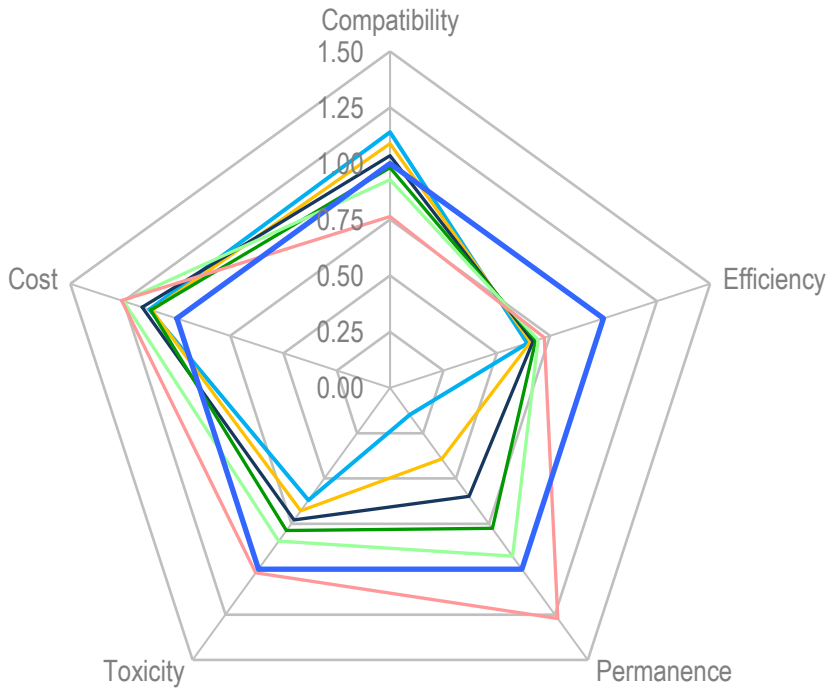

Figure 2-5. Results epoxidized mono esters.
(—) MDES - Methyl diepoxystearate, (—) EDES-Ethyl diepoxystearate, (—)IPDES-Isopropyl diepoxystearate, (—)IBDES-Isobutyl Diepoxystearate, (—) IADES-Isoamyl diepoxystearate, (—) DOP-Dioctyl phthalate, (—) ODES:-2-Octyl diepoxystearate

From an overall perspective, the lowest value for the objective function was reached for Isobutyl diepoxystearate (IBDES). Nonetheless, it is important to point out that the predictive methods showed only slight differences between linear and branched molecules of the same number of carbons. This is evident comparing the results for the epoxidized esters of propanol (IDES) and isopropanol (IPES), or butanol (BPES) and isobutanol (IBPES). However, it is well documented that introducing a branched molecule into the polymer-plasticizer structure promotes the permanence of the plasticizer within the solid matrix [133].

As a result of the screening methodology, Isobutanol epoxidized ester (IBDES) was identified as the most promising molecule for a plasticizer application. Thus, soybean fatty acids from isobutanol are expected to have similar properties to those estimated with the

predictive methods. The following sections will address the synthesis of the selected molecules, and their assessment as plasticizers for PVC products.

Finally, it is expected that the here developed methodology could be used not only in the design of plasticizers but also in other industrial applications to guide the design of new additives (bio- or fossil-based compounds).

3. Biobased plasticizer production process

After selecting a potentially suitable plasticizing molecule based on the different performance criteria, the next stage of this work was to design a production process that considers the effect of the main variables during the reaction and separation stages. Although the target molecule is an epoxide of isobutyl soyate, the experimental work was performed using three additional feedstocks: oleic acid, linoleic acid, and a distillation fraction obtained from the SODD. Evaluating feedstocks with similar fatty acid composition provides a better understanding of the reaction and separation stages. The different raw materials used in the experimental work are presented in Table 3-1.

Table 3-1. Fatty acid - raw materials used in the experimental design.

Feedstock	Chemical nature
A) Oleic acid (OA)	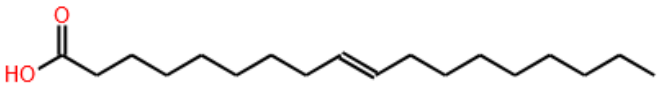
B) Linoleic acid (LA)	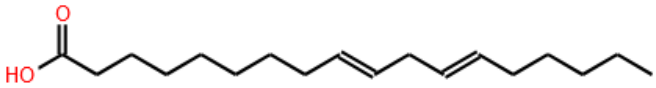
C) Soybean oil deodorizer distillate (SODD)	Mixture of saturated and unsaturated fatty acids (C16-C18) and acylglycerols.

This chapter outlines the production of isobutyl epoxides from soybean oil and its derivates (i.e., linoleic acid, oleic acid, and SODD). The choice of these raw materials was based on the fact that linoleic acid (C18:2) is the main fatty acid in the lipid profile of SODD, while oleic acid has an iodine value similar to that of SODD, which is the valuable agro-industrial residue of interest.

The proposed process involves two reaction steps (i.e. esterification and epoxidation), and different reaction conditions were explored to select the best processing conditions. Besides the production of epoxidized esters, this chapter also delves into the kinetics of epoxidation of isobutyl linoleate catalyzed by a homogeneous acid, and a regressed mathematical expression of the process was obtained. As the processing of each raw material is different, a simplified scheme is presented in Figure 3-1. There are minor differences in the processing of the various raw materials due to their composition, but the unit operations remain largely the same.

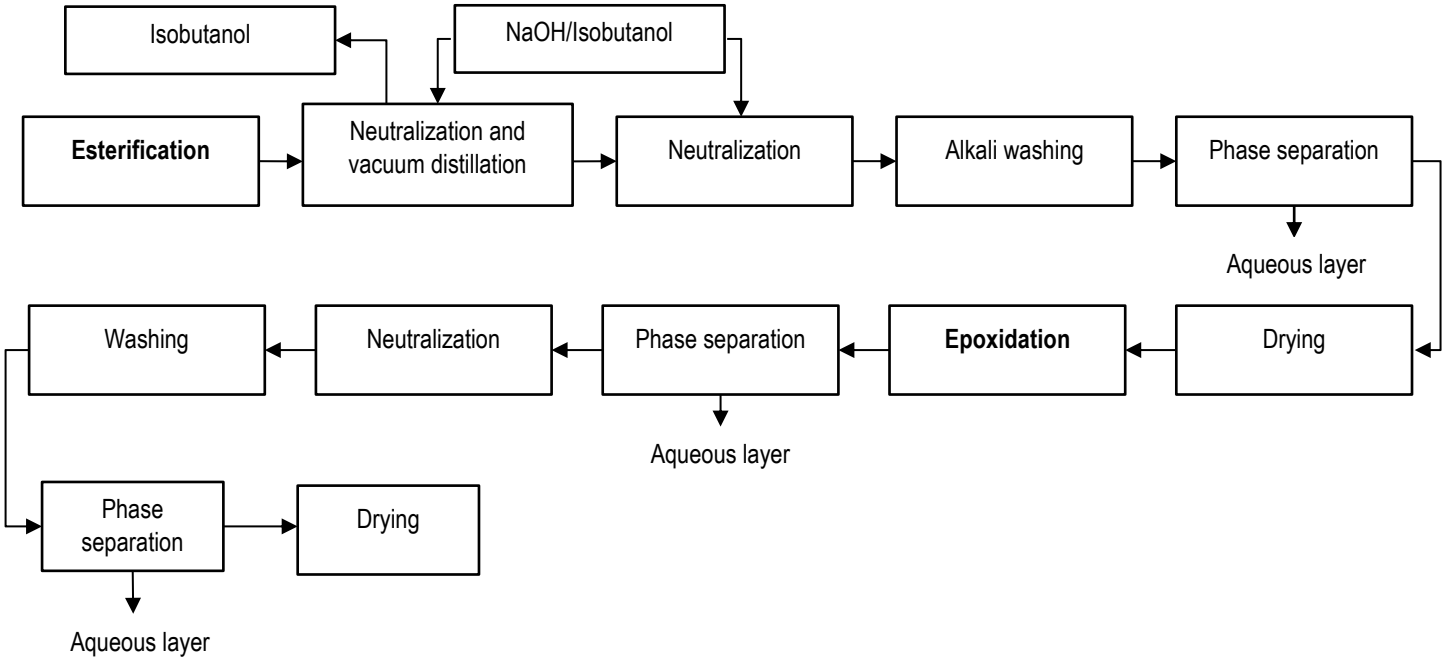

Figure 3-1. Simplified block diagram of the epoxidized isobutyl esters production process

3.1 Methodology

- **Reagents**

Food-grade linoleic acid (≥ 95% wt., Sigma Aldrich), technical-grade oleic acid (>50% wt. Quimiescencias), and soybean oil deodorizer distillate provided by Team Foods were used as the fatty acid reactant during esterification reactions, along with isobutanol (> 99% GC, Merck). Sulfuric acid (96% wt., Merk) was used as a catalyst. Glacial acetic acid (100% wt., J.T Baker), amberlite IRC 120 H (Merck), and aqueous hydrogen peroxide (50% wt., Chemi) were used during epoxidations. Absolute ethanol USP (PanReac), NaOH (99% wt.,

Supelco), and Toluene (99.98% wt., J.T. Baker), chloroform (HPLC grade, J.T. Baker), Wijs reagent (0.2N, PanReac), diethyl ether (99% wt., Loba Chemie PVT LTD), acetone (USP, Panreac), sodium thiosulphate pentahydrate (Supelco), hydrochloric acid (0.5M Panreac), and 2-Propanol USP (PanReac) were used during acid value, iodine index, saponification value, unsaponifiable matter, peroxide value and oxirane oxygen determination.

- **Methods**

The fatty acids (OA, LA, SODD) were characterized through acid value, iodine value, and saponification value following the official method ISO 660, ISO 3961, and ISO 3657 respectively [134],[135],[136]. The peroxide value of the SODD was measured following the official method ISO 3960 [137], while the unsaponifiable matter was measured according to ISO 3596 [138]. Each analysis was performed in triplicate. Fatty acid profiles were obtained for all raw materials by gas chromatography using a reported standard method for FAMEs quantification (AOCS Ce 1-e91). FAMEs were prepared from the corresponding fatty acid samples following AOCS Ce 2-66 standard method. A 7890A Agilent GC with a flame ionization detection (GC-FID) was employed using hydrogen as carrier gas.

The acid number and moisture content were analyzed using a Karl Fisher volumetric titrator (Mettler Toledo). Each analysis was performed in duplicate.

Differential Scanning Calorimetry analysis (DSC) was performed using a Mettler Toledo calorimeter 500/2722. Thermal properties of the samples, including crystallization (T_c) and melting temperatures (T_m), were evaluated by performing the following thermal cycle at a constant rate of 5 K/min: heating from 25 to 60 °C, isotherm holding for 10 min, cooling from 60 to -60°C, isotherm holding for 10 min, and heating from -60 to 60°C under a constant flow rate of N_2 of 50 ml/min.

Thermogravimetric analysis (TGA) was performed on a TGA SF/1100/268. Samples were heated from 30 to 700°C at a constant heating rate of 10°K/min. Nitrogen was used as purge gas at a flow of 60ml/min and the balance purge flow of air.

Rheological properties were measured at 20 and 40°C. Density was measured in a Densito 30PX Mettler Toledo equipment and viscosity was measured using a viscosimeter Koehler instrument equipped with a capillary viscosimeter and thermocouple.

The cloud point of the fatty acids was measured according to the standard ASTM D2500 [139]. Samples of 25 ml were cooled in a flask in a thermostatic bath set at -24°C.

FTIR spectra were carried out in an FT-IR Perkin Elmer Spectrum BX. The spectra were scanned in the range of 800 to 200 cm^{-1} at a scan rate of 600 nm/min.

3.2 Esterification

3.2.1 Results

- **Characterization of Fatty acids**

The fatty acid profiles of the oleic acid (OA), linoleic acid (LA), and SODD used in this work are reported in Table 3-2. As expected, unsaturated acids, mainly oleic and linoleic, are the major components of these raw materials. The total percentages of unsaturated acids were 93.7, 99.8 and 81.3 % respectively. Considering the total number of unsaturated acids, the concentration of oxirane oxygen (OO) in the final epoxidized fatty esters is expected to follow the order LA > OA > SODD. The lipid profile of SODD was found to be consistent with that of soybean oil [140], and this is also presented in Table 3-2. For comparison purposes, a picture of the as-received fatty acid feedstocks is presented in Figure 3-2, The SODD was dark and semi-solid while the OA was a clear liquid.

Table 3-2. Fatty acid composition

Fatty acid	**OA**	**LA**	**SODD**	**Soybean oil** [140]
C16:0	3.47	0.20	13.79	8-14
C18:0	2.80	0.05	4.91	3-5
C18:1	55.06	2.35	30.00	20-25
C18:2	34.15	97.21	47.61	50-57
C18:3	0.37	0.19	3.70	6-8
C20:2	2.89	-	-	-
C20:3	1.26	-	-	-
SFA (%)	6.27	0.25	18.70	11-19
MUFA (%)	55.06	2.35	30.00	20-25
PUFA (%)	38.67	97.40	51.31	56-65

SFAA: saturated fatty acids,
MUFA: monounsaturated fatty acids,
PUFA: polyunsaturated fatty acids

a) b) c)

Figure 3-2. Pictures of the employed fatty acids during esterification experiments
a) Oleic acid b) Linoleic acid c) SODD

The main physicochemical characteristics of the fatty acids used as reactants in this study are presented in Table 3-2. As can be seen, all these raw materials have a high iodine value (> 114 mg KOH/g) which is consistent with their high content of unsaturations. These high values of unsaturations are suitable for the epoxidation processes.

Table 3-3. Physicochemical properties of fatty acid feedstocks

Property	**OA**		**LA**		**SODD**	
Acid value (mg KOH/g)	194.0	± 0.8	193.7	± 0.3	89.2	± 0.1
FFA (oleic) (%)	97.7	± 0.4	97.5	± 0.2	44.9	± 0.1
Iodine value (g I_2/100g)	120	± 0.6	176	± 0.2	114.5	± 0.07
Saponification value (mg KOH/g)	--		--		162	± 1
Peroxide value (meg/kg)	--		--		6.2	
Unsaponifiable matter (%)	--		--		16	
Neutral oil (% wt.)	--		--		39	
Moisture (%wt.)	0.1	± 0.004	0.21	±0.01	--	
Density (20ºC) (kg/m^3)	901.4	± 0.1	913.0	± 0.1	911.8	± 0.8
Density (40º) (kg/m^3)	883.2	± 0.1	893.0	± 0.1	893.8	± 0.1
Kinematic Viscosity cSt (40ºC)	18.8	± 0.1	21.3	± 0.1	26	± 0.24
Dynamic Viscosity cP (40ºC)	16.6	± 0.1	19.1	± 0.1	23.2	± 0.2
Calculated						
MW (g/gmol)	282.0		280.5		277.9*	
Iodine value Theoretical (g I_2/100g)	120.2		178.6		123.1	
Average instaurations	1.3		2.0		1.3	

* Acylglycerols: 100-FFA-Unsaponifiable matter
* Average molar mass of FFA calculated based on the lipid profile

Regarding the SODD, its FFA content was around 45% wt., in addition to these FFAs, this feedstock also contains a significant amount of other components, such as monoglycerides (MG), diglycerides (DG), and triglycerides (TG). The presence of these acylglycerols is confirmed by its high saponification value (162 mg KOH/g), indicating that the SODD contains various saponifiable species. Based on the saponification value of SODD, and assuming only acylglycerides of linoleic acid, it is possible to estimate their total content in the sample, as is shown in equation (3-1).

$$SV_{SODD} = x_{FFA} * SV_{FFA} + x_{TG} * SV_{TG} + x_{DG} * SV_{DG} + x_{MG} * SV_{MG} + x_{UM} * SV_{UM} \quad (3\text{-}1)$$

$$162 = x_{FFA} * 201.9 + x_{TG} * 193.1 + x_{DG} * 183.4 + x_{MG} * 159.5 + 0.16 * SV_{UM}$$

$$x_{FFA} + x_{TG} + x_{DG} + x_{MG} + x_{UM} = 1$$

$$x_{TG} + x_{DG} + x_{MG} = 0.39$$

Here, x_{MG}, x_{DG}, x_{TG}, x_{UM} are the mass fraction of monoglycerides (MG), diglycerides (DG), triglycerides (TG), and unsaponifiable matter (UM) respectively. SV_{MG}, SV_{DG}, SVx_{TG}, are the saponification value of monoglycerides (MG), diglycerides (DG), and triglycerides (TG), respectively. As observed, the total content of acylglycerides remaining in SODD is around 39% wt.

Regarding the content of unsaponifiable matter (16%), it agrees with the reported values (11-33%) [16]. This high value is derived from the content of typical secondary metabolites encountered in soybean oil such as tocopherols, lecithin, sterols, and squalene. The peroxide value (6.2 meq O_2/kg) was measured to estimate the oxidative stability of the SODD. This result indicates a low content of oxidative components such as ketones and aldehydes.

The results from the physicochemical and rheological characterization of samples are also presented in Table 3-3. Among the assessed properties, viscosity is an important parameter for a plasticizer application. According to these values, the viscosity of FFA decreases in the order: SODD>LA>OA. It is expected that the epoxides of the respective FFA would follow the same trend.

- **Thermal characterization of the fatty acids**

To study the thermal properties of the feedstocks (OA, LA, and SODD), the samples were analyzed using two thermal cycles, one cycle of cooling (crystallization cycle) and one of heating (melting cycle) through controlled thermal conditions. The results are displayed in Figure 3-3, Figure 3-4, and Figure 3-5, and are summarized in Table C-1, Table C-2, and Table C-3 in Annex C – Thermal properties.

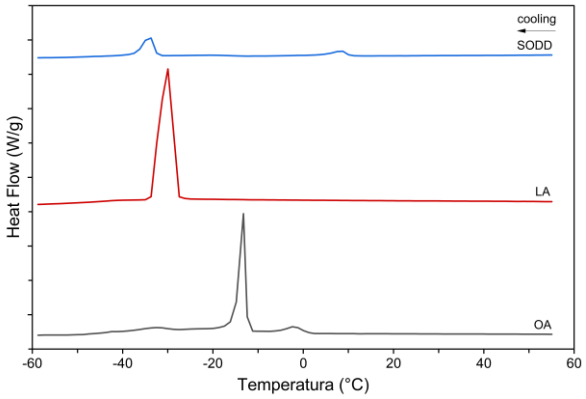

Figure 3-3. Crystallization DSC curves of FFA

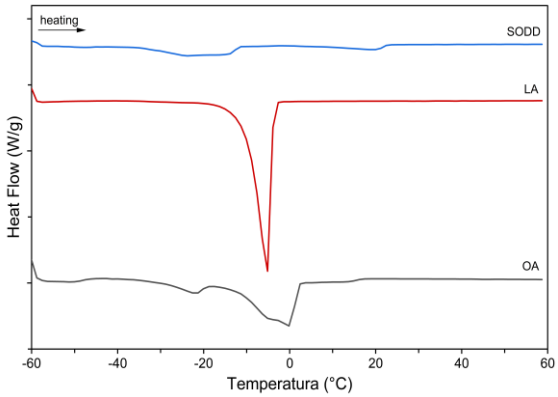

Figure 3-4. Melting DSC curves of FFA

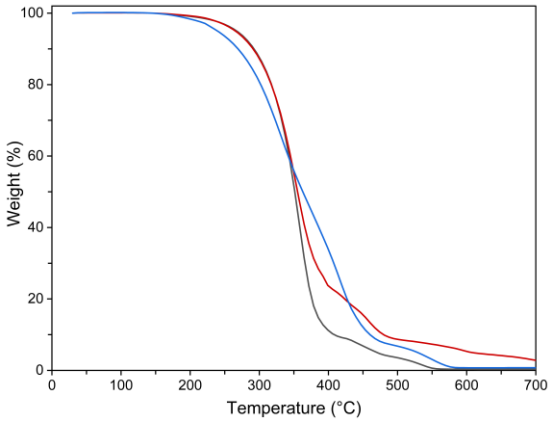

Figure 3-5. Thermal degradation of FFA.

(— OA) (—LA) (—SODD)

Melting and crystallization curves for oleic acid show two characteristic peaks, as reported in the literature [141]. In the cooling cycle (exothermic phase transition), OA exhibits two peaks at -1.7°C and -13.1°C which are associated to the crystallization of the meta-stable

α-form and the γ polymeric transformation [142]. For the melting cycle (endothermic phase transition), the major peak is found at 0°C. This point differs from the melting temperature of OA which ranges from 13.2°C to 16.3°C [130]. This significant difference was expected as a commercial brand of Oleic acid with a technical grade purity of ~50% wt. was employed in this study. The crystallization temperature (Tc) and cloud point of LA were -30°C and -22°C, respectively. According to these curves, low freezing temperatures were achieved due to a high content of unsaturated fatty acids. These low freezing temperature values indicate good low-temperature performance, which is valuable for lubricant or plasticizing applications. The measured melting temperature of LA was -5.6°C, which is very close to the reported value -5 °C [130].

Finally, the SODD presented two characteristic peaks in crystallization and melting cycles. These peaks are less sharp compared to those of the other fatty acids under study, which can be attributable to their higher content of acylglycerides. The SODD exhibited two crystallization events at 8.38°C and -34°C, and two melting peaks at -23.7°C and 19.7°C, respectively. Such behavior is consistent with the high content of oleic and linoleic acid. Also, the thermal behavior of SODD is highly dependent of other compounds present in the mixture such as acylglycerides, tocopherols, squalene, phytosterols, and soaps.

In terms of thermal degradation, pure fatty acids such as oleic and linoleic acid, exhibited a single degradation stage near 346°C. In contrast, SODD has two degradation peaks at 331.3 and 415.7°C. This is consistent with the high content of unsaturated fatty acids and other high molecular weight components in the feedstock.

- **Procedure**

Esters of isobutanol, namely isobutyl oleate (IBO), isobutyl linoleate (IBL), and isobutyl soyate (ISO), were obtained via Fisher esterification of fatty acids and isobutanol using sulfuric acid as a catalyst in an inert nitrogen atmosphere. The esterification reaction was carried out in a 150 ml glass four-necked jacketed reactor equipped with a thermometer, a magnetic agitator, and a continuous heating fluid flow from a thermostatic bath (MV-4, Julabo). The system also featured a vigreux column, a condenser, and a cylindrical separatory funnel to recover condensates. The experimental setup for the esterification reaction is illustrated in Figure 3-6.

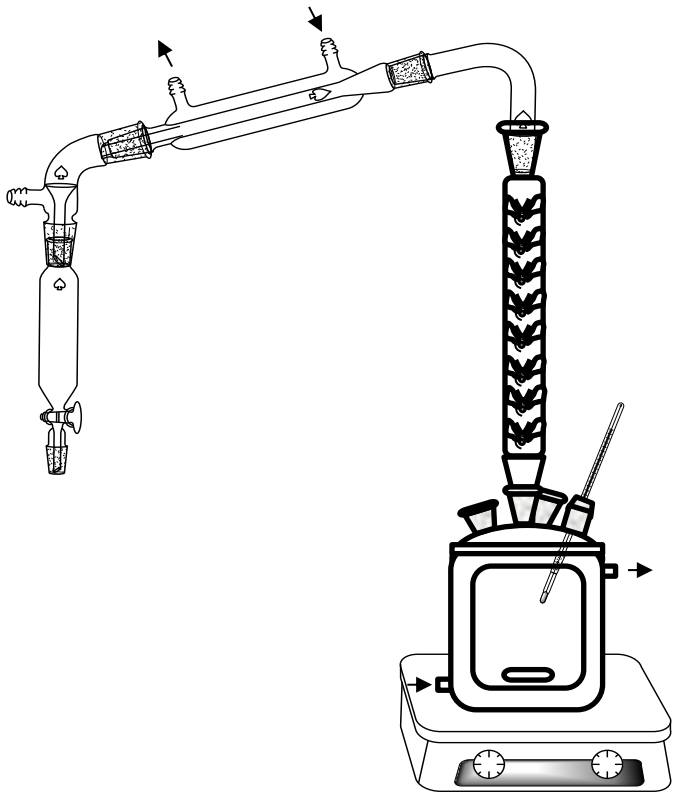

Figure 3-6. Experimental setup during esterification experiments

All esterification experiments were performed under a stirring rate of 650 rpm and 94°C of temperature at the local pressure of 74.6 kPa. Two different reaction conditions were used: 3:1 molar ratio of isobutanol to a fatty acid, 1% wt. sulfuric acid as catalyst, and 5:1, 2% wt. catalyst. Fatty acids were heated up until the reaction temperature was reached. Then a mixture of catalyst and isobutanol was dosed to the reactor. After 20 minutes, some water and isobutanol were evaporated, condensed, and recovered in the side cylindrical collector. The top vapor temperature reached a maximum of 80 °C before the temperature profile dropped. As expected due to the large excess of isobutanol, and the liquid-liquid equilibrium of the system presented in Figure 3-1 [143], the condensed vapor underwent a liquid-liquid splitting. According to the phase equilibria, at the temperature of the condensate (~293K) the heavy phase was mainly composed of water (~ 92% wt.), and the light phase was mainly composed of isobutanol (~ 84% wt. isobutanol).

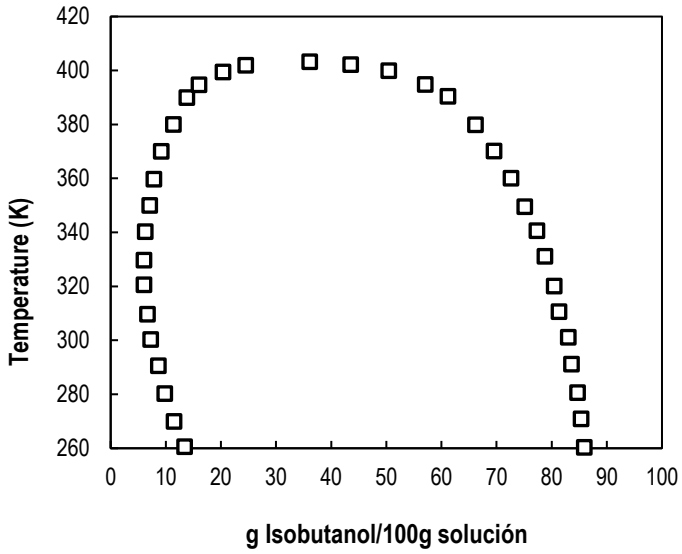

Figure 3-7. Liquid – Liquid Equilibrium for the mixture isobutanol-water
Adapted from [134]

Samples of 1g were extracted at different time intervals during the reaction, and the progress of esterification was monitored by measuring the acid value. After 6 hours, the reaction mixture containing the ester, the acid catalyst, and the residual alcohol was neutralized using 80% of the required stoichiometric amount of a saturated NaOH solution in isobutanol, followed by vacuum distillation. The mixture was then neutralized again until the acid value was lower than 0.06 mg KOH/g. Then the solution was washed with water until pH 7 and dried under vacuum. The neutralization of the remaining fatty acids in the reaction medium was slow due to the low solubility of NaOH in isobutanol. However, alcoholic neutralization in the absence of water reduced soap formation and facilitated separation processes.

- **Esterification kinetics**

The conversion of the esterification reaction was monitored by measuring the acid value along the reaction time. The conversion is expressed as follows:

$$X = \frac{W_{FFA}(t)}{W_{FFA}(t_o)} * 100 \qquad (3\text{-}2)$$

In Equation (3-2), $N_{FFA}(t)$ is the mass of fatty acid at time (t) and $W_{FFA}(t_o)$ is the initial mass of fatty acid. Using the definition of acid value, this equation can be written as:

$$X = \frac{VA_t\ (t) * w_t - VA_{H_sSO_4} * w_{H_sSO_4}}{VA_r(t_0) * w_r} \quad (3\text{-}3)$$

In Equation (3-3), $VA_r(\mathrm{t}_0)$ and w_r are the initial acid value of the fatty acid in the reactor and the initial mass of the FFA. $VA_{H_2SO_4,r}$ is the acid value of sulfuric acid and $w_{H_sSO_4}$ is its weight in the reactor mixture. $VA_r(\mathrm{t})$ is the acid value in the reactor along the time and w_t is the corresponding mass of the reactor mixture at sampling time t. Assuming that the total mass of fatty acids in the reactor was constant (negligible change by evaporation or by samples withdrawal) and that the total acid content in the condensate was negligible (< 0.54 mg KOH/g), Equation(3-3) can be rewritten as:

$$X = \frac{VA_r(\mathrm{t}) - VA_{H_sSO_4,r}}{VA_r(\mathrm{t}_0)} \quad (3\text{-}4)$$

By using this Equation, conversion along reaction was monitored for 3 hours. However, from initial calculations of acid values, it was possible to verify that a secondary reaction was occurring. At high conversions, the acid equivalents of the sulfuric acid catalyst in the reactive media resulted lower that the initially loaded ones. According to previous reports [144],[145], the inorganic acid catalysts can sulfate the alcohol to produce an alkyl sulfuric acid ($ROSO_3H$). The sulfation reaction between isobutyl alcohol and sulfuric acid is depicted in Equation (3-5).

$$ROH + H_2SO_4 \rightarrow ROSO_3H + H_2O \quad (3\text{-}5)$$

In the reported studies, it was found that monovalent isobutyl sulfuric acid was produced irreversibly during the esterification process, and its formation could reduce the acid value of the catalysts to half of the initial acidity at all tested temperatures (57 to 87°C) and alcohol to acid molar ratios (i.e. 10^2 of to 10^3). Figure 3-10 illustrates the observed conversions during the reaction, as reported in the aforementioned studies [145].

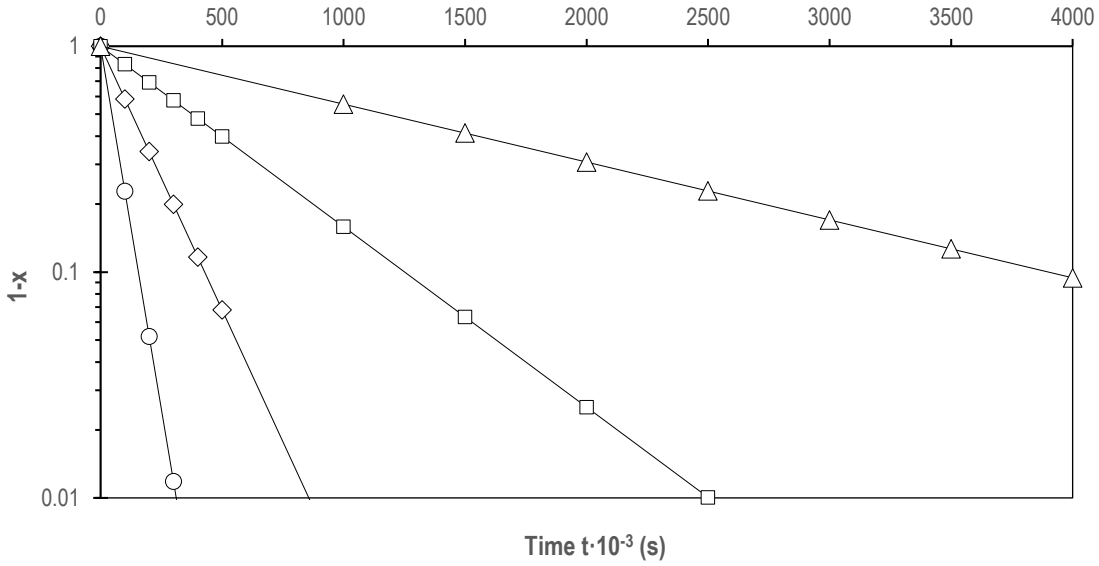

(-○-) 360K. (-◊-) 350K. (-□-) 340K. (-Δ-) 330K reported by [145]
Figure 3-8. Sulfuric acid concentration with reaction time.

To evaluate the variation of the inorganic acidity due to the side reaction, isobutanol, and sulfuric acid were reacted in the absence of fatty acids. The two experiments were run at 1.3 and 1.5% wt. sulfuric acid in isobutanol with a molar ratio sulfuric acid: isobutanol of 104 and 87 respectively. The mixture was heated to 94°C at 650 rpm under reflux in a flask equipped with a condenser, a thermometer, and a magnetic stirrer. Aliquots of 1 g were withdrawn at different time intervals and the acid value was measured. In this case, the acid value was equivalent to the sum of the acidity of sulfuric acid and monovalent isobutyl sulfuric acid [145]. The conversion of the side reaction using a 1.3% wt. sulfuric acid in the alcohol is presented in Figure 3-8, and the results from both experiments are summarized in Table 3-4. As observed, the side reaction is almost complete within the first five minutes. Similar results were obtained for the case of a 2% wt. sulfuric acid loading. As a result, the acid value of the catalyst decreased by 41 and 45% respectively for each reaction condition.

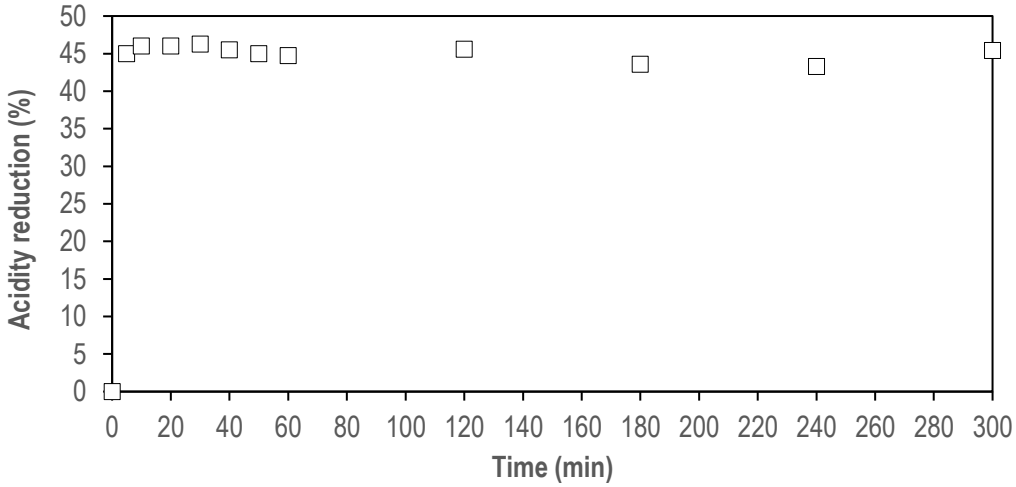

Figure 3-8. Reduction of acidity during sulfation of isobutyl alcohol under 1% wt. of sulfuric acid at 94°C

Table 3-4. Operating conditions and results during sulfation of isobutanol with sulfuric acid

Reaction conditions			Acid value reduction
% Catalyst	**°T**	**Ratio OH:FFA**	**(%)**
2%	94°C	5:1	41.1 ± 3
1%	94°C	3:1	45.2 ± 1

The obtained results were similar to those observed in previous studies. At higher temperatures (above 340K) the acid value decreased with time and achieved a constant value within an hour of reaction. Then, it was verified that the side reaction of isobutyl alcohol and sulfuric produces a significant reduction of the acid value of the catalyst. The experimental reduction of the acidity as reported in Table 3-4 and the mass balance of the system were used to correct the calculated acid value along reaction time (i.e. $VA_r(\mathrm{t})$). The conversion of the esterification was then computed according to Equation (3-4). The conversion of the esterification reaction of oleic acid, linoleic acid, and SODD over time are presented in Figure 3-9, Figure 3-10, and Figure 3-11, respectively. Table 3-5 presents the final conversion of each fatty acid.

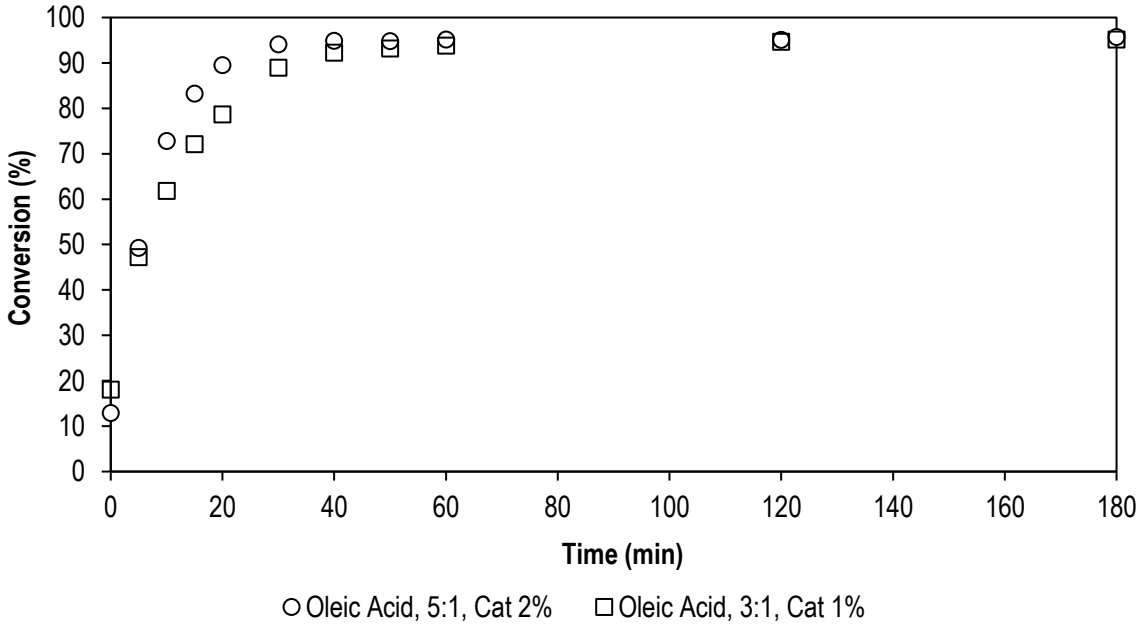

Figure 3-9. Esterification of oleic acid with isobutanol at 94°C

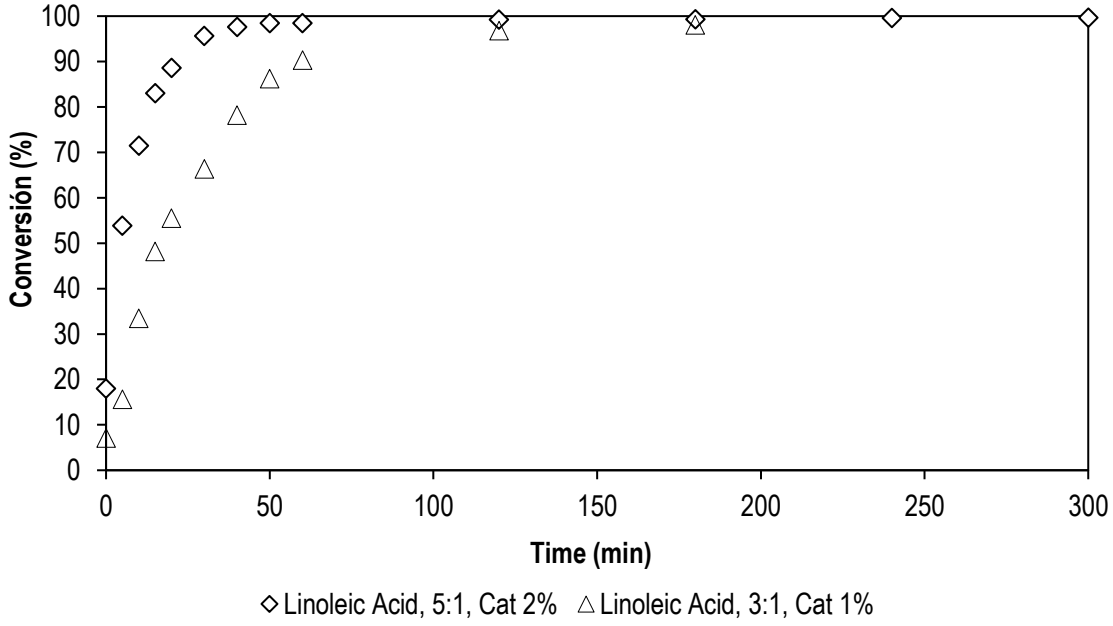

Figure 3-10. Esterification of linoleic acid with isobutanol at 94°C

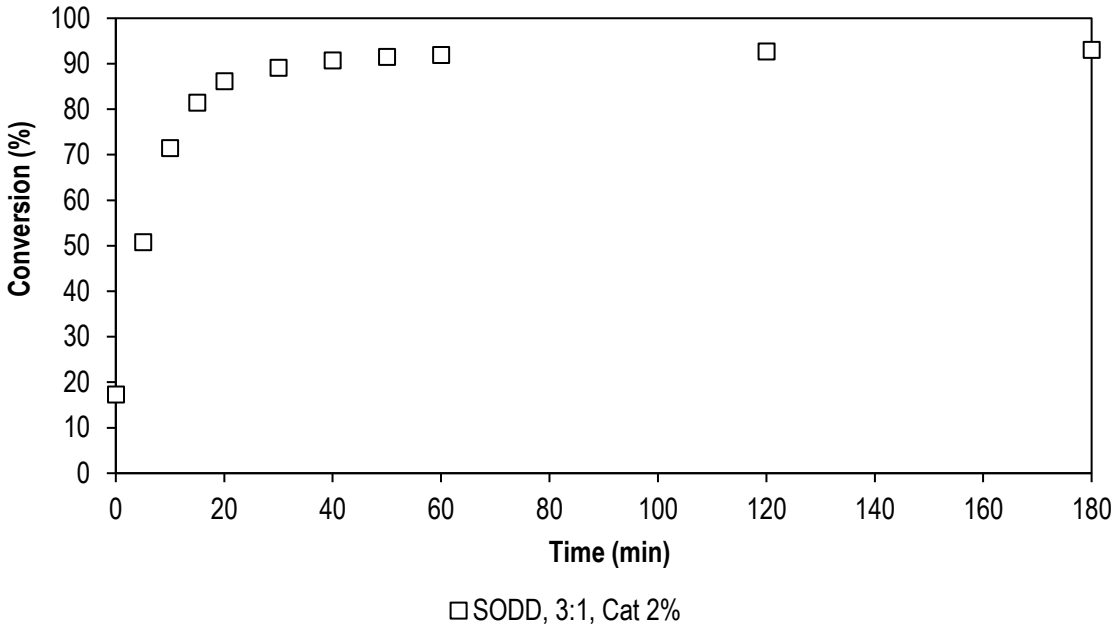

Figure 3-11. Esterification of SODD with isobutanol at 94°C

Table 3-5. Final conversion of fatty acids by esterification with isobutanol

Fatty Acid	Ratio 5:1, Cat 2%	Ratio 3:1, Cat 1%	Ratio 3:1, Cat 2%
Linoleic Acid	99.7	98.0	--
Oleic Acid	96.4	96.2	--
SODD	--	--	93.0*

* Based on the acid content

High conversions were obtained for the esterification of oleic acid and linoleic acid, ranging from 99 to 96%, by removing the water produced during the ester formation. Similar conversions were achieved in reference works [146],[147]. Regarding the SODD, a 93% conversion was achieved based on its acid content. As mentioned above, this feedstock contains glycerides and unsaponifiable material that affect the esterification kinetics and can consume the acid catalyst. To obtain a purer ester from SODD, isobutyl soyate (ISO) was distilled under vacuum to remove undesired compounds.

- **Distillation of Isobutyl soyate (ISO)**

The obtained Isobutyl soyate (ISO) was distilled in a 150 ml two-necked jacketed flask equipped with a thermometer, a magnetic agitator, and a condenser. The system was

coupled to a high vacuum pressure pump and a thermostatic bath (MV-4 Julabo) for circulation of the cooling fluid. The distillation was performed at 180°C and 0.1 mbar. The first drop of distillate was obtained at a head temperature of 118°C, and after this point, the temperature gradually raised until it reached 178°C at the end of the distillation. The complete set of temperatures observed during vacuum distillation is presented in Table 3-6. According to the observed behavior, it can be inferred that the boiling point of isobutyl soyate at 0.1 mbar is around 118°C. According to the mass balance, the target distillation fraction was 0.45 of the feed.

Table 3-6. Observed temperatures during isobutyl soyate distillation.

Boiling temperature (°C)	Head temperature (°C)
180	118
180	124
180	144
180	162
182	164
183	166
185	178

Based on the fatty acid composition of the SODD presented in Table 1-1 and Table 3-2, it is expected that the major components of the distillate product were fatty acid esters of C16 chains and fractions of C18:0, C18:1, C18:2, C18:3. On the other hand, it would be expected that major components in the bottoms were fatty acid esters of C18:0 and minor fractions of C16, C18:1, C18:2, C18:3. Distilled isobutyl soyate (ISD) was recovered and used together with the other esters, namely isobutyl oleate (IBO), isobutyl linoleate (IBL), isobutyl soyate (ISO), in subsequent epoxidation process.

- **Characterization of the esters**

The results from the physicochemical characterization of the obtained esters are summarized in Table 3-7, and the appearance of such products can be observed in Figure 3-12. All esters exhibited low acid values (< 0.5 mg KOH/g) and iodine values above 102 I_2/100g, which is desirable for the epoxidation process. According to these values, the maximum theoretical oxirane content in the epoxidized isobutyl esters of IBO, IBL ISD, and ISO would be 6.0, 8.4, 6.1, and 6.4% wt., respectively. Concerning the unsaturation content, the average instauration of isobutyl oleate and isobutyl linoleate were 1.4 and 1.9

respectively. The molecular weight of IBO and IBL was calculated based on the saponification value, but this parameter is not presented for ISD and ISO since these esters have an unknown mixture of glycerides. Finally, because of the esterification process, the density and viscosity of the isobutyl esters decreased compared to those obtained for the feedstocks.

Table 3-7. Results characterization of isobutyl esters

Parameter	IBO	IBL	ISD	ISO
Acid value (mg KOH/g)	0.41 ± 0.02	0.3 ± 0.1	0.4 ± 0.1	0.3 ± 0.1
Iodine value (g I2/100g)	101.1 ± 0.5	146.3 ± 0.7	102.9 ± 0.3	108 ± 0.2
Saponification value (mg KOH/g)	166.5 ± 0.6	165.3 ± 0.2	139.4 ± 0.1	126 ± 1
Density (20°C) (kg/m^3)	871.4	874.8	869.5	882.5
Density (40°C) (kg/m^3)	853.4	856.8	853.5	864.5
Kinematic Viscosity (40°C) (cSt)	6.43 ± 0.03	5.20 ± 0.06	5.72 ± 0.07	8.7 ± 0.2
Dynamic Viscosity (40°C) (cP)	5.49 ± 0.03	4.45 ± 0.06	4.88 ± 0.07	7.57 ± 0.2
Color	Yellow	Orange	Yellow	Brown
	Calculated			
Calculated MW (g/mol)	337.7	340.0	--	--
II theoretical (g I_2/100g)	106.3	148.7	--	--
reported MW (g/mol)	338.60	336.55	--	--
Average instaurations	1.4	1.9	--	--

a) b) c) d)

Figure 3-12. Appearance of the obtained isobutyl esters.
a) Isobutyl Oleate b) Isobutyl Linoleate c) Distilled isobutyl soyate d) isobutyl soyate

- **Thermal properties of esters**

To study the thermal properties of the esters (IBO, IBL, ISD, and ISO), the samples were analyzed using the same thermal cycles (crystallization and melting), that were employed to evaluate the thermal properties of free fatty acids. The crystallization and melting cycles of isobutyl esters are shown in Figure 3-13 and Figure 3-14, and the thermal degradation of these esters is presented in Figure 3-15.

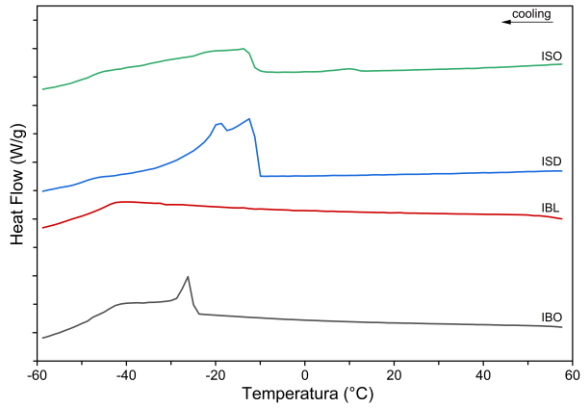

Figure 3-13. Crystallization DSC curves of isobutyl esters

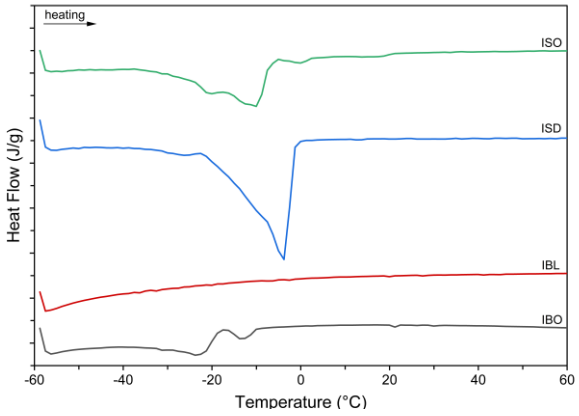

Figure 3-14. Melting DSC curves of isobutyl esters

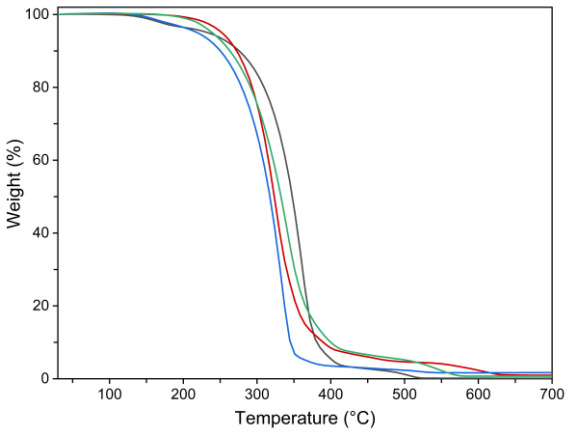

(— IBO) (—IBL) (—ISD) (— ISO)

Figure 3-15. Thermal degradation of isobutyl esters

According to the obtained calorimetric profiles, the crystallization temperatures of isobutyl esters were -26.3, -13.5, and -11.9 °C for IBO, ISO, and ISD, respectively. The melting temperatures were -22,- 9.8 and 3.9 °C for IBO, ISO, and ISD, respectively. Regarding the thermal properties of isobutyl linoleate, it is very likely that these values were outside the

range of measurement since no attenuated peaks were found in both cycles. As expected, the isobutyl esters exhibited lower crystallization and melting temperatures than those obtained for the FFA, showing a more liquid-like behavior. This is because the introduction of an ester group of a branched alcohol increases intermolecular distances and hindrance their interactions. Regarding degradation temperatures of the esters, they remained similar to those of the fatty acids. This might indicate that degradation initially occurs in the same type of moieties that are present in both molecules, namely the unsaturation of the fatty acid chain. However, the IBL presented a slight decrease of around 13°C of this parameter.

3.3 Epoxidation

According to the context developed in Chapter 1, three variables were selected for the kinetic study during the epoxidation step: temperature, molar ratio of H_2O_2, and Acetic acid (AA) to unsaturation content. The epoxidation kinetic study was performed only using isobutyl linoleate, as this was the only ester of well-define nature. As identified in previous works [85],[148], optimal epoxidation yields are obtained in the following range of conditions; temperature: 50-80 °C, catalyst loading 1-2% wt., and molar ratio C=C/AA/H_2O_2 1:0.5:2. Hence, these conditions were selected for the experiment design. Additionally, a stirring rate of 600 rpm was used to maintain a well-mixed reactive medium and a suitable temperature control. It has been reported that operating between stirring rates of 300 and 900 rpm, neither mass transfer limitations nor significant differences in the epoxide content during the reaction are present [84],[95].

- **Box Behnken design for the epoxidation reaction**

The effect of the variables on the epoxidation process was studied through a Box Behnken design of 3 variables and 3 levels. The parameters considered were temperature, molar ratio AA:C=C, and molar ratio C=C:H_2O_2. Furthermore, three additional runs were proposed to evaluate the effect of the catalyst loading and temperature. The complete set of conditions of all experiments is presented in Table 3-8. The reaction progress was monitored by measuring the oxirane oxygen content and iodine value. The main response variables were the conversion of double bonds, epoxide yield, and selectivity.

Table 3-8. Box Behnken experimental design

Run	Factors						Catalyst (% wt.)	Run
	X_1	X_2	X_3	°T (°C)	Ratio AA:C=C	Ratio C=C:H_2O_2		
1	-1	-1	0	50	0.3	1.5	2.0	L10
2	1	-1	0	70	0.3	1.5	2.0	L14
3	-1	1	0	50	0.5	1.5	2.0	L11
4	1	1	0	70	0.5	1.5	2.0	L15
5	0	0	0	60	0.4	1.5	2.0	L8
6	0	-1	-1	60	0.3	1	2.0	L7
7	0	-1	1	60	0.3	2	2.0	L6
8	0	1	-1	60	0.5	1	2.0	L5
9	0	1	1	60	0.5	2	2.0	L4
10	0	0	0	60	0.4	1.5	2.0	L2
11	-1	0	-1	50	0.4	1	2.0	L13
12	-1	0	1	50	0.4	2	2.0	L12
13	1	0	-1	70	0.4	1	2.0	L16
14	1	0	1	70	0.4	2	2.0	L17
15	0	0	0	60	0.4	1.5	2.0	L9
16	0	1	0	80	0.5	1.5	2.0	L18
17	0	0	0	60	0.4	1.5	1.0	L1
18	0	0	0	60	0.4	1.5	1.5	L3

L1, L3 and L18 were carried out using variable catalyst and L18 was performed at a higher temperature (80°C)

- **Procedure**

Epoxidized isobutyl linoleate (EIL) was produced by epoxidation of isobutyl linoleate using peracetic acid generated in situ, and sulfuric acid as a catalyst. The reaction was carried out in a 150 ml glass five-necked jacketed and coiled reactor equipped with a thermometer, and a mechanical stirrer. The reactor was connected to two thermostatic baths, one to provide heating and the other to provide cooling circulating fluids. The immersed coil was used to remove the heat of the reaction, and the jacket was used to maintain the reaction temperature. The system was provided with a calibrated syringe pump to dose the H_2O_2 feed and a reflux condenser to recover the volatile species. The experimental setup for the epoxidation reaction is presented in Figure 3-16.

.

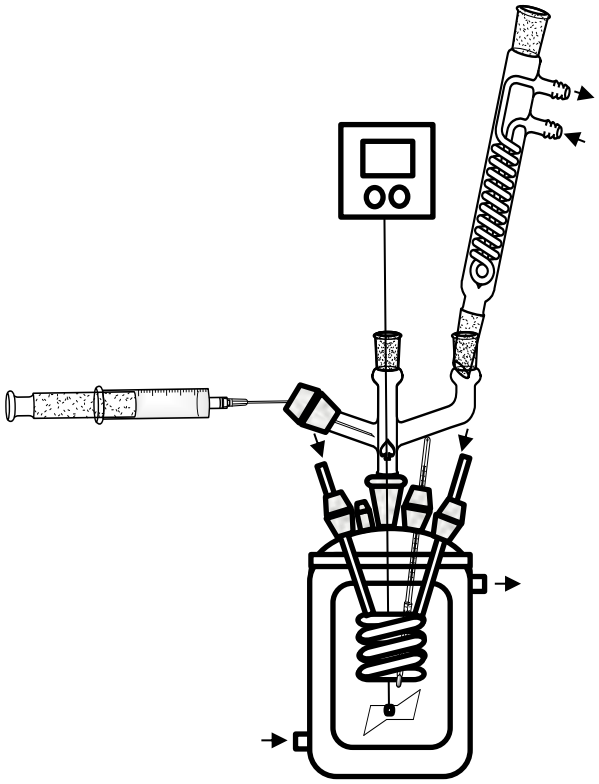

Figure 3-16. Experimental setup used during epoxidation of fatty esters.

In the setup, 70 g of isobutyl linoleate and the corresponding amount of acetic acid, according to the experiment design, were added to the reactor and heated up to the reaction temperature. A mixture of sulfuric acid and aqueous hydrogen peroxide was then added dropwise to the reactor over a period of 10 minutes. The temperature of the reaction was held isothermal by using a coil connected to a thermostatic bath which refrigerated the reaction medium. Samples of 0.5 g were withdrawn at different time intervals and quenched by immersing the sample holder in cold water to stop the reaction. The reaction progress was monitored by measuring the acid value, iodine value, and oxirane oxygen content in the samples. After 3 hours, the reaction was stopped, and the content of the reactor was removed and transferred to a glass funnel for separation. The water phase was discarded. Subsequently, the oil phase containing the epoxide was neutralized using a 5% wt bicarbonate solution and rinsed with water at 40°C until the aqueous effluent reached a neutral pH. Finally, the epoxide was dried over $MgSO_4$ to remove the residual water.

3.3.1 Results

The results of the epoxidation study are summarized in Table 3-9. The effect of catalyst loading (1, 2, and 1.5% wt.) was studied at 60°C in runs L1, L2, and L3. The oxirane content achieved in those runs was about 5.1%, and the conversions were 73%, 81 and 88.6%, respectively. Nevertheless, the highest selectivity was reached using 1% wt. catalyst. As expected, high catalyst concentrations also trigger ring-opening reactions in the presence of water and decrease the yield of the reaction [86],[94],[147].

Table 3-9. Run results and reaction conditions.

Run	°T(°C)	Ratio C=C: CA: H_2O_2	Catalyst (%)	II (gI_2/100g)	OO (%)	Y (%)	X (%)	S (%)
L1	60	1 : 0.4 : 1.5	1.0	40.2	5.0	58.9	72.5	81.2
L2	60	1 : 0.4 : 1.5	2.0	16.6	5.1	60.3	88.6	68.0
L3	60	1 : 0.4 : 1.5	1.5	27.7	5.1	60.6	81.1	74.8
L4	60	1 : 0.5 : 2.0	1.4	16.7	5.2	61.6	88.6	69.5
L5	60	1 : 0.5 : 1.0	1.6	29.1	3.8	44.8	80.1	55.9
L6	60	1 : 0.3 : 2.0	2.0	16.6	5.2	61.8	88.6	69.7
L7	60	1 : 0.3 : 1.0	2.2	24.1	4.7	55.1	83.5	66.0
L8	60	1 : 0.4 : 1.4	1.9	14.6	5.0	59.4	90.0	66.0
L9	60	1 : 0.4 : 1.4	1.9	16.3	5.1	60.3	88.8	67.9
L10	50	1 : 0.3 : 1.5	2.0	41.6	4.8	56.5	71.6	79.0
L11	50	1 : 0.5 : 1.5	2.0	25.3	4.9	58.6	82.7	70.8
L12	50	1 : 0.4 : 2.0	2.1	30.8	5.0	59.4	78.9	75.3
L13	50	1 : 0.4 : 1.0	2.1	43.3	4.2	49.9	70.4	70.9
L14	70	1 : 0.3 : 1.5	2.0	5.3	4.7	56.0	96.4	58.1
L15	70	1 : 0.5 : 1.5	2.0	4.3	0.5	6.3	97.0	6.5
L16	70	1 : 0.4 : 1.0	2.1	19.2	2.9	34.4	86.9	39.6
L17	70	1 : 0.4 : 2.0	2.0	1.5	2.6	30.7	99.0	31.0
L18	80	1 : 0.5 : 1.5	2.0	5.6	0.0	0.0	96.1	0.0

Y: yield, X: conversion S: selectivity.

The dependence of epoxidation conversion on the catalyst loading is presented in Figure 3-17. It is possible to verify that final conversion linearly increases with catalyst loading, which is characteristic when using a homogenous catalyst, and mass transfer limitations are absent. In further experiments, a 2% wt. H_2SO_4 loading was used to enable higher reaction rates.

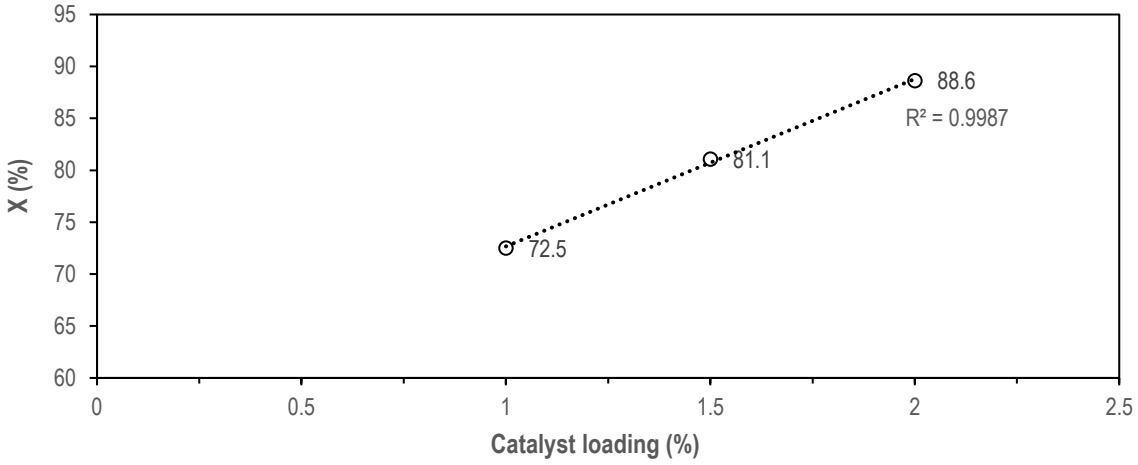

Figure 3-17. Acid homogeneous catalyst loading vs conversion.

The effect of the temperature was studied from 50°C to 80°C. As expected, high temperatures enhance the rate of epoxidation but also have a negative effect on the selectivity and yield to oxirane groups. This is clear when comparing the final concentration of oxirane at 60°C, 70°C, and 80°C, which is almost zero at the highest temperature. Therefore, when the epoxidation is carried out above 60°C, it is necessary to identify the point of maximum oxirane production to quench and stop the reaction [85].

Previous works have reported that degradation reactions are highly dependent on temperature and catalyst loading in the reactive medium [86],[89]. High temperatures and high catalyst concentrations trigger the nucleophilic attack on the oxirane ring at the interphase and the oil phase. In the used epoxidation route, the main nucleophiles are the acetic acid which is partially soluble in the oily phase, and the water which is in large excess. Hydrogen peroxide has low solubility in the oil phase due to its polar nature and tends to react with carboxylic acids, so its oxirane cleavage capacity can be considered negligible. According to these considerations, the most likely degradation reactions are mainly caused by the attack of acetic acid and water over the oxirane ring.

From the epoxidation results in Table 3-9, it is observed that the increasing of the molar ratio of hydrogen peroxide increases the rate of epoxidation (runs L4 and L5). However, a large loading of aqueous H_2O_2 also increases the content of water in the reaction medium up to a level where its concentration is 4 to 8 times that of acetic acid. Besides becoming a

major issue for oxirane ring stability, an excess of water under acidic conditions can promote hydrolysis of the ester [86]. This was characterized during epoxidation experiments, and Figure 3-18 shows the measured acid value of the reactive medium over time. As observed, the acid value increased with the reaction time. At 50°C and 60°C it displayed a slightly linear growth, but acidity exponentially increased when operating at 70°C and 80°C. This trend indicates that the hydrolysis reaction is promoted by the acid catalyst under large water excess and high temperatures.

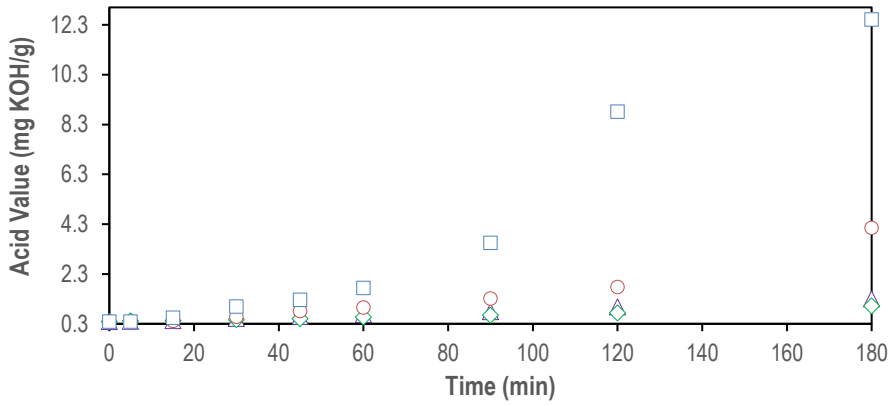

(-□-) Run L18 - 80°C. (-○-) Run L15 - 70°C. (-Δ-) Run L7 - 60°C. (-◊-) Run L11 - 50°C.
Figure 3-18. Acid value of the reactive medium along time during epoxidation reactions at different temperatures.

Increasing the molar ratio of acetic acid also has a significant effect on the ring-opening reactions. According to runs L15 and L18, a complete ring opening was attained using a molar ratio of 0.5 at temperatures of 70 and 80°C. This fact, coupled with degradation by water, resulted in the lowest selectivity and yield in these experimental runs.

Conversely, the highest oxirane oxygen 5.2% was reached in runs L6 and L4 at 60°C after 3 hours of reaction. This oxirane content represents a yield of 62% and a conversion of 89%.

In this regard, it can be concluded that moderate oxirane cleavage is achieved at mild conditions, but operating under such conditions hinders the maximum oxirane concentration, which, in the case of isobutyl linoleate, is 8.4%.

Regarding the effect of reaction time, evaluating the oxirane content as a function of time for each run enables to define the highest oxirane production along the reaction. In this case, an oxirane content of 5.5% wt. was achieved using the following reaction conditions: 70°C, 1:0.3:1.5, and 2% wt. catalyst, and 90 min reaction (Run L14). After reaching the maximum oxirane content, it gradually decayed as observed in the kinetic profiles presented in Annex C - L14. Despite a similar yield could also be achieved in runs L10 or L1 at 50°C with a longer reaction time, the conversion of these runs was moderate (~72%) and it was balanced by high selectivity values (~80%). The corresponding selectivity, yield, and conversion of all the experiments are graphically presented in Figure 3-19.

As can be seen, conversions are above 80% in most of the experiments, but selectivity is highly affected by reaction conditions, also impacting the obtained yield. The highest selectivities were obtained in runs L1, L10, and L12. In these runs, the conversion was between 70 – 80%. In this sense, to reach the highest oxirane content, a balance between conversion and selectivity must be achieved [149].

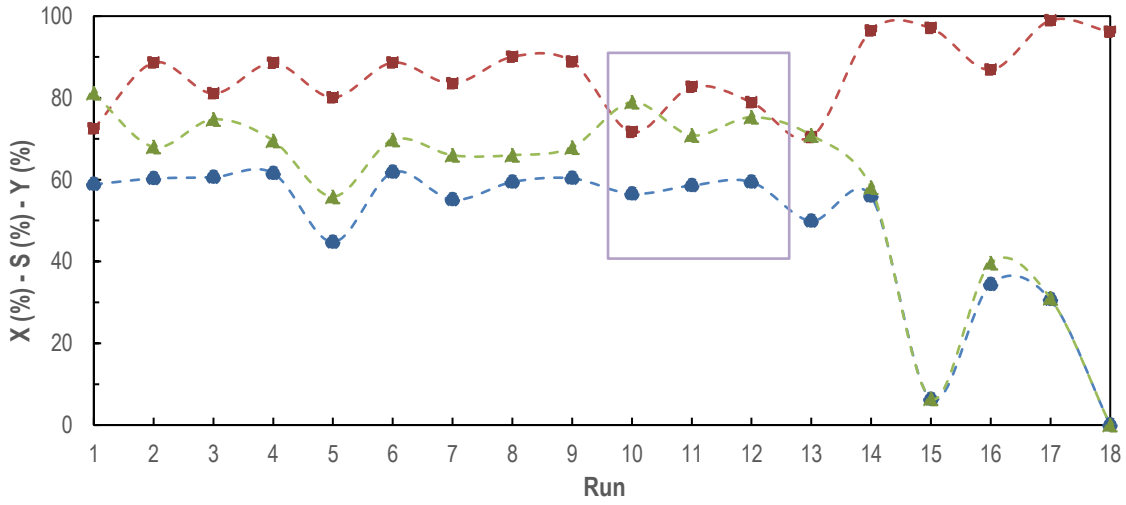

Conversion (■) Selectivity (▲) Yield (●)

Figure 3-19. Epoxidation results.

Other degradation reactions, such as H_2O_2 and peracetic acid decomposition, can also decrease the concentration of the reagents and affect the epoxidation rate. However, these reactions were not considered in the present study [87].

3.4 Two-phase epoxidation kinetic model

The epoxidation of unsaturations in which the aqueous and oil phases are well mixed can be modeled using a two-phase reaction system [79],[84],[99]. As is described in Chapter 1, the unsaturation present in the ester molecule reacts with the in situ peracetic acid to produce an oxirane ring, as is shown in Equation (3-6) and Equation (3-7).

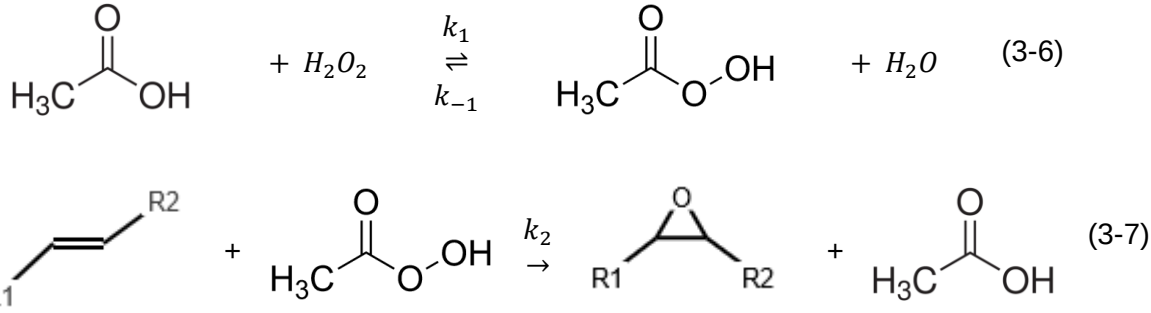

The oxirane ring can further react with nucleophilic agents present in the reaction mixture (water, hydrogen peroxide, acetic acid, and peracetic acid) [81]. However, in the modeling of the system, it is assumed that the cleavage of oxirane is only caused by acetic acid and water, as described in Equation (3-8) and Equation (3-9).

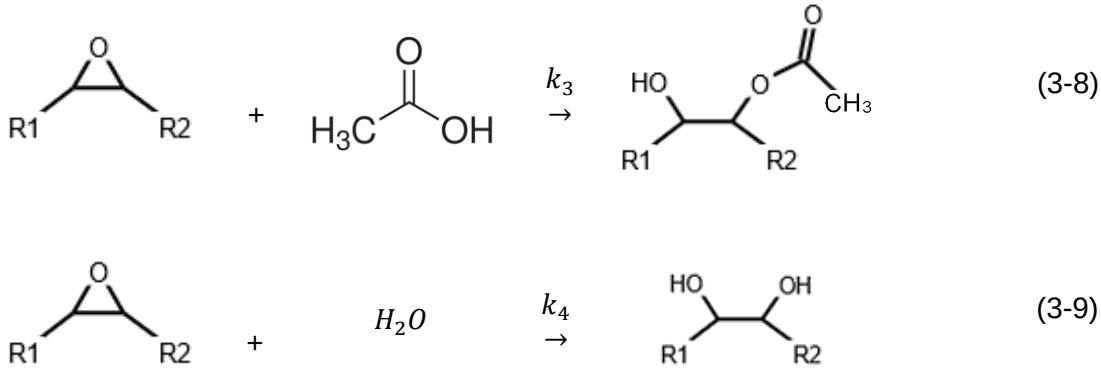

Additionally, the kinetic model considers the following assumptions:

- The epoxidation and degradation reactions are irreversible.
- The rate of reaction and mass balances are a function of the molar concentration in each phase and their corresponding volumes.

- Acetic and peracetic are distributed in both phases, while hydrogen peroxide, sulfuric acid, and water are insoluble in the organic phase [150].
- The degradation reactions are carried out at the oil phase (attack by acetic acid) and the liquid-liquid interphase (attack by water) [151], and they are produced by the attack of carboxylic acid and water.
- The mass transfer coefficients for acetic and peracetic acid are equal ($k_{t,PAA}a = k_{t,AA}\ a$)
- The system is isothermal and well-mixed, and mass transfer limitations are negligible.
- The addition of the first drop of the catalyst mixture and aqueous H_2O_2 is considered time zero for the reaction.
- The degradation reaction by acetic acid is assumed to be of second order for acetic acid. On the other hand, the degradation reaction by water is considered of first order for epoxide and water. Likewise, this reaction considers the influence of acid catalyst in the medium. [79],[84],[150] [152].
- Volume and density slightly change along the reaction time.

According to these assumptions, the mass balance of the reaction system is described by first-order differential equations for each component in the aqueous (w) and oil phase (o). The system was modeled as a semi-batch reactor since the mixture of catalyst and hydrogen peroxide was dosed continuously in the first 10 minutes.

- **Mass balance in a semi-batch reactor**

$$\frac{dN_i}{dt} = \sum_{k=1}^{4} \vartheta_{i,k} r_{i,k} V^p + F_i \tag{3-10}$$

In this equation, N_i is the total number of moles of component i in the reactor, t is the time coordinate, $r_{i,k}$ is the rate of appearance/disappearance, and $\vartheta_{i,k}$ is the corresponding stoichiometric coefficient of component i in reaction k. V^p is the volume of the corresponding reactive phase p. F_i is the constant feed flow rate of component i during the

initial loading of the reactants and the catalyst. There are four reactions taking place, namely peracetic acid formation and decomposition (r_1, r_{-1}), isobutyl fatty ester epoxidation (r_2), and ring-opening reactions by acetic acid (r_3) and water (r_4). Rates of reactions are expressed in mol L^{-1} min^{-1}, and they correspond to equations (3-11) to (3-20) The kinetic models were described as the following power-law expressions:

$$r_1 = k_1 C_{H_2O_2} C_{AA}^W C_{H^+}$$
$$r_{-1} = k_{-1} C_{PAA}^W C_{H_2O} C_{H^+}$$
$$r_2 = k_2 C_{C=C} C_{PAA}^O$$
$$r_3 = k_3 C_{EPO} {C_{AA}^O}^2$$
$$r_4 = k_4 C_{EPO} C_{H_2O} C_{H^+}$$

Here, $C_{H_2O_2}$ is the concentration of H_2O_2, C_{AA}^W is the concentration of acetic acid, $C_{H^+}$is the concentration of the catalyst, C_{PAA}^W is the concentration of peracetic acid, and C_{H_2O} is the concentration of water, all in the aqueous phase. On the other hand, C_{AA}^O is the concentration of acetic acid, C_{PAA}^O is the concentration of peracetic acid, $C_{C=C}$ is the concentration of the isobutyl ester, and C_{EPO} is the concentration of the epoxidized ester, all in the oily phase. The model depends on the following parameters: peracetic forward and backward kinetic constant k_1, k_{-1}, (L^2 mol^{-2} min^{-1}), epoxidation kinetic constant k_2, (L mol^{-1} min^{-1}), kinetic constants for the degradation products k_3 (L^2 mol^{-2} min^{-1}), k_4 (L^2 mol^{-2} min^{-1}), partition coefficients of acetic acid (K_{AA}) and peracetic acid (K_{PAA}), mass transfer coefficients: $k_{t,PAA}a = k_{t,AA}\,a = k_m a$, (min^{-1}), and phases volume V^W and V^O (L). The resulting material balances of all species are on a molar basis (mol/time). N_{DEG1} corresponds to the degradation product from the ring-opening reaction by acetic acid (r_3), and N_{DEG2} is the degradation product generated from the ring-opening reaction by water (r_4).

Aqueous phase

- Hydrogen peroxide (H_2O_2):

$$\frac{dN_{H_2O_2}}{dt} = \dot{F_{H_2O_2}} + (-k_1 C_{H_2O_2} C_{AA}^W C_{H^+} + k_{-1} C_{PAA}^W C_{H_2O} C_{H^+}) V^W \quad (3\text{-}11)$$

- Peracetic acid (PAA):

The peracetic acid, as well as acetic acid, is distributed between the two phases, thus the mass balance equation includes the mass transfer rate. The mass transfer is described as the flux of the component between phases: $N_A = k_m a\,(c_A - c_A{}^*)$. According to the two-film theory, phase equilibrium is achieved at the interface and $c_A{}^*$ is the composition of the oil that is in equilibrium with the bulk liquid and is equal to $K_{PAA}C_{PAA}^W$.

$$\frac{dN_{PAA}^W}{dt} = (k_1 C_{H_2O_2} C_{AA}^W C_{H^+} - k_{-1} C_{PAA}^W C_{H_2O} C_{H^+}) V^W - k_m a \left(K_{PAA} C_{PAA}^W - C_{PAA}^O\right) V^O \quad (3\text{-}12)$$

- Acetic acid (AA):

$$\frac{dN_{AA}^W}{dt} = (-k_1 C_{H_2O_2} C_{AA}^W C_{H^+} + k_{-1} C_{PAA}^W C_{H_2O} C_{H^+}) V^W + k_m a \left(C_{AA}^O - K_{AA} C_{AA}^W\right) V^O \quad (3\text{-}13)$$

- Water (H_2O):

$$\frac{dN_{H_2O}}{dt} = \dot{F_{H_2O}} + (k_1 C_{H_2O_2} C_{AA}^W C_{H^+} - k_{-1} C_{PAA}^W C_{H_2O} C_{H^+})\, V^W - k_4 C_{EPO} V^O \quad (3\text{-}14)$$

Oil phase

- Unsaturations (C=C)

$$\frac{dN_{C=C}}{dt} = -(k_2 C_{C=C} C_{PAA}^O)\, V^O \quad (3\text{-}15)$$

- Epoxide (EPO):

$$\frac{dN_{EPO}}{dt} = (k_2 C_{C=C} C_{PAA}^O - k_3 C_{EPO} {C_{AA}^O}^2 - k_4 C_{EPO})\, V^O \quad (3\text{-}16)$$

- Peracetic acid (PAA)

$$\frac{dN_{PAA}^O}{dt} = -\left(k_2 C_{C=C} C_{PAA}^O\right) V^O + k_m a \left(K_{PAA} C_{PAA}^W - C_{PAA}^O\right) V^O \quad (3\text{-}17)$$

- Acetic acid (AA)

$$\frac{dN_{AA}^O}{dt} = (k_2 C_{C=C} C_{PAA}^O - k_3 C_{EPO} {C_{AA}^O}^2) V^O - k_m a \left(C_{AA}^O - K_{AA} C_{AA}^W\right) V^O \quad (3\text{-}18)$$

- Degradation products from epoxide (N_{DEG1})

$$\frac{dN_{DEG1}^{O}}{dt} = (k_3 C_{EPO} {C_{AA}^{O}}^2) V^O \quad (3\text{-}19)$$

- Degradation products from epoxide (N_{DEG2})

$$\frac{dN_{DEG2}^{O}}{dt} = (k_4 C_{EPO} C_{H_2O} C_{H^+}) V^O \quad (3\text{-}20)$$

The flow of catalyst and hydrogen peroxide is modeled in a time interval of 10 minutes.

$$F_i = \frac{\dot{F} * x_i}{PM_i} \quad \text{t} \leq t_a \quad (3\text{-}21)$$

$$F_i = 0 \qquad \text{t} \leq t_a$$

In Equation (3-21), PM_i and x_i are the molar mass and the mass fraction of the components of the mixture, respectively.

The partition coefficient K_i is denoted as follows [150]:

$$K_i = \frac{C_i^{o*}}{C_i^{W*}} = \frac{N_i^o / V^o}{N_i^W / V^W} \quad (3\text{-}22)$$

Here, C_i^o and C_i^W are the molar concentration in the oil phase and the aqueous phase of component i, respectively.

$$N_i = N_i^o + N_i^W \quad (3\text{-}23)$$

Using Equation (3-22), the molar mass of the phases can be written as a function of the partition coefficients and the volume of the phases:

$$N_i^o = \frac{K_i V^O N_i}{V^W + K_i V^O} \quad (3\text{-}24)$$

$$N_i^W = \frac{V^W N_i}{V^W + K_i V^O} \quad (3\text{-}25)$$

Then, the total volume of the phases can be expressed as:

$$V^W = V_{H_2O} + V_{H_2O_2} + V_{AA}^W + V_{PAA}^W + V_{H_2SO_4} \quad (3\text{-}26)$$

$$V^O = V_{AA}^O + V_{PAA}^O + V_{EPO} + V_{ES} + V_{DEG1} + V_{DEG2} \quad (3\text{-}27)$$

Likewise, the density of the phases can be expressed as:

$$\rho^W = \frac{W_{H_2O} + W_{H_2O_2} + W_{AA}^W + W_{PAA}^W + W_{H_2SO_4}}{V^W} \quad (3\text{-}28)$$

$$\rho^O = \frac{W_{AA}^O + W_{PAA}^O + W_{EPO} + W_{ES} + W_{DEG1} + W_{DEG2}}{V^O} \quad (3\text{-}29)$$

In addition to these variables, the modified Arrhenius equation is used to correlate a kinetic constant $k(T)$ with the activation energy Ea and preexponential factor $A\,prex$ [153]. The selected reference temperature was 70°C.

$$k(T) = exp\left[A + B\left(\frac{T - T_{ref}}{T}\right)\right] \quad (3\text{-}30)$$

$$A = \ln\left(k_{ref}\right) \quad (3\text{-}31)$$

$$B = \frac{Ea}{RT_{ref}} \quad (3\text{-}32)$$

$$A\,prex. = \frac{k_{ref}}{\exp\left(-\frac{Ea}{RT_{ref}}\right)} \quad (3\text{-}33)$$

In Equations (3-30) to (3-33), A and B are the constants of the modified Arrhenius equation. Ea and $A\,prex$ are the activation energy and the preexponential factor, respectively.

3.4.1 Kinetic parameters regression

The modeling of the epoxidation reaction was performed using *MATLAB 2022a* and the operating conditions of the 18 experimental runs. The system of differential equations described from (3-11) to (3-20) was solved by numerical integration using the multistep solver *ode15s*, based on differential-algebraic equations (DAEs). The objective function in Equation (3-38) was minimized and corresponds to the difference between experimental values (Equations (3-35) and (3-37)) and the predicted values (Equation (3-34) and Equation (3-36)). The minimization problem was solved by adjusting the corresponding kinetics parameters using the Global Search algorithm implemented in Matlab. To determine the number of moles, the molecular weights of the ester and epoxide were

calculated using the saponification and acid values presented in Table 3-7. The molecular weight of the degradation products was obtained from the reaction stoichiometry.

$$[\boldsymbol{NDB}]_{model} = \frac{N_{ES}}{W_{ES} + W_{EPO} + W_{DEG1} + W_{DEG2}} \quad (3\text{-}34)$$

$$[\boldsymbol{NDB}]_{\boldsymbol{exp}} = \frac{IN}{2 * Ai} \quad (3\text{-}35)$$

In Equations (3-34) and (3-35) NDB is the number of double bonds, IN is the experimental iodine value and Ai is the molecular mass of iodine.

$$[\boldsymbol{EPO}]_{model} = \frac{N_{EPO}}{W_{ES} + W_{EPO} + W_{DEG1} + W_{DEG2}} \quad (3\text{-}36)$$

$$[\boldsymbol{EPO}]_{\boldsymbol{exp}} = \frac{OO}{100 * Ao} \quad (3\text{-}37)$$

In Equations (3-36) and (3-37) EPO is the number of oxirane groups, OO is the experimental oxirane value (%) and Ao is the molecular mass of oxygen. As mentioned above, the objective function to minimize is described in Equation (3-38), and the corresponding statistical parameters are described in Equations (3-39) to (3-41).

- **Objective Function**

$$\boldsymbol{F} = \sqrt{\frac{\mathbf{1}}{\boldsymbol{n}} \sum_{\boldsymbol{L}:\mathbf{1}}^{\mathbf{18}} \sum_{\boldsymbol{n}:\mathbf{1}}^{\mathbf{9}} \left[\left(\frac{([\boldsymbol{NDB}]_{\boldsymbol{exp}} - [\boldsymbol{NDB}]_{\boldsymbol{model}})^{\mathbf{2}}}{([\boldsymbol{NDB}]_{\boldsymbol{exp,max}})^{\mathbf{2}}} \right) + \left(\frac{([\boldsymbol{EPO}]_{\boldsymbol{exp}} - [\boldsymbol{EPO}]_{\boldsymbol{model}})^{\mathbf{2}}}{([\boldsymbol{EPO}]_{\boldsymbol{exp,max}})^{\mathbf{2}}} \right) \right]} \quad (3\text{-}38)$$

- **Standard deviation**

$$SD = \sqrt{\frac{(x_{i,cal} - x_{i,exp})^2}{\sum_{i:1}^{NR} NS_i}} \quad (3\text{-}39)$$

- **Absolute error**

$$AE = \frac{1}{\sum_{i:1}^{NR} NS_i} * \sum_{j:1}^{NR} \sum_{k:1}^{NS} (x_{i,cal} - x_{i,exp}) \quad (3\text{-}40)$$

In Equations (3-39) to (3-40), NR is the number of runs, and NS_i is the number of samples.

- **Relative Error**

$$E_{rel} = \frac{\sum_{samples} \left| \frac{x_{i,cal} - x_{i,exp}}{x_{i,exp}} \right|}{n\ samples} * 100 \quad (3\text{-}41)$$

In equation (3-41) $x_{i,cal}$ is the calculated value and $x_{i,exp}$ is the experimental value.

3.4.2 Results of kinetic model regression

The corresponding kinetic model of the epoxidation of isobutyl linoleate with H_2O_2 was obtained by adjusting 19 parameters while minimizing the objective function described in Equation (3-38) [154]. The fitted kinetic parameters are summarized in Table 3-10 along with the corresponding confidence intervals. Table 3-10 presents other statistical measures of the model regression.

Table 3-10. Fitted kinetic parameters for the epoxidation of isobutyl esters.

Parameter	Units	Value	Upper limit	Lower limit
$\boldsymbol{E_{A,1}}$	J/mol	$6.11 \cdot 10^4$	$6.00 \cdot 10^4$	$6.21 \cdot 10^4$
$\boldsymbol{A_1}$	$L^2\ mol^{-2}\ min^{-1}$	$5.88 \cdot 10^7$	$3.82 \cdot 10^7$	$9.04 \cdot 10^7$
$\boldsymbol{E_{A,-1}}$	J/mol	$6.63 \cdot 10^4$	$6.53 \cdot 10^4$	$6.73 \cdot 10^4$
$\boldsymbol{A_{-1}}$	$L^2\ mol^{-2}\ min^{-1}$	$1.04 \cdot 10^9$	$7.10 \cdot 10^8$	$1.52 \cdot 10^9$
$\boldsymbol{E_{A,2}}$	J/mol	$5.74 \cdot 10^4$	$5.70 \cdot 10^4$	$5.78 \cdot 10^4$
$\boldsymbol{A_2}$	$L\ mol^{-1}\ min^{-1}$	$5.96 \cdot 10^8$	$5.03 \cdot 10^8$	$7.06 \cdot 10^8$
$\boldsymbol{E_{A,3}}$	J/mol	$4.00 \cdot 10^4$	$3.93 \cdot 10^4$	$4.06 \cdot 10^4$
$\boldsymbol{A_3}$	$L^2\ mol^{-2}\ min^{-1}$	$8.52 \cdot 10^3$	$5.91 \cdot 10^3$	$1.23 \cdot 10^4$
$\boldsymbol{E_{A,4}}$	J/mol	$9.97 \cdot 10^4$	$9.79 \cdot 10^4$	$1.01 \cdot 10^5$
$\boldsymbol{A_4}$	$L^2\ mol^{-2}\ min^{-1}$	$1.21 \cdot 10^{11}$	$5.33 \cdot 10^{10}$	$2.74 \cdot 10^{11}$
$\boldsymbol{KAA_{50°C}}$	--	0.659	0.655	0.664
$\boldsymbol{KAA_{60°C}}$	--	0.687	0.684	0.692
$\boldsymbol{KAA_{70°C}}$	--	0.783	0.780	0.785
$\boldsymbol{KAA_{80°C}}$	--	0.892	0.808	0.975
$\boldsymbol{KPAA_{50°C}}$	--	0.442	0.378	0.506
$\boldsymbol{KPAA_{60°C}}$	--	0.490	0.467	0.512
$\boldsymbol{KPAA_{70°C}}$	--	0.704	0.641	0.767
$\boldsymbol{KPAA_{80°C}}$	--	0.848	0.771	0.924
$\boldsymbol{kt \cdot a}$	min^{-1}	24.46	24.26	24.66

In general, the resulting model exhibits a good fit for the experimental data. The range of the relative error is between 13% and 15% for the instaurations content and oxygen-oxirane content, respectively.

Table 3-11.Errors in the curve fitting

	DB	OO
Absolute Error (AE)	5.05	0.25
Relative Error (RE)	13.30	15.39
Standard Deviation (SD)	6.76	0.42

According to the results, the epoxidation reaction has a kinetic constant of $k_{0,2} = 5.96 \cdot 10^{-1}$ (L mol^{-1} min^{-1}) at 333K, which is similar to that observed for the epoxidation of soybean oil [87]. However, the obtained value was higher than that observed in the epoxidation of methyl linoleate (i.e. $4.33 \cdot 10^{-2}$ L mol^{-1} min^{-1}) [155]. This constant is one order of magnitude lower than the one reported in this work. However, in that model, oxirane cleavage reactions were not considered, so low values for this constant compensate the oxirane loss caused by ring-opening reactions. Also, the kinetic constant for the epoxidation reaction is higher than the peracetic acid formation $1.57 \cdot 10^{-2}$ (L^2 mol^{-2} min^{-1}), verifying that peracid formation is the controlling step of the reaction [90].

As expected, due to the higher mobility and lower steric hindrance, the double bonds in the fatty esters are more reactive than those in TAGs. Consequently, the kinetic constant was larger than the other reported values. Similarly, the fatty acid composition of the feedstock has a significant effect on the rate constant of epoxidation. This is expected because conjugated double bonds in highly unsaturated fatty chains can be more prone to epoxidation. This has been previously observed and the reactivity of fatty acids in the epoxidation reaction follows the order: linolenic acid > linoleic acid > oleic acid as reported before [45].

Regarding the kinetic constants of oxirane degradation by acetic acid ($k_{0,3}$) and water ($k_{0,4}$), a ratio of $k_{0,3}/k_{0,4} = 48$ was obtained at 80°C. This result agrees with literature reports, which suggest that the attack by acetic acid proceeds at a higher rate. However, the concentration of acetic acid in the reaction medium is lower compared to the concentration of water. Moreover the degradation constants $k_{0,3}$ and $k_{0,4}$ increase rapidly with

temperature. Above 70°C these reactions are even competitive with the main epoxidation reaction [156].

At low temperatures, the rate of degradation is moderate, and the concentration of epoxide continuously increases. However, at high temperatures, the rate of epoxide degradation becomes higher than the rate of production, resulting in a decrease in the epoxide content. It's worth highlighting that the initial amount of acetic acid is lower than the amount required to degrade the epoxide, which confirms that water is also contributing to the degradation of the epoxide.

An example of a reasonably good fit of the obtained model is shown in Figure 3-20 which presents the experimental and regressed values for run *L11* performed at 50°C and molar ratios C=C:AA: HP (1:0.3:1.0). As observed, the predictions of double bonds and oxirane groups are well predicted. The complete set of experimental and fitted values is presented in annex D, where it is possible to confirm that the mathematical regression fits well all the experimental values.

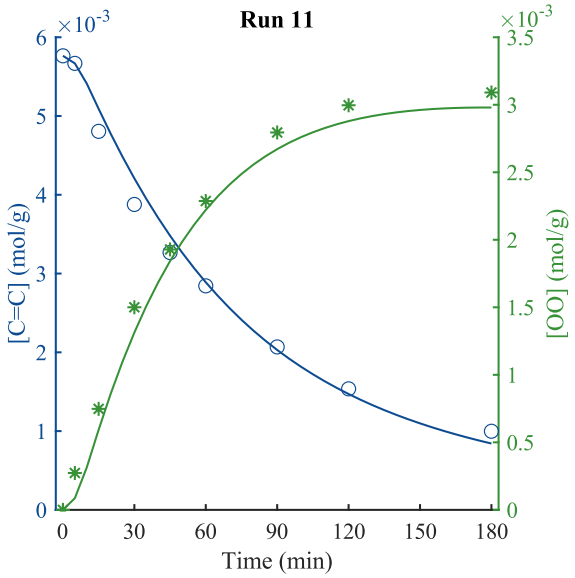

Figure 3-20. Fitted curves and experimental values for run L11.

Figure 3-21 presents the molar profiles (N) of each of the components over time. As seen, hydrogen peroxide (H_2O_2) and water (H_2O) are added dropwise into the reactor during the first 10 minutes. The molar profile of acetic acid in the oil phase (NAA_o) decayed after 120

minutes due to the oxirane degradation reaction ($NDeg_1$). In the case of peracetic acid, its concentration remains low as the reaction progresses. The aqueous phase is composed mostly of water, whose concentration remains steady over time.

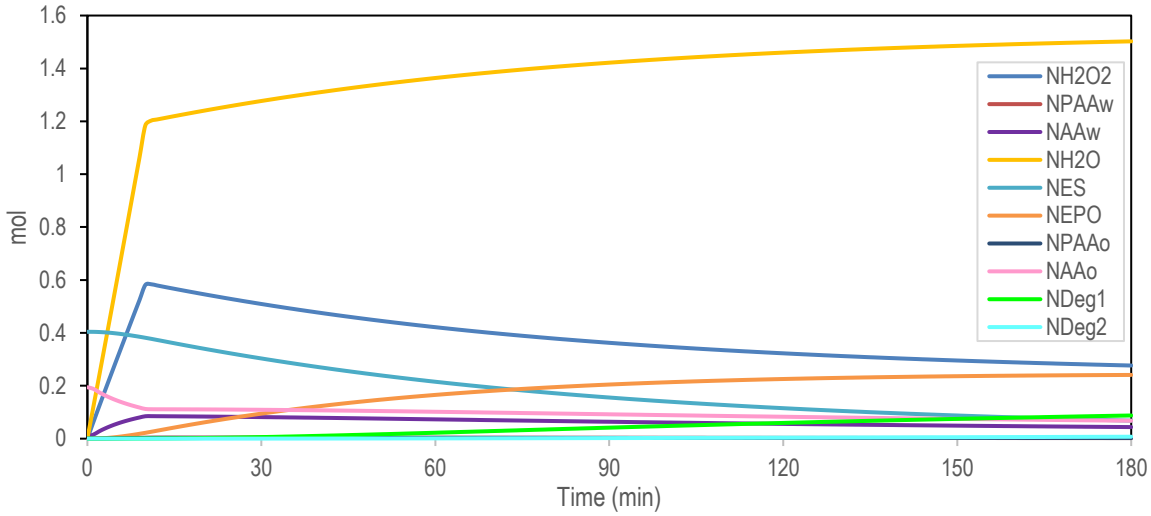

Figure 3-21. Molar profiles along the reaction time

Figure 3-22 shows the time evolution of the density and the volume of the two phases calculated over time. It can be verified that the volume and the density of each phase did not change significantly during the reaction.

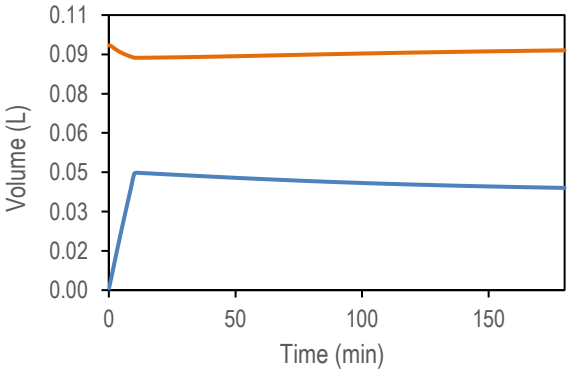

Figure 3-22. Volume along the reaction time

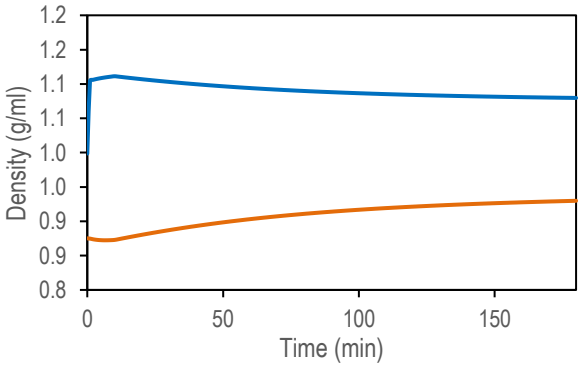

Figure 3-23. Density along the reaction time

Figure 3-24 presents the partition coefficients obtained from the regression parameters. In the epoxidation of isobutyl esters, the partition coefficient of acetic acid was found to be higher than that of peracetic acid. As the temperature increased, both partition coefficients increased in favor of a higher concentration of these compounds in the oleic phase. This

regression will employ to model the partition coefficient of acetic and peracetic acid in the optimization of the process conditions.

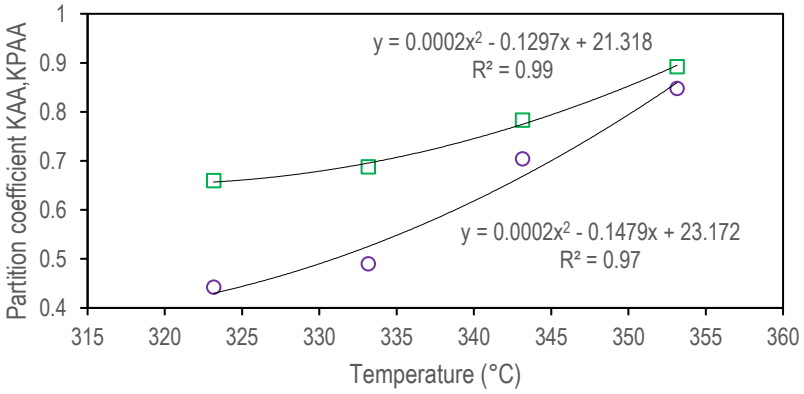

(□) Acetic acid partition coefficient (KAA) (○) Peracetic acid partition coefficient (KPAA)

Figure 3-24. Regressed Partition coefficient

To visualize the good fit of the model, parity plots of all the experimental data and the predicted results used in the regression are presented in Figure 3-25 and Figure 3-26. In general, large differences were observed when operating at 70 and 80°C, as well as at long reaction times when the oxirane cleavage becomes more important and dilution effects caused by degradation products are significant. Regarding the iodine content, deviations from experimental values become noticeable at the end of the reaction. Experimental error plays a key role in the deviation of iodine value as at low concentrations, measurements are less accurate than at high concentrations.

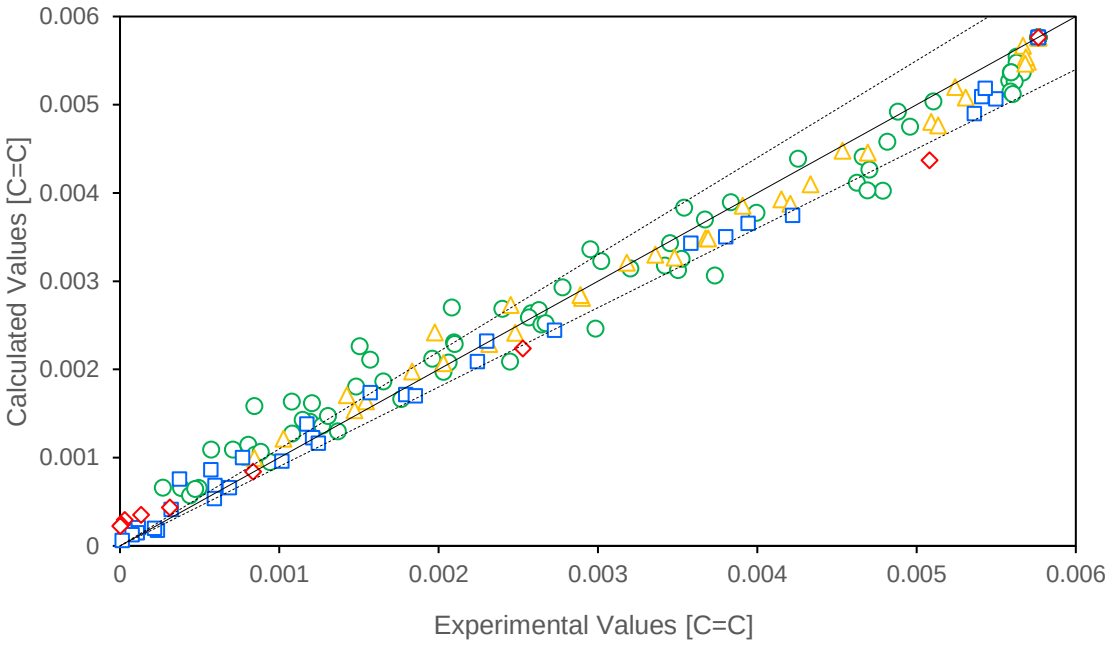

(○) 60°C (△) 50°C (□) 70°C (◊) 80°C (---) ±10%

Figure 3-25. Parity plot of unsaturation content for all experimental runs

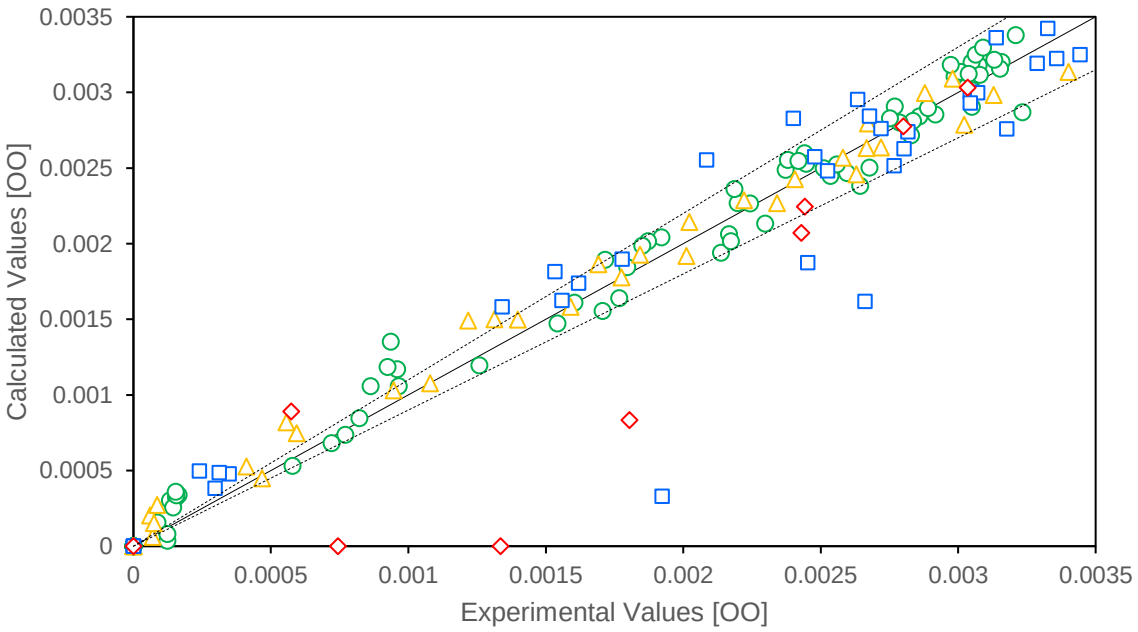

(○) 60°C (△) 50°C (□) 70°C (◊) 80°C (---) ±10%

Figure 3-26. Parity plot of oxirane oxygen content for all experimental runs

An important outcome of this work is that the regressed kinetic model can be used to estimate epoxidation rates for isobutyl esters of SODD and oleic acid [155]. It was stated that double bonds in oleic and linoleic acid exhibit similar epoxidation reactivity [155]. This model may have wider applications in the epoxidation of other raw materials, particularly during feasibility assessments and process design stages.

3.5 Optimization

The final step in this section is to identify the optimal reaction conditions for the epoxidation of fatty esters in a semi-batch reactor using the regressed kinetic parameters. The optimization objective is to maximize the oxirane oxygen of the epoxide and the global productivity of the process (Equation (3-43).

$$Productivity = \frac{mass\ of\ epoxide}{total\ mass} * 100 \quad (3\text{-}42)$$

As described in the previous section, besides the epoxide formation other undesirable reactions occur in the reaction medium. Hence, to achieve high epoxide yields, the production of these degradation products must be minimized. With this goal in mind, the objective function was constructed, as shown in Equation (3-43).

$$Objective\ function\ = Conversion * Selecitivy \quad (3\text{-}43)$$

The parameters to be optimized are temperature, molar ratio of reagents, and the amount of catalyst. Table 3-12 displays the optimization parameters of the search space during the optimization process. For the assessment, 70g of isobutyl ester was considered. It is important to note that a high oxirane content can be achieved not only by carrying out the epoxidation at moderate temperatures but also by limiting the reaction time at higher temperatures. The first route accounts for less use of catalyst than the second.

Table 3-12. Optimization variables range

Variable	Lower limit	Upper limit
Temperature (°C)	40	80
Molar ratio H_2O_2:C=C	1	2.5

Catalyst %(w/w)	0.50	5
Molar ratio AA:C=C	0.2	1
Time (min)	5	540

The optimal conditions for the epoxidation of isobutyl esters, determined using the regressed model and a semi-batch reactor, are presented in Table 3-13. Under these conditions, the highest yield of oxirane was (80.3%) using sulfuric acid as a catalyst.

Table 3-13. Optimization results

Variable	**Value**
Temperature (°C)	60.5
Molar ratio C=C: H_2O_2	3.0
Catalyst %(w/w)	1.57
Molar ratio C=C: AA	0.21
Time (min)	355
OO(%)	6.58
Yield (%)	80.3
Conversion (%)	95.4
Selectivity (%)	84.2

As a result of the optimization, mild conditions for temperature and catalyst loading were obtained. The molar profile of each component is displayed in Figure 3-28. These operation conditions favor the production of epoxide while minimizing the formation rates of degradation products. Additionally, controlled rates of oxirane cleavage are achieved due to the low concentration of sulfuric acid and acetic acid in the system. The resulting oxirane content is 6.6%, which corresponds to 78% of the maximum theoretical value of oxirane. This outcome highlights the importance of seeking new catalysts with high activity and selectivity for the synthesis of epoxides, such as ion exchange resins.

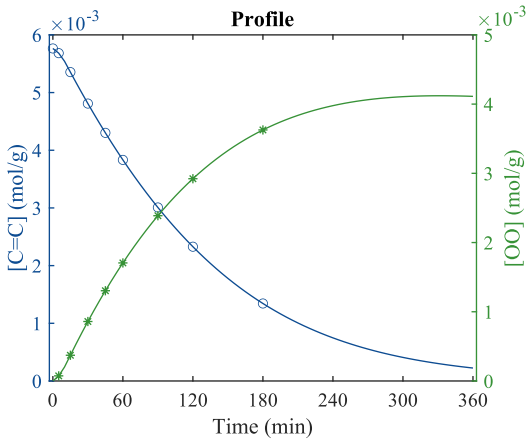

Figure 3-27. Concentration of oxirane and double bonds for the optimum conditions

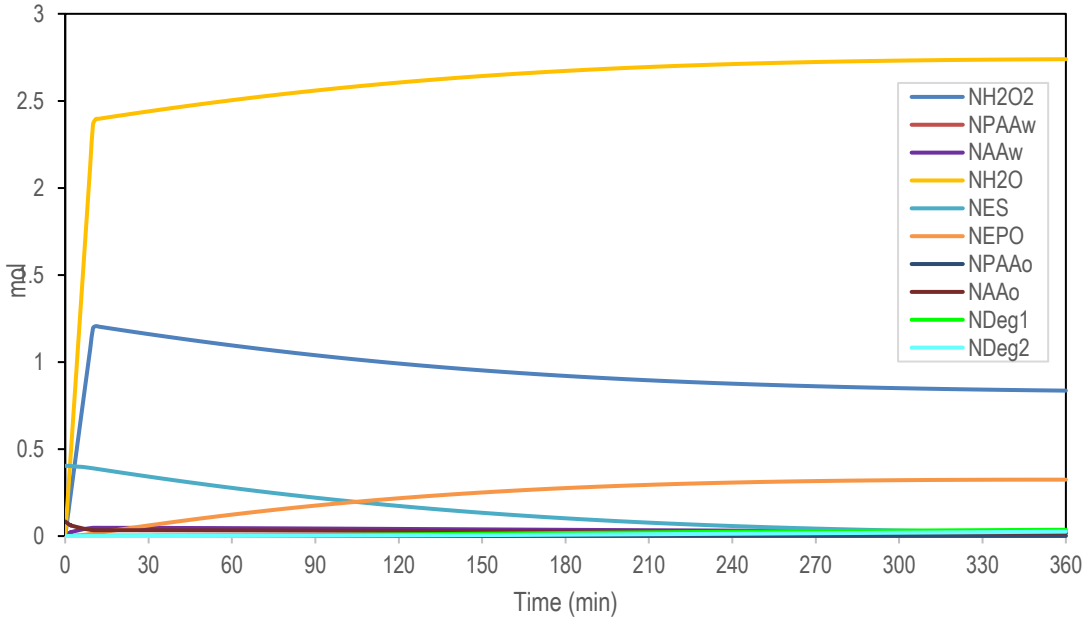

Figure 3-28. Molar profiles along the reaction time for the optimum conditions

3.6 Plasticizers production at bench scale and characterization

Epoxides of isobutanol, namely: epoxide of isobutyl oleate (EIO), epoxide of isobutyl linoleate (EIL), epoxidized isobutyl soyate distillate (EID), and epoxide of isobutyl soyate

(EIS), were produced at bench scale by following the methodology described in the previous section. However, the main goal of this stage was to produce enough amount of epoxides for further evaluation as plasticizers, and thus it was necessary to maximize oxirane content, reduce ring-opening decomposition, and avoid product darkening. For this reason, larger bench-scale batches were carried out at the conditions that optimized oxirane productivity but with a different catalyst. In this case, an ion exchange resin (Amberlyst IRC 120 H) was used as a catalyst with the same acid equivalents of H_2SO_4 determined under the optimal conditions. Considering the ion exchange capacity of the resin, and the molecular weight of H_2SO_4, it was found that the equivalent loading of the resin to the acid was 5.48 ± 0.07 g resin/g H_2SO_4. As the heterogeneous catalyst is less active and might present lower mass transfer rates, the reaction time was set at 6 hours. Once completed, the heterogeneous catalyst was removed from the reaction mixture by filtration, and there was no need for neither further neutralization or bleaching.

The main physicochemical characteristics of the obtained epoxides at the bench scale are presented in Table 3-14, and the appearance of the resulting products is shown in Figure 3-29.

Table 3-14. Characterization of isobutyl epoxides

Property	EIO	EIL	EID	EIS
Acid value (mg KOH/g)	0.8 ± 0.2	1.1 ± 0.3	1.0 ± 0.2	2.0 ± 0.2
Iodine value (g I_2/100g)	9.3 ± 0.7	12.5 ± 0.9	8.9 ± 0.4	12.7 ± 0.1
Oxirane Oxygen (%)	4.47 ± 0.1	6.31 ± 0.1	4.1 ± 0.2	4.2 ± 0.1
Moisture (%)	0.12	0.15	0.16	0.10
MW calculated	359.3 ± 0.7	371.4 ± 0.9	429.7 ± 0.4	476.7± 0.1
Density (20°C) (kg/m^3)	929.7	955.5	920.2	936.0
Density (40°C) (kg/m^3)	911.7	937.5	902.2	920.0
Kinematic Viscosity (40°C) (cSt)	14.8 ± 0.1	17.1 ± 0.1	11.6 ± 0.1	20.9 ± 0.6
Dynamic Viscosity (40°C) (cP)	13.5 ± 0.1	16.0 ± 0.1	10.5 ± 0.1	19.2 ± 0.6
Color	Yellow	Yellow	Yellow	Orange

a) b) c) d)

Figure 3-29. Produced epoxidized isobutyl esters at the bench scale.
(a) Isobutyl Oleate (EIO) (b) Epoxidized Isobutyl Linoleate (EIL) (c) Epoxidized isobutyl soyate distillate (EID) (d) Epoxidized Isobutyl Soyate (EIS)

The molar weight of the isobutyl epoxides in Table 3-14 was calculated based on the molar weight of the esters and their iodine value. Isobutyl epoxides EIO, EIL, EID, and EIS meet most of the parameters of epoxidized esters as listed in Table 1-10. However, it is necessary to reduce their final iodine value (9-13 cg I_2/g). For further epoxidation, it would be necessary to extend the reaction time to decrease the iodine value below the recommended level for oleochemical plasticizers. In the case of epoxidized isobutyl soyate, a bleaching treatment would be necessary to improve the color of the final product. If this is not possible, the application of these epoxides would be limited to products that do not require clear or translucent specifications.

The dynamic viscosity of the final product follows the order EIS> EIL>EIO>EID with viscosity values ranging from 10.5 to 19.2 cP. This is about three times higher than their corresponding isobutyl ester. As expected, the introduction of oxygen in the double bond increases the viscosity of the product due to the more polar interaction of the oxirane rings. The obtained viscosity of the epoxidized isobutyl ester is in the range of other oleochemical epoxides and even of some phthalates. Reference plasticizers such as epoxidized soybean and DOP have dynamic viscosities of 13 cP at 40°C and 26 cP at 40°C, respectively [79], [157].

- **Thermal properties of epoxides**

To study the thermal properties of the epoxides (EIO, EIL, EID, and EIS), the samples were analyzed using the same thermal cycles (crystallization and melting) that were employed to evaluate the thermal properties of esters.

The crystallization and melting cycles of isobutyl epoxides obtained at the bench scale are shown in Figure 3-30 and Figure 3-31. Furthermore, the thermal degradation of these epoxides is presented in Figure 3-32.

As observed, isobutyl epoxides exhibited several peaks in the DSC thermogram, which explains why they crystallize and melt over a wide range of temperatures. The results were analyzed based on the main thermal peaks. In general, isobutyl epoxides exhibited good thermal properties for plasticizing purposes. All these epoxides have low crystallization temperatures in the range of -22 to -35°C. Likewise, they exhibited low melting points between -14 and -17°C. This indicates that they can also be used in different industrial applications, such as lubricants, surfactants, or even as additives for fuels where good fluidization at low temperatures is required [158].

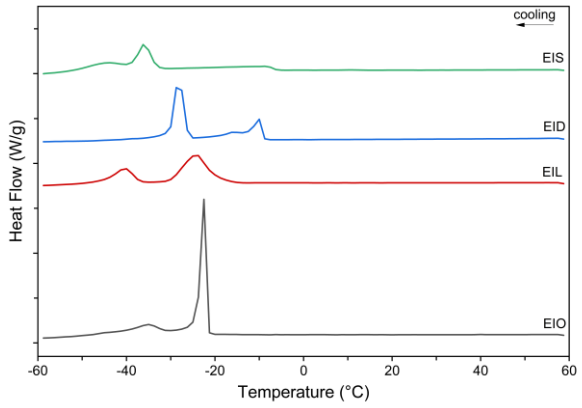

Figure 3-30. Crystallization DSC curves of isobutyl epoxides

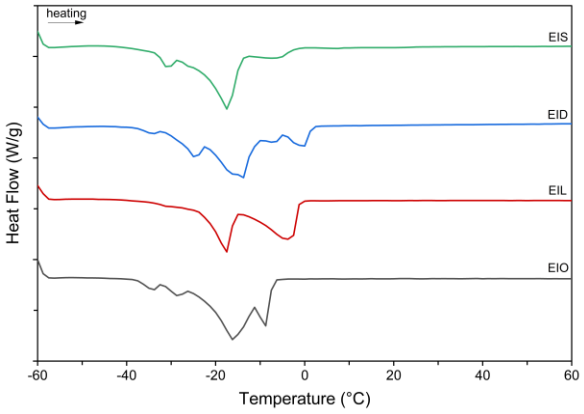

Figure 3-31. Melting DSC curves of isobutyl epoxides

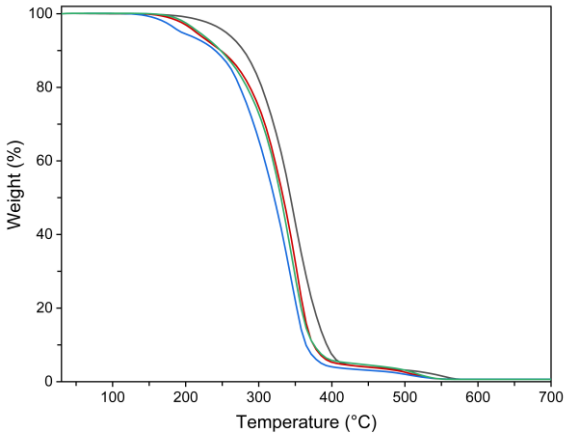

(— IBO) (—IBL) (—ISD) (— ISO)

Figure 3-32. Thermal degradation of isobutyl epoxides

In particular, the thermal properties of the isobutyl esters and epoxides are enhanced after the functionalization of the molecule by esterification and epoxidation. Similar results have been found in the study of the cold flow properties of epoxidized castor oil [159]. The thermal stability of epoxides is slightly higher than the corresponding ester and fatty acids, which is attributed to the incorporation of oxygen instead a double bound that is more easily oxidized.

- **FTIR of bench-scale epoxides**

The main groups of the assessed epoxide molecules were identified through FTIR spectra. The peak at 819 cm^{-1} is associated with oxirane oxygen vibration. Additionally, the peaks at 1724 cm^{-1} and 1285 are related to the C=O and C-O vibrations of ester groups respectively [160]. Figure 3-33 presents the characteristic absorbance of these compounds.

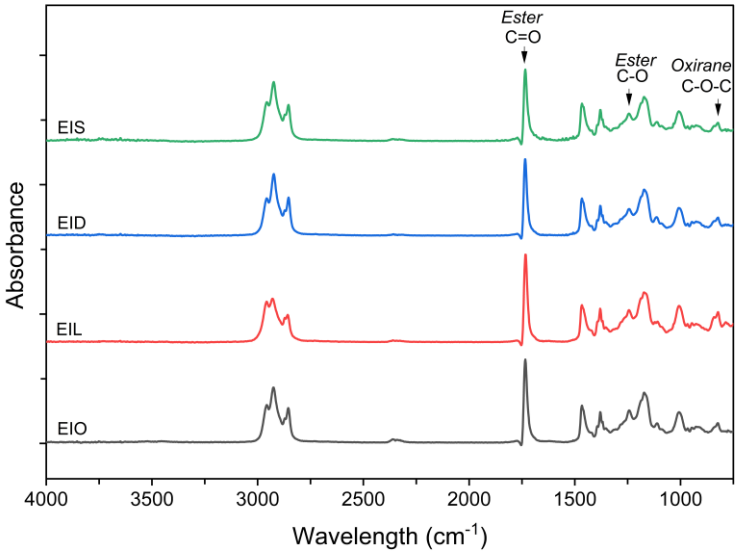

Figure 3-33. FTIR spectra of isobutyl epoxides

4. Performance evaluation of biobased plasticizers

After producing the biobased epoxidized isobutyl esters (i.e. EIO, EIL, EID, EIS), at the bench scale their performance as plasticizers in PVC films was evaluated. While this may seem straightforward, processing PVC may require suitable equipment to avoid corrosion due to the potential evolution of chloride compounds, especially when operating at high temperatures.

Several methods can be used to obtain flexible PVC products, including thermocompression, extrusion molding, blow molding, and solvent casting. In the latter, a polymer is dissolved in a suitable organic solvent, which is then evaporated to form a polymer film. This avoids thermal treatment and the potential generation of corrosive gases. Therefore, the solvent casting method is widely used for research purposes.

In general, a formulation for flexible PVC incorporates between 20 to 50% of plasticizer, aside from the primary polymer [161]. Higher amounts can lead to exudation and lower compatibility with the polymer. The potential molecular interactions of the epoxide plasticizers with PVC polymer are shown schematically in Figure 4-1. These interactions not only provide plasticity but also help stabilize the polymer to prevent decomposition. In this regard, this chapter investigates the performance as well as the plasticization effect of the epoxidized isobutyl esters and compares the results with those obtained for standard PVC plasticizers. The performance of the proposed oleochemical plasticizers will be analyzed in terms of mechanical and thermal properties, contact angle, water vapor transmission permeability, migration, and volatility rate of the plasticizer in PVC films.

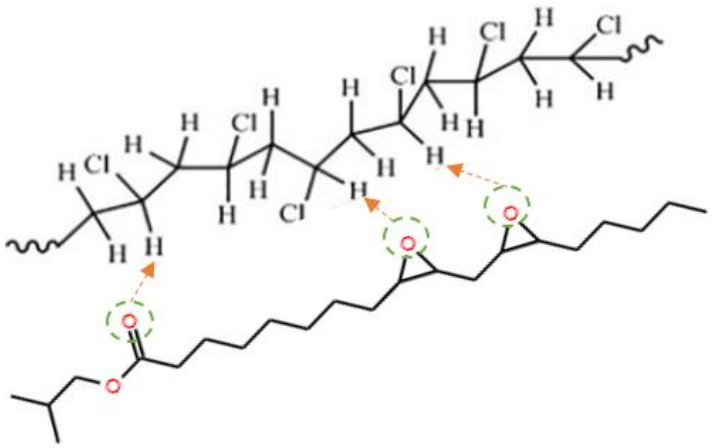

Figure 4-1. Plasticized PVC with epoxidized isobutyl esters

4.1 Methodology

To evaluate the performance of the epoxidized plasticizers, PVC films were prepared using the solvent casting technique with a fixed plasticizer content of 70 phr (41% wt). Additionally, DOP and ESO were selected as industrial benchmark plasticizers for a comparative performance evaluation. Four films of each formulation were prepared and conditioned for analysis.

- **Reagents**

PVC resin Lacovyl PB1172H (K value 68) supplied by Atofina, and tetrahydrofuran (THF, 99.5% Merk) were used in the solvent casting method for polymeric film production. The assessed biobased plasticizers were synthesized and purified as described in the previous chapter and they are denoted as EIO (epoxidized isobutyl oleate), EIL (epoxidized isobutyl linoleate), EID (epoxidized isobutyl soyate distillate), and EIS (epoxidized isobutyl soyate). The industrial benchmark plasticizers were dioctyl phthalate (DOP, 99.5%, Traquisa) and ESO (epoxidized soybean oil 99.5% Traquisa). Silica gel was used as a desiccant and ethanol (96%, Merck) was used to perform migration tests.

- **Film preparation**

PVC films were prepared by solvent casting method, following a methodology previously reported [162]. The PVC resin was mixed with the corresponding plasticizers at 70 phr (41% wt) and 9 ml of THF per 0.4g of PVC resin was added. The formulation of each film is presented in Table 4-1.

Table 4-1. Formulation of PVC Films

Material	PVC	PVC/DOP	PVC/ESO	PVC/EIO	PVC/EIL	PVC/EID	PVC/EIS
PVC (g)	1.60	0.80	0.80	0.80	0.80	1.20	0.80
Plasticizer(g)	0.00	0.56	0.56	0.56	0.56	0.84	0.56
THF(ml)	27.0	18.0	18.0	18.0	18.0	27.0	18.0

The mixture was homogenized at room temperature using a magnetic stirrer until all the PVC was dissolved. The solution was then poured into a 10 cm diameter petri dish and allowed to air dry until a constant mass was obtained. Once dry, the films were conditioned at a constant humidity of 30% inside a chamber at room temperature before characterization.

- **Methods**

The thickness of the films was measured using an electronic RS PRO micrometer at multiple points throughout the film. Ten measurements were taken, and the reported thickness corresponds to the average value.

Thermogravimetric analysis (TGA) was conducted using a Linseis PT1000 thermogravimetric balance (Selb, Germany). Samples of about 10 mg were heated at a constant heating rate of 20 K/min from 30 to 700°C under a nitrogen purge gas flow rate of 50 ml/min. Additionally, Differential Scanning Calorimetry (DSC) analysis was performed on a Mettler Toledo 821 calorimeter following a programmed temperature protocol at a constant heating rate of 10 K/min. The temperature ramp was initiated by heating from 30 to 100°C, then cooling from 100°C to -50°C, and finally heating from -50°C to 200 °C using a flow rate of N_2 of 55 ml/min.

The mechanical properties of the films, including tensile strength, elongation at break, and Young's modulus, were characterized at room temperature using a DUOTRAC-10/1200. The films were cut into rectangular strips measuring 80 x 10 mm following the ASTM D882

standard [163]. The grip spacing and crosshead speed were set to 50 mm and 10 mm/s respectively, using a 0.1kN cellule.

Fourier transform infrared spectrometry (FTIR) was performed using a Perkin Elmer Spectrum BX scanning over the range of 4000 to 500 cm^{-1} at a resolution of 4 cm^{-1}. In addition, to evaluate the transparency of the PVC films, UV-vis spectra were measured using a G9821A UV-Vis spectrophotometer over the range of 800 to 200 nm at a scan rate of 600 nm/min.

The water contact angle between a drop of water and the film surface was measured using an optical goniometer FM140 (KRÜSS GmbH) under ambient conditions. The contact angle was measured ten times per material, and the average value is reported.

Water vapor transmission permeability (WVTP) was analyzed gravimetrically by measuring the moisture gain of the films over time according to ISO 2528 [164]. Films measuring 3.6 in diameter were placed inside a constant humidity chamber (90%) at 23°C for 7 hours. WVTR is calculated using Equation (4-1), based on the definition of water vapor.

$$WVTR = \frac{\Delta m}{t \cdot A} \tag{4-1}$$

In Equation (4-2) Δm (g/h) is the slope of the curve obtained by linear regression of the weight gained by the film over time, where t is the time (h), and A is exposed area (m^2). Then, WVTP is calculated using (4-2).

$$WVTP = \frac{WVTR}{S \cdot (RH_1 - RH_2)} \cdot e \tag{4-2}$$

In Equation (4-2), S is the saturation pressure at the test conditions, RH_1 is the relative humidity inside the chamber, RH_2 is the relative humidity inside the cup, and e is the film thickness (mm).

The migration rate of the plasticizers was evaluated at three different temperatures: 50, 40°C, and 23°C for 24 hours in aqueous ethanol (96% and 50%) following the standard method ASTM D1239 [165]. Samples were weighed and immersed in 100ml of the solvent. After 24 hours, the samples were dried in an oven at 40°C for 24 hours and the final weight was reported. The extraction loss was calculated according to Equation (4-3).

$$Weight\ loss\ (\%) = \frac{W_1 - W_2}{W_1} * 100 \quad (4\text{-}3)$$

In Equation (4-3) W_1 is the initial weight of the test specimen, and W_2 is the final weight of the test specimen.

Volatility tests were conducted following the standard method ISO 176 [166]. Samples in the form of disks with a diameter of 50 mm were weighed and immersed in circular flasks filled with activated charcoal. The test was performed at 70°C for 24h. Volatility loss was calculated according to Equation (4-3).

4.2 Results

4.2.1 Film preparation

A visual comparison of the different plasticized films is presented in Figure 4-2. All the films were prepared with a fixed plasticizer content of 70 phr (41% wt).

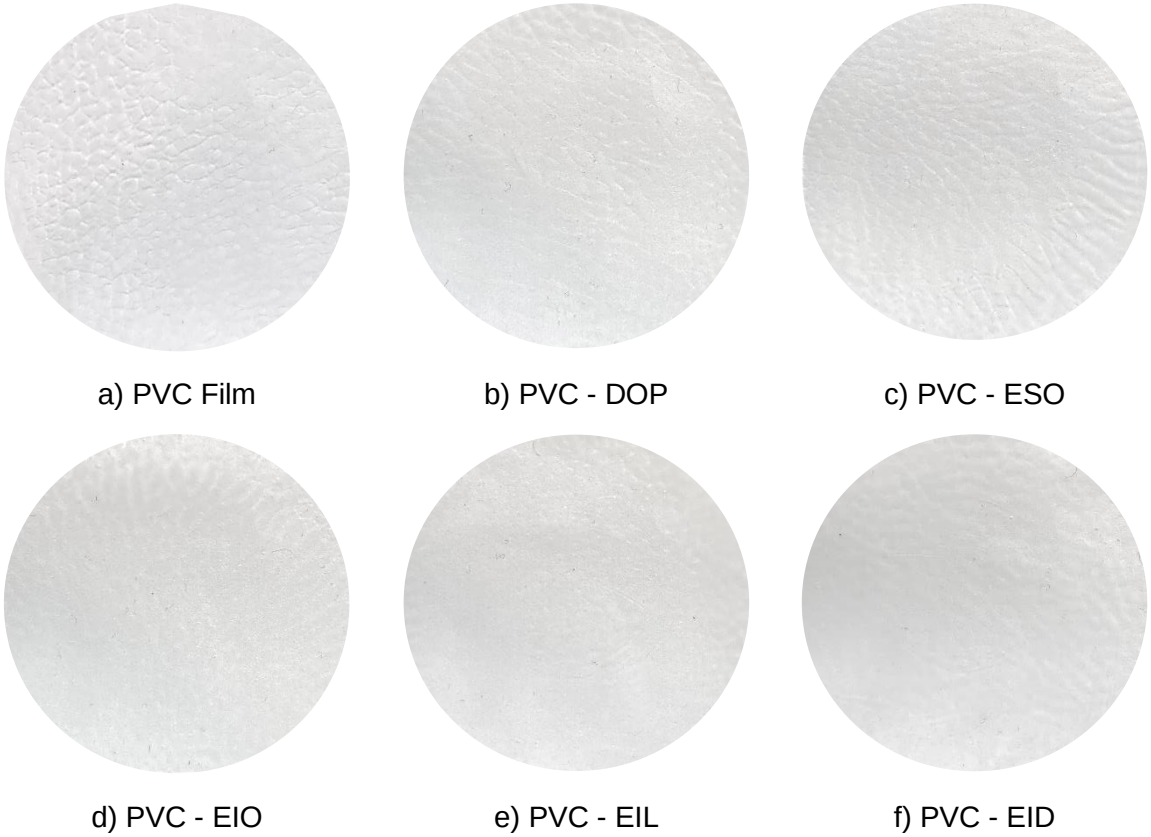

a) PVC Film b) PVC - DOP c) PVC - ESO

d) PVC - EIO e) PVC - EIL f) PVC - EID

g) PVC - EIS

Figure 4-2. PVC films prepared by solvent casting.

In general, the different PVC films prepared by the solvent casting process were homogeneous, sparkling, and transparent with a characteristic film thickness ranging between 0.17 to 0.26 mm. An increase in the average film thickness was observed with the addition of plasticizers. In particular, the films prepared with EIO, EID, and EIS developed a yellowish color, being more intense in the PVC/EIS film as observed in Figure 4-2. This was expected as the original epoxides had a characteristic yellowish tone after purification, and if found suitable, their use as plasticizers would be possible only in dark plastic products or after a suitable bleaching process.

4.2.2 Mechanical Properties

The average thickness, as well as the mechanical properties of the films, are presented in Table 4-2. Thickness, Elongation at break (E), Tensile strength (TS), and Young's modulus (YM) were measured for the films prepared with and without plasticizer. As can be seen, the pure PVC film had a lower thickness compared to the films prepared with additives. This is expected since the plasticizer creates more space between the polymer macromolecules and reduces their intermolecular forces, promoting high thickness and low density in the film. Regarding the mechanical properties, the pure PVC film achieved a tensile strength of 37.7 MPa, an elongation at break of 24.6%, and Young's modulus of 1023.6 MPa. These values agreed with the mechanical properties reported by other authors [18],[48],[167]. Comparatively, the addition of all types of additives derived in a much larger elongation confirmed their plasticizing effect. In contrast, both tensile strength and Young's modulus were much lower for pure PVC which is consistent with plastic behavior [168].

Table 4-2. Average thickness and mechanical properties of plasticized PVC

Material	Thickness (mm)	E (%)	TS (Mpa)	YM (MPa)
PVC	0.166 ± 0.006	24.60 ± 2	37.7 ± 2	1023.6 ± 56
PVC/DOP	0.240 ± 0.007	362.1 ± 15	9.1 ± 0.6	5.5 ± 1
PVC/ESO	0.237 ± 0.011	442.8 ± 8	13.7 ± 0.9	6.7 ± 1
PVC/EIO	0.233 ± 0.008	453.6 ± 20	9.6 ± 0.2	4.0 ± 1
PVC/EIL	0.256 ± 0.011	323.0 ± 10	5.6 ± 0.3	3.1 ± 1
PVC/EID	0.229 ± 0.023	466.8 ± 28	10.9 ± 0.9	4.5 ± 1
PVC/EIS	0.223 ± 0.005	498.8 ± 14	11.2 ± 0.6	4.3 ± 1

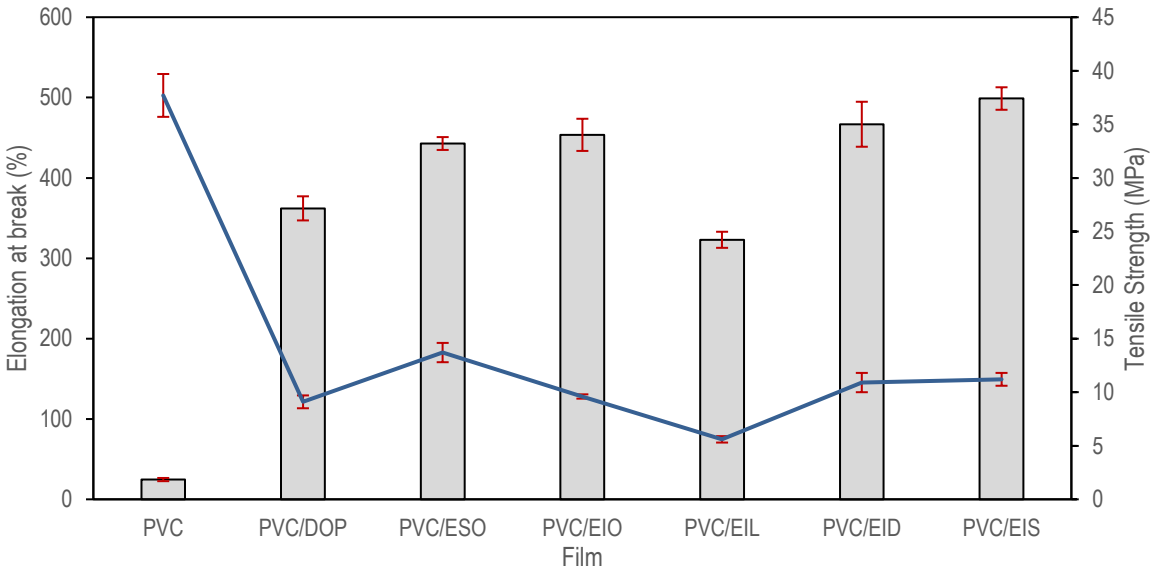

Elongation at break (■) and tensile strength (—)

Figure 4-3. Mechanical properties of plasticized PVC.

In particular, the assessed biobased isobutyl plasticizers reached an elongation at break between 323 and 499%, along with low tensile strength values (13.7 – 5.6 MPa). These results are comparable to those achieved by the reference plasticizers DOP and ESO. The film PVC/EIS showed the highest elongation at break (499%), which is 20 times higher than that of pure PVC. The improvement in these properties is mainly attributed to the intermolecular forces (hydrogen bond, polar, and dispersion forces) between the polymer and plasticizer which reduce the interaction forces between polymer-polymer. Such interactions improve the mechanical properties of the polymer making it more flexible and ductile, thereby facilitating workability and processing [161],[169].

In the case of PVC/EIL, this film did not reach the same elongation values as those obtained by the other isobutyl epoxides. However, EIL significantly reduced the tensile strength (5.6 MPa) and Young's modulus (3.1 MPa). Additionally, it exhibited similar behavior to the film containing the traditional DOP plasticizer. Comparatively, all other isobutyl plasticizers were more like traditional epoxidized soybean oil plasticizers.

The observed results agreed with those reported by other authors. For instance, in previous research, butyl epoxidized esters of palm kernel oil (EEPKO) were evaluated as effective plasticizers for PVC [37]. In that study, different formulations of PVC were prepared at different processing temperatures using the dispersion technique. As a result, the tensile strength of plasticized PVC/EEPKO at 65 phr ranged between 6-10 MPa. Similar results were obtained by PVC plasticized with DOP (10-15 MPa). Regarding elongation at break, values of 410% and 350% were obtained for PVC/EEPKO and PVC/DOP, respectively, when the PVC was processed at 200°C.

4.2.3 Thermal Properties

- **Glass transition temperature**

Plasticizers increase the chain mobility in the polymer matrix, lowering the glass transition temperature (Tg), which occurs over a range of temperatures depending on the composition and purity of the plasticizers [169], [170]. The glass transition temperature of neat PVC and plasticized PVC was obtained from DSC analysis, and the obtained scanning profiles are presented in Figure 4-4.

As observed, the glass transition temperature of pure PVC was about 83.4°C which is consistent with literature reports [167], [171]. In some additives, no significant endothermic shift in the baseline (Tg) was observed as the temperature increased [167]. This was the case of PVC plasticized with EIL and DOP. Therefore, the glass transition temperature of the different plasticizers was confirmed by DMTA analysis, as indicated in Figure 4-4.

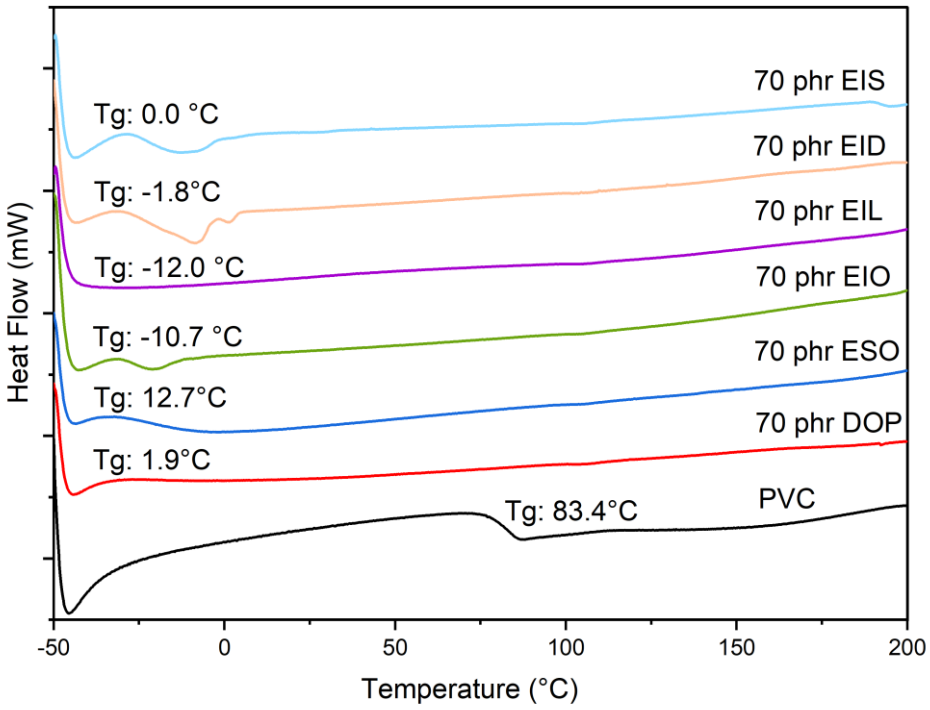

Figure 4-4. Glass transition temperature of plasticized PVC

As expected, films prepared with the different epoxidized molecules exhibited low Tg values demonstrating the plasticization effect. These values agreed with the Tg reported by other authors. For instance, in the study of butyl epoxidized esters of Palm kernel oil, glass transition temperatures of -23°C and -32°C were found for PVC plasticized with EEPKO and DOP, respectively [37].

- **TGA**

TGA and DTGA curves of the evaluated PVC films are presented in Figure 4-5 and Figure 4-6 respectively. The corresponding maximum weight loss peak is reported in Table 4-3.

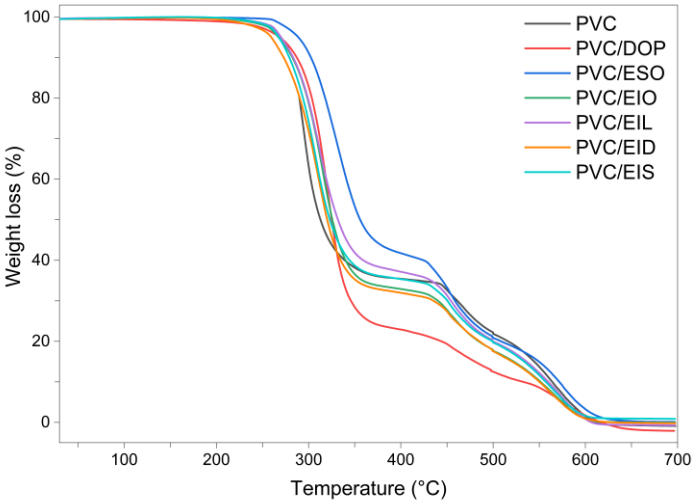

Figure 4-5. TGA curves of PVC films

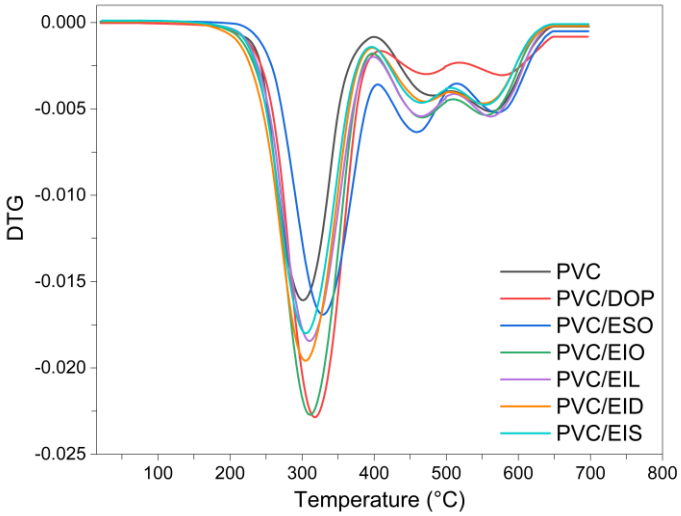

Figure 4-6. First TG derivate curves of PVC films

Table 4-3. DTG of PVC films

Material	1		2		3	
	Tm	Weight loss(%)	Tm	Weight loss(%)	Tm	Weight loss(%)
PVC	301.6	39.0	480.9	74.7	561.9	89.4
PVC/DOP	317.4	37.5	471.8	83.9	578.3	95.7
PVC/ESO	329.2	29.6	457.9	39.7	570	89.5
PVC/EIO	311.4	33.0	467.0	76.6	555.6	90.9
PVC/EIL	311.3	31.8	464.3	73.0	561.8	90.5
PVC/EID	304.1	32.2	470.9	77.5	550.7	90.1
PVC/EIS	301.8	27.6	467.0	74.7	553	89.0

In general, plasticizers induce higher thermal stability in polymers due to their molecular interaction with active groups and their scavenging capacity of labile chlorine atoms from the polymer [170].

As observed, all TGA curves exhibited three characteristic thermal degradation stages. The first stage occurred between 250 to 350°C which is associated with the decomposition of plasticizers and the dichlorination of PVC, followed by the release of HCl. The second stage, which occurred above 430°C, corresponds to the crosslinking reaction of C=C bonds to form aromatic compounds. The last stage, above 560°C, is related to the complete oxidation of the material to produce a char residue [48].

From these profiles, it is possible to observe a thermal stabilization effect of the epoxidized esters in terms of the corresponding degradation temperature. Tm represents the temperature at which the maximum weight loss occurs [69]. In this sense, there was a slight shift towards high decomposition temperatures (Tm) when the blends contained the different assessed plasticizers. The epoxides EIL, ESO, and DOP increased the thermal stability of PVC by 10, 16, and 28 °C respectively. On the other hand, EIO, EIS, and EID exhibited low shifting ranging from 10 to 1°C.

The inflection point of the first stage of thermal degradation provides information about the maximum rate of weight loss. During this stage, a weight loss of 39% was observed for pure PVC. The plasticizers that were assessed exhibited low weight losses ranging from 27.6% to 37.5%. Although the thermal stability of EIS seems to be marginal as it only increased the Tm by 1°C, it resulted in the lowest weight loss during this stage. This result can be explained by considering the particular composition of the SODD, which is rich in antioxidants and vitamins [13].

Generally, like commercial DOP, films plasticized with biobased epoxidized esters exhibited high thermal stability below 250°C. This suggests that they can be utilized in PVC products that require thermal processing, without experiencing significant degradation.

4.2.4 Water Vapor Permeability

Water vapor permeability (WVP) is a measure of the amount of water that passes through a surface per unit of area, time, and pressure. WVP is an important barrier property of packaging material as it protects food from environmental factors such as water, water vapor, odors, exudation, moisture, grease, oil, etc. Suitable barrier properties depend on the specific nature of the food being packed. For example, fruits and vegetables require a low gas barrier to release carbon dioxide, whereas meat products require a high gas barrier to prevent moisture loss [172]. PVC is one of the main thermoplastic materials used in food packaging and has a wide range of applications [172].

The corresponding WVP values of the PVC films assessed are presented in Figure 4-7 As observed, the lowest WVP was observed for the neat PVC film, which was around $3.0 \cdot 10^{-13}$ (g $\cdot m^{-1} \cdot s^{-1} \cdot Pa^{-1}$) at 23°C and 90% RH. This result is consistent with those reported in the literature for this material, which ranges from ($4 \cdot 10^{-14}$ to $2 \cdot 10^{-13}$ g $\cdot m^{-1} \cdot s^{-1} \cdot Pa^{-1}$) [3]. The incorporation of a plasticizer in the PVC film breaks the orderly structure of the polymer

chains and increases the free volume, thereby allowing water to pass more easily through the film [173].

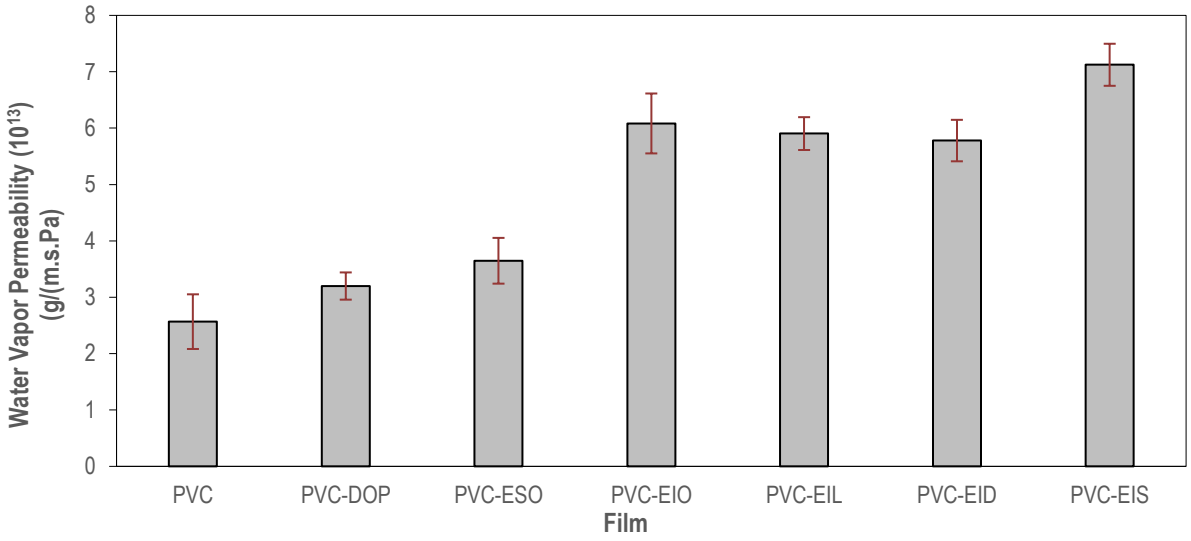

Figure 4-7. Water Vapor transmission rate

As observed, the WVPR increased with the addition of plasticizer, thereby modifying the barrier properties of the PVC. Isobutyl epoxides achieved higher permeability rates, ranging from 7.0 to $8.2 \cdot 10^{-13}$ $g \cdot m^{-1} \cdot s^{-1} \cdot Pa^{-1}$ compared to the reference plasticizers (DOP and ESO), which exhibited a WVPR of 3.7 and 4.2 10^{-13} $g \cdot m^{-1} \cdot s^{-1} \cdot Pa^{-1}$ respectively. In the case of isobutyl epoxidized, polar groups may interact with water molecules promoting water adsorption instead of its transport through the film. Although, the reference plasticizers DOP and ESO also exhibited hydrophilic affinity, their permeation rates were lower. In this sense. a moderate water vapor barrier can be advantageous for certain packaging applications that require dynamic gas transport through the film.

4.2.5 Contact Angle

The contact angle is a useful parameter to assess surface wettability, mainly for packaging applications. The effect of the plasticizer incorporation in the PVC films on their contact angles is observed in Figure 4-8 and the corresponding values are reported in Table 4-4.

.

Table 4-4. Contact Angle of plasticized PVC

Film	Contact Angle (°)
PVC	81.7 ± 2
PVC/DOP	52.0 ± 3
PVC/ESO	48.8 ± 5
PVC/EIO	67.3 ± 2
PVC/EIL	65.6 ± 2
PVC/EID	67.5 ± 3
PVC/EIS	61.2 ± 1

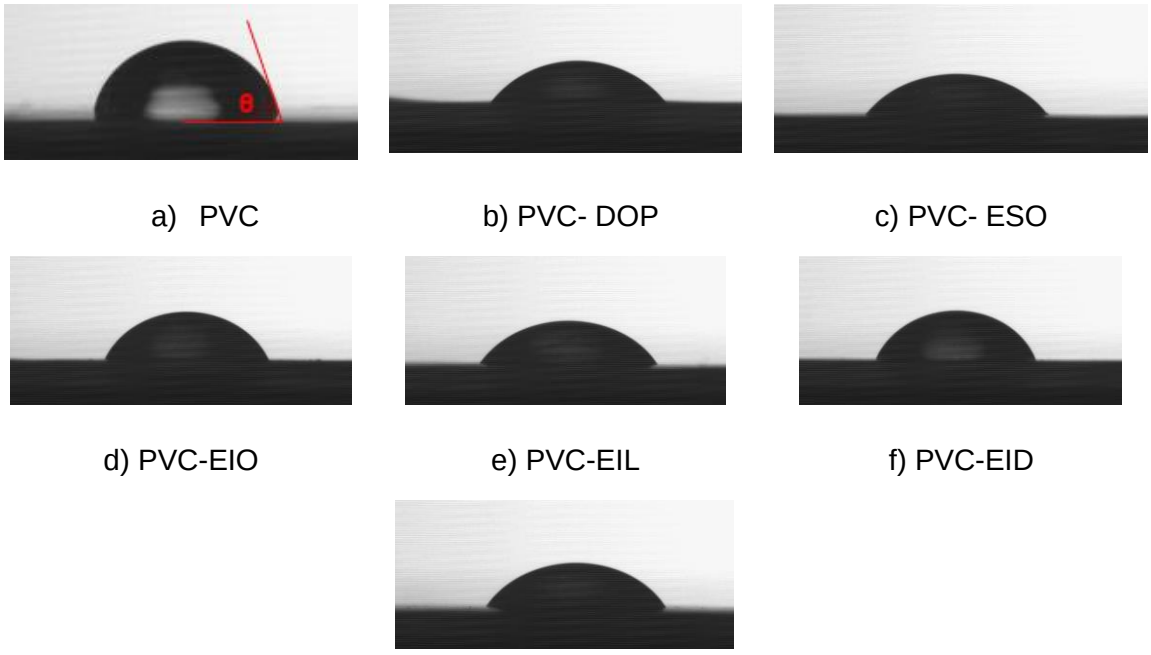

a) PVC b) PVC- DOP c) PVC- ESO

d) PVC-EIO e) PVC-EIL f) PVC-EID

g) PVC-EIS

Figure 4-8. Contact angles of PVC films

Initially, the observed contact angle of pure PVC film was about 81.7°, which is consistent with that reported in previous works [174]. However, when plasticizers were added, the contact angle decreased as the PVC films became slightly more hydrophilic, mainly due to the hydrogen bonding tendency of the oxygen-containing plasticizing molecules. The reduction in the contact angle was more evident in DOP and ESO films. This may be related to the higher content of oxygen atoms and their larger molecular sizes, which facilitate accessibility and interaction with water molecules. On the other hand, epoxidized isobutyl esters exhibited high contact angles ranging from 61 to 67°, being the films PVC/EIO and

PVC/EID the most hydrophobics. Their small molecular size enables a denser packaging of the PVC polymer, which repels water from the surface.

Although some of these results seem to contradict the tendency obtained in the WVP, is important to consider that the roughness of the film surface and loss of plasticizer due to migration can also affect the contact angle. Nonetheless, the slightly hydrophobic behavior of the epoxidized isobutyl esters may be advantageous in food packaging applications and for film coatings on cleanable surfaces.

4.2.6 Optical properties

- **FTIR**

FTIR is a useful technique to identify the principal functional groups in the structure of polymers and the potential presence of functional groups from certain additives or impurities. The characteristic absorption bands of pure PVC and plasticized films are shown in Figure 4-9. As can be seen, the FTIR spectra of the different plasticized materials are different from the spectrum of pure PVC, indicating that the infrared absorption of the plasticizers is stronger than that of PVC [175].

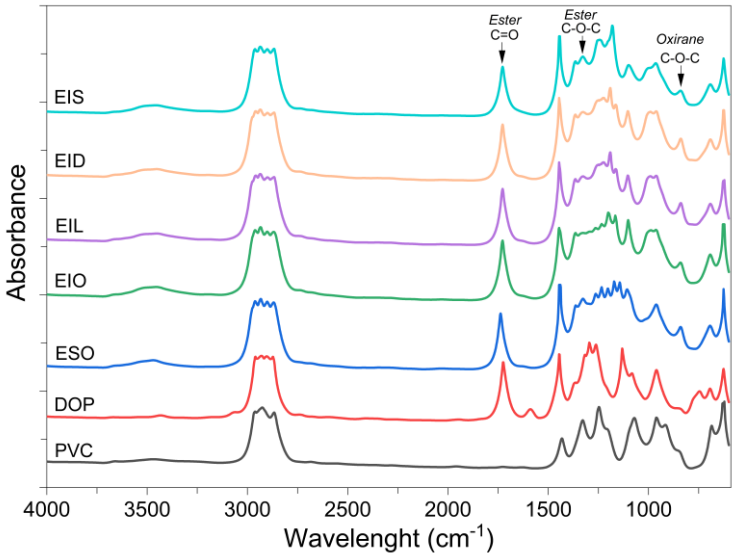

Figure 4-9. FT-IR spectra of plasticized PVC

The incorporation of epoxidized isobutyl esters into the PVC matrix was confirmed by a higher intensity of the peak at 819 cm^{-1}, which is associated with the oxygen oxirane

vibration. The peaks at 1724 cm^{-1} and 1285 are related to C=O and C-O vibration of the ester groups, respectively. Characteristic peaks of the PVC structure were found at 680-605 cm^{-1}, 1000 – 1100 $cm^{-1,}$ and 1425 cm^{-1} which belong to the vibration of HC-Cl, C-C, and aliphatic bond C-H of the PVC backbone [176]. Besides, $-CH_2$ symmetric stretching vibration is identified at 2951 cm^{-1}. Additionally, in the case of DOP, the peak at 1597 cm^{-1} is linked to the C=C on the benzene ring and the peaks at 788 and 690 cm^{-1} belong to the four hydrogen atoms adjacent to the aromatic ring [160].

- **UV-VIS**

Film transparency is an important property in packaging materials as ultraviolet light can cause adverse effects on food quality. These effects range from the destruction of proteins, antioxidants, and nutrients to changes in food smell and color [173]. The transparency of the films was estimated by measuring the ultraviolet-visible light in the range of 200 to 800nm. The absorption spectra of PVC and plasticized PVC films are shown in Figure 4-10.

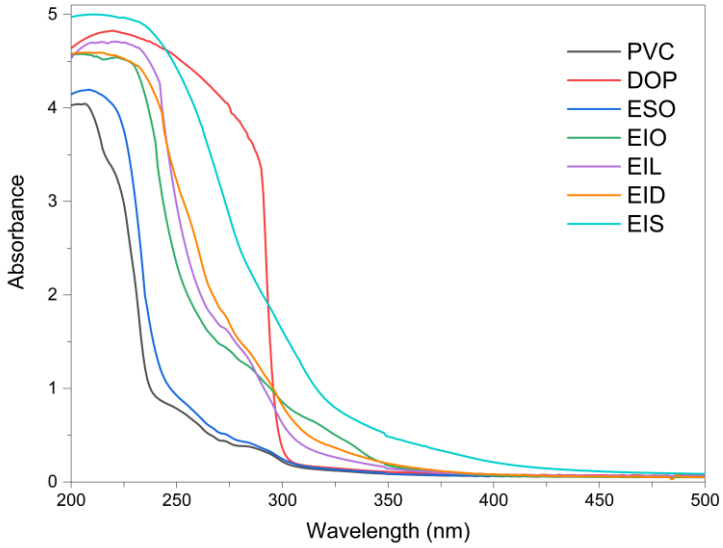

Figure 4-10. UV spectra of plasticized PVC

As can be seen, pure PVC film was the most transparent. The yellowish coloring of some epoxides, especially those derived from soybean oil distillates increases the absorption of visible light, resulting in a loss of transparency. In this sense, the absorption of the visible light of materials decreases in the following order: EIS> DOP >EID>EIL> EIO>ESO>PVC.

The epoxides derived from the soybean oil distillates have a characteristic color due to the pigments present in the raw material. This might indicate a need for a bleaching step during the downstream purification of the different epoxides. Alternatively, those plasticizers can be directed to dark PVC products only.

4.2.7 Migration and volatility losses

Migration and volatility rates depend mainly on the chemical structure, molecular weight, solubility, and compatibility of the plasticizer [48], [174]. To evaluate the migration losses of the plasticized films, aqueous ethanol at 96% and 50% was employed as solvent. The migration losses of plasticized PVC are summarized in Figure 4-11.

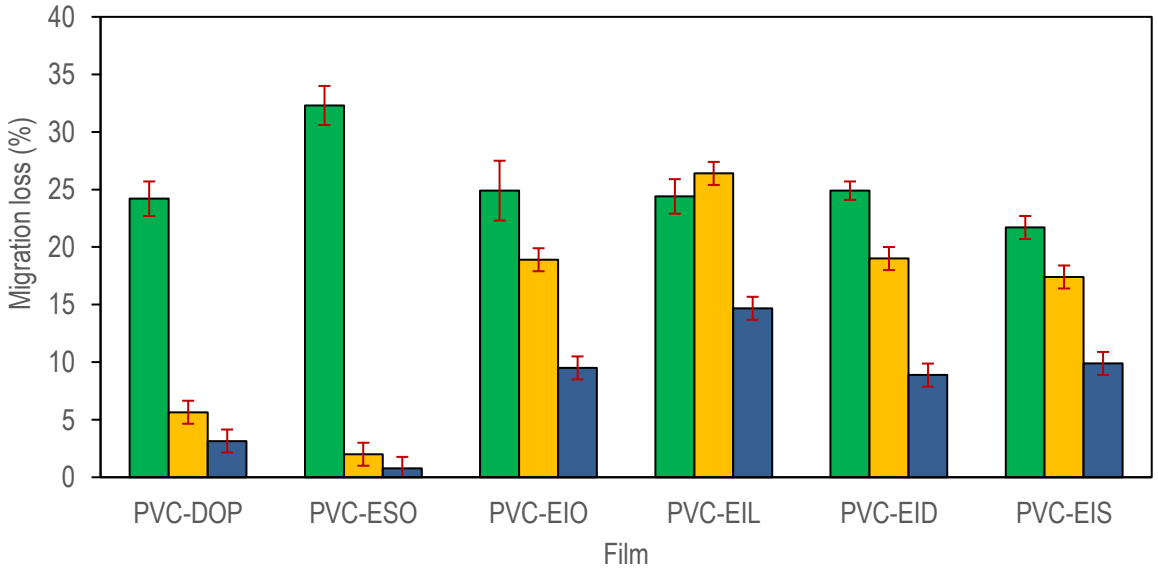

(■) 50°C (95% ethanol). (■) 40°C (50% ethanol). (■) 23°C (50% ethanol)

Figure 4-11. Migration loss of the evaluated plasticizers.

Within the conditions evaluated for the migration assays, the films immersed in 96% wt. ethanol presented the highest migration rates. Under these conditions (96% and 50°C), the migration losses were higher than 20% for all films. The PVC-ESO film exhibited the highest migration loss (32%) and the film PVC-EIS the lowest (21.7%). These values are close to the maximum possible migration, which is 41% (70 phr). Under these test conditions, all the plasticizers may have migrated into the solvent due to the thin thickness of the films (~0.2 mm). These high migration rates are related to the principle of “like dissolves like”, so

isobutyl plasticizers are expected to be soluble in a polar organic solvent such as ethanol. This might represent a major drawback for the use of isobutyl plasticizers in polymers intended for liquid containers and for materials that would be in continuous contact with organic solvents. At low temperatures (40 and 23°C) and using a diluted ethanolic solution (50%) the migration losses showed a different behavior. In this case, the EIL exhibited the highest migration rate, followed by EIO-EID-EIS with similar migration rates, then DOP with a moderate migration rate, and finally ESO, which exhibited the lowest migration (1 - 2%).

These results can be explained by the small size of isobutyl ester molecules that makes it more susceptible to being dissolved by alcohol. Additionally, the interaction of the oxirane and hydroxyl groups is more effective in smaller molecules. Based on these results, the migration loss of the different plasticizers solvents should be evaluated using solvents of different polarities to determine a suitable application for these additives.

To evaluate volatility losses, the different films were heated at 70°C for 24 hours. Figure 4-12 gathers the results of these test conditions.

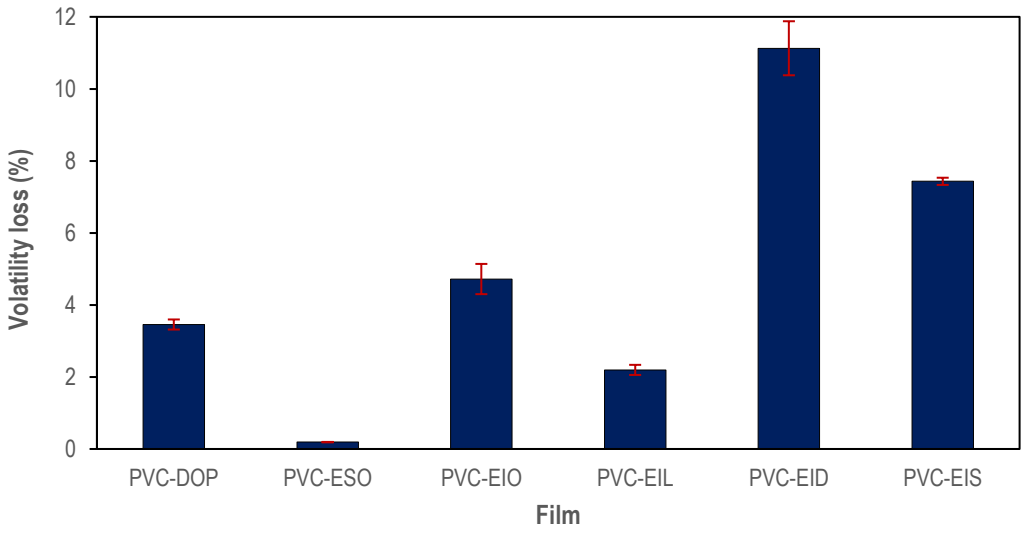

Figure 4-12. Volatility loss of the evaluated plasticizers

Volatility is closely related to the molecular weight and molecular structure of a substance. Although EID and EIS have the highest molecular weight (476.7 and 429.8 g/mol), these plasticizers exhibited high volatility losses of 11.1 and 7.4%, respectively. Nonetheless, it is important to note that the molecular weight of the materials is an average since they are

derived from a mixture of esters and fatty acids of varying molecular weights. As a result, it is expected that EID and EIS may contain volatile components such as short-chain fatty acids, aldehydes, and ketones which contribute to their high volatility rates. This is also consistent with their high solvent extraction rates. On the other hand, EIL and ESO exhibited low volatility losses, ranging from 2% to 0.2%, respectively. This is due to their high oxirane content, which enhances the permanence of the plasticizer in the polymer.

4.2.8 Overall performance

In general terms, it was verified that the implemented product design methodology was suitable to identify potential plasticizing molecules for PVC polymers. Based on the overall performance of isobutyl esters as plasticizers, these additives improve thermal degradation and provide high elasticity and ductility, and exhibit moderate water barrier properties. However, these additives also exhibit high migration rates in polar solvents on account of the nature of the attractive forces of the ester and oxirane group or possible cleavage of the oxirane group.

In the case of SODD epoxides, the presence of impurities and minor components in the raw material seems to increase the migration and volatility losses of the plasticized films. Therefore, while the PVC/EIS and PVC/EID plasticizers offer a well-balanced flexible polymer, their application needs to be limited considering volatility and migration losses depending on the processing conditions. In the case of isobutyl epoxides, they are smaller molecules compared to ESO and DOP, which increases their migration and volatility rates. This represents a major issue and can limit the potential use of these molecules for PVC plasticization.

Although it was verified that the implemented methodology can assist in guiding the design of new plasticizing molecules, there is still need for a more robust methods to predict performance properties. Specifically, there is a need to improve the estimation of key performance properties such as permeation and weight loss. For example, such models could evaluate the differences between linear and branched molecules, as well as the impact of minor components.

5. Conclusions and recommendations

5.1 Conclusions

This work developed a simplified product design methodology and evaluated its effectiveness in designing biobased plasticizers. The methodology was based upon a comparative assessment of the performance properties of the potential candidate molecules to those of the most used general-purpose plasticizers. This approach was successfully implemented in the design of oleochemical plasticizers based upon epoxidized fatty acid esters to exploit and valorize agro-industrial oleochemical streams. Soybean oil deodorization distillates were used as raw material, and the intended molecules were obtained by esterification and subsequent epoxidation process. After applying the molecular design approach to epoxides of fatty acids present in the deodorization distillates with different biobased alcohols, it was identified that isobutyl epoxides could be promising plasticizing molecules for PVC. Then, after suitable synthesis and separation steps at different scales, isobutyl epoxides were characterized and assessed as potential PVC plasticizers.

During the experimental esterification and epoxidation processes, high conversions were achieved. The esterification step resulted in high productivity and a high ester content after purification. However, the epoxidation reaction only achieved a maximum yield of 62%, representing an oxirane equivalent content of 5.2% wt. The low yield was due to competitive ring-opening reactions that degraded the oxirane, resulting in losses of oxirane. Nevertheless, the oxirane content of the final products falls within the range of commercial epoxides. Subsequently, a kinetic model for the epoxidation of isobutyl linoleate was developed through modeling of the reaction. Based on this model, reaction conditions were

optimized for the synthesis of plasticizers on a bench scale, using acid oleochemical streams as raw material.

After synthesis and purification of the different materials at the bench scale, they were assessed as plasticizers and exhibited good performance properties. Isobutyl epoxides exhibited good mechanical properties comparable to those obtained by the reference plasticizer (DOP). In addition, they also exhibited good low-temperature properties, high resistance to thermal degradation, and moderate transparency. Although the color of the final epoxide was enhanced after the epoxidation process, SODD derivatives would require a bleaching process to meet technical color specifications. Alternatively, their use should be limited to specific applications (e.g. dark products). In addition, these additives are partially soluble in polar solvents due to their polar nature, which may limit their applicability when polar substances are present.

Finally, the valorization of agro-industrial streams such as SODD to produce bio-based plasticizers offers a wide field of action and the possibility of tailoring a wide range of transformations to meet the industry requirements.

5.2 Recommendations

Future research can focus on evaluating more efficient catalysts for the epoxidation process that facilitate the separation and purification stages. Especially for the case of epoxidized esters more selective catalysts are required since the acidity of the reaction medium triggers ring-opening reactions and increases the rate of ester hydrolysis. Advanced heterogeneous catalysts, such as ion exchange resins, amorphous Ti/SiO_2, rhenium, or tungsten-based catalysts, could be used to achieve higher yields and selectivity, thereby having further industrial applications.

On the other hand, SODD is a complex matrix containing FFA, glycerides, and unsaponifiable material. Its processing can involve acid removal treatments such as solvent extraction process with polar solvents, to isolate and purify fatty acids for different applications, including plasticizers production.

Furthermore, the epoxides derived from the SODD contain valuable compounds (e.g. vitamins, antioxidants, tocopherols, etc.). These minor components could provide additional

functional action (e.g. antioxidant activity) to the plasticizers that could be valuable in food applications. This could be the object of study of a future work.

Annex A: Analytical methods

Annex A describes the conditions that were employed for the characterization of raw materials and products according to ISO standards. The amounts described in the official methodologies were modified to reduce the consumption of reagents. These procedures were evaluated in previous work to ensure their reproducibility [57].

A.1 Acid value

The acidity expressed as acid value or acid number was determined according to ISO 660 by the titration method.

- **Reagents:** 0.1M and 0.01M sodium hydroxide solution (NaOH), potassium biphthalate, ethanol, toluene, and phenolphthalein.
- **Standardization:**

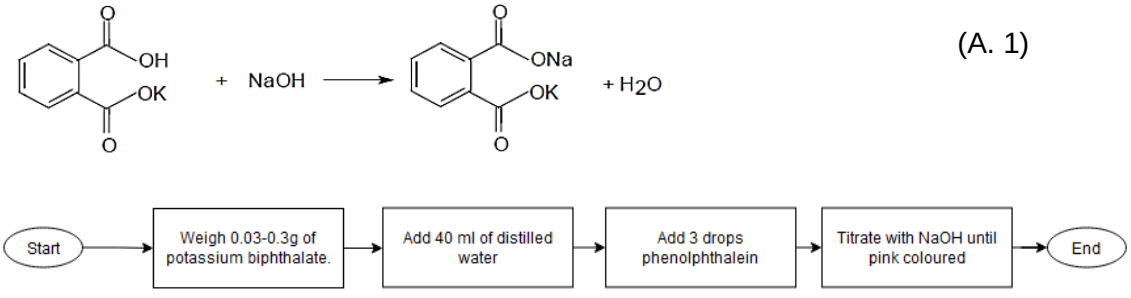

(A. 1)

Figure A-1. Standardization of NaOH for acidity value analysis

- **Measurement:**

$$RCOOH + NaOH \rightarrow RCOONa + H_2O \quad \text{(A. 2)}$$

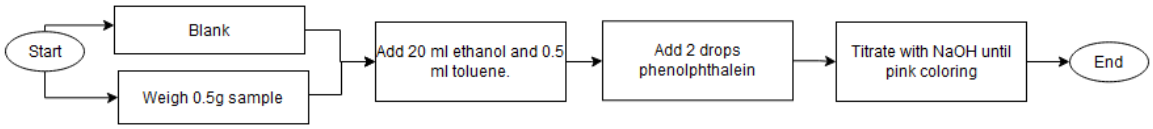

Figure A-2. Procedure for acid value analysis

- **Calculations:** The acid number is expressed as mg of NaOH required to neutralize the fatty acids of 1g of the sample.

$$AV = \frac{56.1 * C * (V_1 - V_0)}{m} \quad \text{(A. 3)}$$

In Equation (A.3) C is the NaOH concentration (mol/L), V_1 and V_0 are the volume (ml) of NaOH solution used in the sample and the blank respectively, and m is the mass of the sample. The acidity expressed as the fatty acid content (%) can be calculated as follows:

$$\%\, Acidity = \frac{(V_1 - V_0) * \mathrm{C} * \mathrm{M}}{10 * m} \quad \text{(A. 4)}$$

In Equation (A.4) M is the molar mass of the reference fatty acid used for the calculation of acidity

$$\%\, Acidity = 0.5 * \mathrm{VA} \quad \text{(A. 5)}$$

A.2 Iodine Value

The iodine value was carried out according to ISO 3961.

- **Reagents:** Wijs reagent 0.2N, potassium iodide KI (10%), potassium iodate KIO_3 (0.013N), starch solution (1%), sodium thiosulphate $Na_2S_2O_3$ $5H_2O$ (0.06N), HCl 4M, chloroform ($CHCl_3$).
- **Standardization:** Molar concentration of sodium thiosulphate ($Na_2S_2O_3$ $5H_2O$) is standardized using KI as a primary standard and a KIO_3 solution.

$$IO_3^- + 5I^- + 6H^+ \rightarrow 3I_2 + 3H_2O$$
$$I_2 + 2S_2O_3^{2-} \rightarrow 2I^- + S_4O_6^{2-} \quad \text{(A. 6)}$$

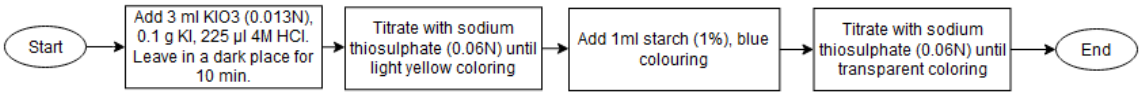

Figure A-3. Standardization for iodine value analysis

- **Measurement:**

$$R_1C = CR_2 + ICl_{(excess)} \rightarrow ClC - CI + ICl_{(remaining)}$$
$$ICl_{(remaining)} + I^- \rightarrow Cl^- + I_2 \quad \text{(A. 7)}$$
$$I_2 + 2\,S_2O_3^{2-} \rightarrow 2I^- + S_4O_6^{2-}$$

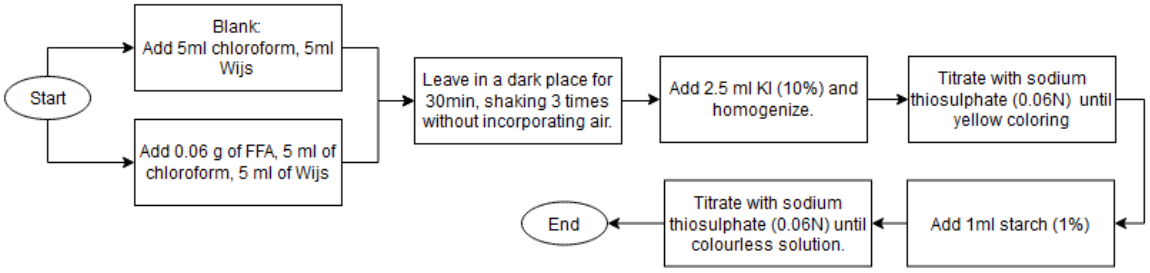

Figure A-4. Procedure for iodine value analysis

- **Calculations:** The iodine value is defined as I_2 absorbed (g) per 100 g of sample:

$$II = \frac{(\boldsymbol{V_0 - V_1}) * \mathbf{C} * \mathbf{12.69}}{\boldsymbol{m}} \quad \text{(A. 8)}$$

In Equation (A.8) C is the concentration of the solution of sodium thiosulphate (mol/L), V_0 and V_1 are the volume (ml) of the thiosulphate solution used in the titration of the blank and the sample respectively and m is the mass of the sample in (g).

A.3 Peroxide Value

The peroxide value was determined according to ISO 3960.

- **Reagents:** saturated potassium iodide solution KI, potassium iodate KIO_3 (0.0013N), sodium thiosulphate $Na_2S_2O_3$ $5H_2O$ (0.0015N), and starch solution (1%).
- **Standardization:** the standardization of the sodium thiosulphate solution is carried out according to the procedure described in A.2.

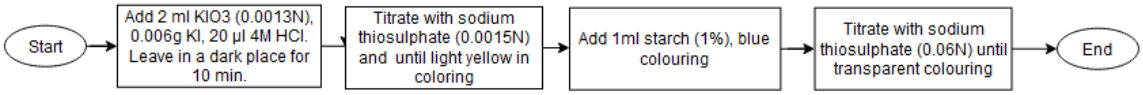

Figure A-5. Standardization for peroxide value analysis

- **Measurement:**

$$\begin{matrix} OOH \\ | \\ R_1CHR_2 \end{matrix} \quad 2\,I^- + 2H^+ \longrightarrow \begin{matrix} OH \\ | \\ R_1CHR_2 \end{matrix} \quad + \; 2\,H_2O + I_2 \qquad \text{(A. 9)}$$

$$I_2 + 2\,{S_2O_3}^{2-} \rightarrow 2I^- + {S_4O_6}^{2-}$$

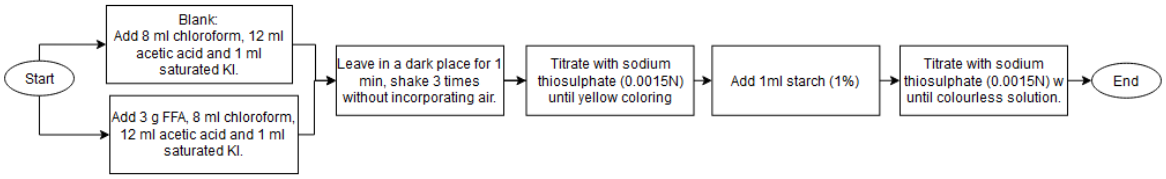

Figure A-6. Procedure for peroxide value analysis

- **Calculations:** The peroxide value is the amount of active oxygen (meq or mmol) chemically bound to fat in the form of peroxides and hydroperoxides per kg of fat.

$$PI = \frac{(\boldsymbol{V_1 - V_0}) * \mathbf{C} * \mathbf{1000}}{\boldsymbol{m}} \qquad \text{(A. 10)}$$

In Equation (A.10) V_1 and V_0 are the volumes of sodium thiosulphate (ml) used in the titration of the blank and sample respectively, C is the concentration of sodium thiosulphate (mol/L), and m is the mass of the sample (g).

A.4 Saponification value

The saponification number was determined according to ISO 3657.

- **Reagents**: Sodium hydroxide NaOH (0.3M), hydrochloric acid HCl (0.3M), ethanolic potassium hydroxide KOH.
- **Standardization**: HCl (0.3M) is standardized using a solution of NaOH (0.3M). This solution is previously standardized using potassium biphthalate according to the procedure described in standardization A.1.

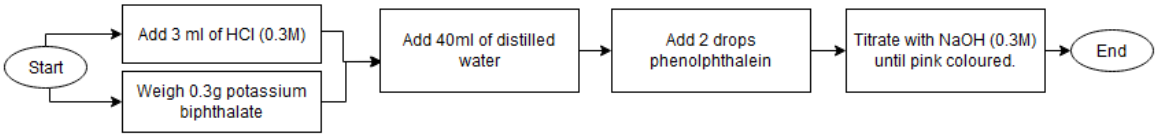

Figure A-7. Standardization of NaOH for saponification value analysis

- **Measurement:**

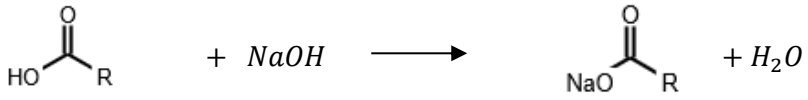

(A. 11)

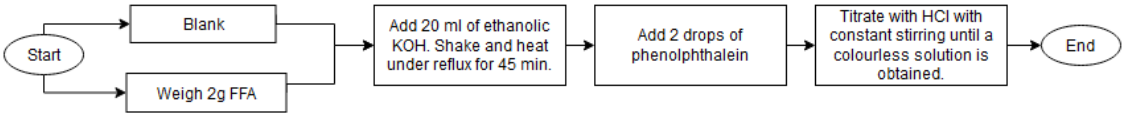

Figure A-8. Procedure for saponification number analysis

- **Calculations:** the saponification value is the amount of KOH (mg) required to saponify 1 g of product.

$$SI = \frac{(V_0 - V_1) * \mathrm{C} * 56.1}{m} \qquad \text{(A. 12)}$$

In Equation (A.12) V_0 and V_1 are the volumes of HCl (ml) used to titrate the blank and sample respectively, C is the concentration of HCl (mol/L), and m is the mass of the sample in (g).

A.5 Unsaponifiable matter

The unsaponifiable matter is measured according to ISO 3596.

- **Reagents:** ethanolic potassium hydroxide KOH (1M), potassium hydroxide (0.5M), diethyl ether, acetone, phenolphthalein.

- **Procedure:**

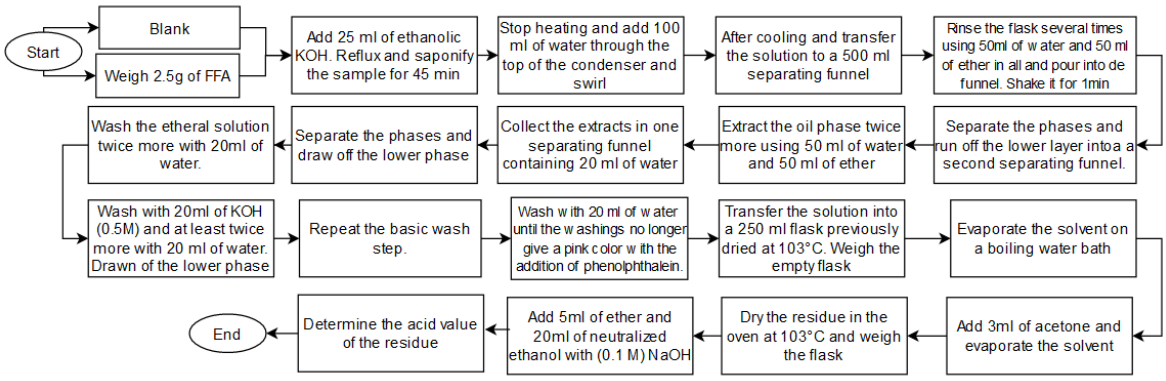

Figure A-9. Procedure for the analysis of unsaponifiable material

- **Calculations:**

$$UM\ (\%) = \frac{(m_1 - m_0) * 100}{m} \qquad \text{(A. 13)}$$

In equation (A.13) m is the mass of the sample in (g), m_1 is the mass of the residue and m_0 is the mass of the residue obtained in the blank.

$$Neutral\ oil\ = 100\% - \%\ unsaponifiable - \%FFA$$

A.6 Oxirane Value

The analysis was carried out based on NTC 2366

- **Reagents:** Chlorohydric acid HCl in isopropanol, sodium hydroxide NaOH (0.1M), potassium biphthalate

- **Standardization:** the standardization of the NaOH solution is carried out according to the procedure described in A.1.

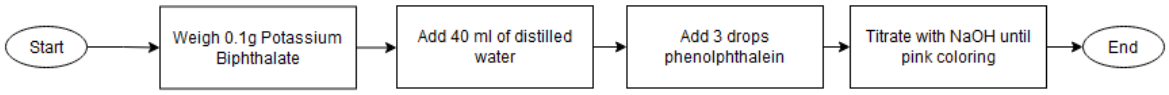

Figure A-10. Standardization of NaOH for acidity value analysis

- **Procedure:**

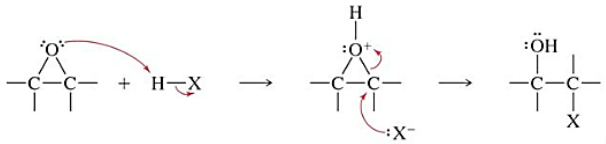

(A. 14)

$$X: Cl$$

$$HCl + NaOH \rightarrow NaCl + H_2O \quad \text{(A. 15)}$$

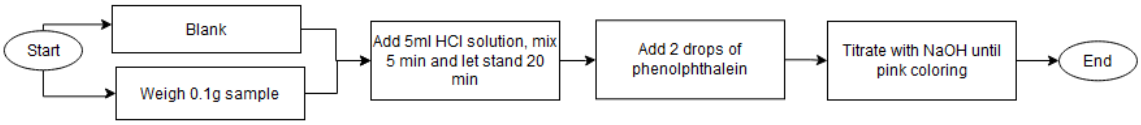

Figure A-11. Procedure for the oxirane oxygen analysis

- **Calculations:**

$$\boldsymbol{OO = \frac{\left[V - V_1 + \frac{V_2}{G} * W\right] * N * 0.016}{W} * 100} \quad \text{(A. 16)}$$

In Equation (A. 16) V is the volume of NaOH solution used to titrate the blank sample (ml). V_1 is the total volume of NaOH used to titrate the test sample (ml); V_2 is the volume of NaOH solution used to titrate the free fatty acids (ml), N is the concentration of NaOH (mol/L); W is the mass of the test sample (g); G is the mass of the test sample employed to determinate the acid value [68]**.**

Annex B: Selection criteria of epoxidized esters

Table B-1. Reference price (2019) used to estimate the cost of the different plasticizers.

Substance	Price (USD/t)	Ref.
DEHP/DOP	1050	[55]
DNOP	1190	[55]
DEHT/DOTP	1220	[55]
DINP	1065	[55]
DIDP	1200	[177]
DBP	1000	[178]
BBP	1700	[179]
Methanol	260	[180]
Ethanol	450	[181]
Propanol	900	[182]
Isopropanol	900	[183]
Butanol	850	[184]
Isobutanol	750	[185]
Isoamyl alcohol	1400	[186]
2-octanol	1400	[187]
Ethylene glycol	575	[188]
1,2 propanediol	1500	[189]
1,3 propanediol	1500	[189]
1,4 butanediol	1500	[190]
Soybean oil	785	[54]
Deodorizer Soybean fatty acids	400	[56]
Epoxidized soybean oil	1700	[52]

Table B-2. Results of the selection criteria for common phthalates and epoxidized esters.

Plasticizer	δt Mpa$^{1/2}$	Φ	Tg (K)	Dp (cm^2/s)	Log (Kow)	Price (USD/t)
PVC	20.3	0.1	342.0	9.1E-07	1.6	
DBP	20.2	1.1	185.4	1.5E-08	4.6	1000
BBP	20.7	0.8	232.3	1.5E-08	4.8	1700
DOP	19.1	3.1	186.5	1.5E-08	8.4	1050
DNOP	19.5	3.1	186.1	1.2E-08	8.5	1190
DOTP	19.3	3.1	179.6	9.0E-09	8.4	1220
DINP	19.0	3.8	186.6	4.6E-08	9.4	1065
DIDP	19.0	4.5	186.6	3.2E-08	10.4	1200
MDEE	20.2	1.5	253.0	2.8E-08	5.2	1185
EDEE	20.1	1.7	250.3	2.4E-08	5.7	1173
PDEE	20.0	1.9	247.8	2.1E-08	6.2	1221
IPDEE	19.8	1.9	248.0	2.1E-08	6.1	1221
BDEE	19.9	2.1	245.5	1.8E-08	6.7	1199
IBDEE	19.7	2.1	245.7	1.8E-08	6.6	1179
IADEE	19.6	2.3	243.6	1.6E-08	7.1	1313
ODEE	19.5	3.0	238.1	1.1E-08	8.6	1322
EEGDL	20.5	3.0	285.5	1.7E-09	10.1	1218
EPGDL	20.3	3.2	283.5	1.6E-09	10.5	1311
EPRDL	20.4	3.2	283.4	1.6E-09	10.6	1311
EBGDL	20.3	3.4	281.4	1.4E-09	11.0	1315
ESBO	20.5	4.6	296.4	2.0E-10	14.8	1700

Annex C: Thermal properties

- **C.1 Thermal properties of FFA**

Table C-1. Thermal properties of the crystallization cycle of fatty acids

Material	Peak (°C)		Onset (°C)		Endset (°C)		ΔH_f (J/g)		Cloud Point (°C)
OA	-13.1	± 0.07	-12.42	± 0.01	-15.1	± 0.01	-73.6	± 0.4	
OA	-1.7	± 0.3	1.3	± 0.2	-5.0	± 0.2	-7.2	± 0.2	6
LA	-29.8	± 0.4	-28.2	± 0.8	-33	± 0.8	-152	± 2	< -22
SODD	-34.08	± 0.2	-32.4	± 0.3	-37.03	± 0.3	-20.66	± 0.3	
SODD	8.38	± 0.3	10.29	± 0.5	4.2	± 0.5	-6.47	± 0.4	

Table C-2. Thermal properties of the melting cycle of fatty acids

Material	Peak (°C)		Onset (°C)		Endset (°C)		ΔH_f (J/g)	
OA	0.0	± 0.1	-12.21	± 0.03	1.755	± 0.007	71.37	± 0.3
OA	-21.8	± 0.5	-26.9	± 0.5	-19.4	± 0.5	5.95	± 0.5
LA	-5.58	± 0.01	-9.24	± 0.01	-3.9	± 0.3	135	± 5
SODD	-23.7	± 0.5	-32.6	± 0.5	-22.4	± 0.5	25.21	± 0.5
SODD	19.72	± 0.5	8.1	± 0.5	22.6	± 0.5	9.59	± 0.5

Table C-3. Results of the thermogravimetric analysis (TGA) of fatty acids.

Material	Weight loss temperature (°C)
OA	343.7 ± 0.7
LA	347.4 ± 0.5
SODD	331.33 ± 0.3
SODD	415.7 ± 0.2

- **C.2 Thermal properties of Esters**

Table C-4. Thermal properties of the crystallization cycle of isobutyl esters

Material	Peak (°C)		Onset (°C)		Endset (°C)		ΔH_f (J/g)		Cloud Point (°C)
IBO	-26.3	± 0.2	-24.6	± 0.2	-28.6	± 0.01	-3.9	± 0.2	
IBO	-41.4	± 0.5	-34.03	± 0.5	-45.8	± 0.5	-2.1	± 0.5	-20
ISD	-11.86	± 0.5	-10.7	± 0.5	-16.9	± 0.5	-7.05	± 0.5	
ISD	-19.4	± 0.5	-17.8	± 0.5	-21.7	± 0.5	-1.6	± 0.5	
ISO	-13.5	± 0.8	-11.1	± 0.5	-31.2	± 1	-18.11	± 1	

Table C-5. Thermal properties of the melting cycle of isobutyl esters

Material	Peak (°C)		Onset (°C)		Endset (°C)		ΔH_f (J/g)	
IBO	-22.0	± 1	-28.9	± 0.2	-19.2	± 0.1	2.5	± 0.2
IBO	-12.8	± 0.1	-16	± 1	-10.4	± 0.2	1.13	± 0.5
ISD	-3.91	± 0.5	-12.8	± 0.8	-1.8	± 0.3	28.43	± 1
ISO	-9.8	± 0.8	-16.5	± 0.5	-7.9	± 0.6	5.08	± 0.7

Table C-6. Results of the thermogravimetric analysis (TGA)

Material	Weight loss temperature (°C)
IBO	340.7 ± 0.6
IBL	321.3 ± 0.9
ISD	331.5 ± 0.7
ISO	339.7 ± 0.9

- **C.3 Therma properties of epoxides**

Table C-7. Thermal properties of the crystallization cycle of isobutyl epoxides

Material	Peak (°C)		Onset (°C)		Endset (°C)		ΔH_f (J/g)	
EIO	-22.1	± 0.3	-21.74	± 0.2	-23.8	± 0.1	-54.8	± 0.2
EIO	-34.95	± 0.4	-31.7	± 0.5	-38.9	± 0.5	-6.5	± 0.5
EIL	-24.13	± 0.1	-19.7	± 0.2	-29.9	± 0.3	-48.5	± 0.3
EIL	-40.3	± 0.2	-37.1	± 0.5	-45.1	± 0.5	-19.2	± 0.5
EID	-28.1	± 0.9	-26.1	± 0.5	-29.7	± 1	-41.2	± 1
EID	-10.14	± 0.6	-9.2	± 0.3	-11.8	± 0.5	-9.3	± 0.5
EIS	-35.81	± 0.3	-33.4	± 0.8	-38.5	± 0.3	-19.0	± 0.4

Table C-8. Thermal properties of the melting cycle of isobutyl epoxides

Material	Peak (°C)		Onset (°C)		Endset (°C)		ΔH_f (J/g)	
EIO	-16.2	± 0.5	-21.6	± 0.3	-11.8	± 0.5	27.6	± 0.2

EIL	-17.45	± 0.9	-22.2	± 0.2	-16	± 0.1	18.6	± 0.6
EIL	-3.77	± 1	-12.1	± 0.6	-1.6	± 0.4	27.7	± 0.1
EID	-14.11	± 0.3	-20.29	± 0.8	-11.9	± 0.8	25.21	± 0.3
EIS	-17.14	± 0.5	-23.33	± 0.3	-15.14	± 1	36.01	± 0.5

Table C-9. Results of the thermogravimetric analysis (TGA) of isobutyl epoxides

Material	Weight loss temperature (°C)
EIO	338.6 ± 0.5
EIL	351.1 ± 0.8
EID	345.3 ± 0.4
EIS	344.0 ± 0.6

Annex D: Epoxidation kinetics

Annex D gathers schematically the concentration of oxirane and double bonds (mol/g) of the experimental runs and curve fitting.

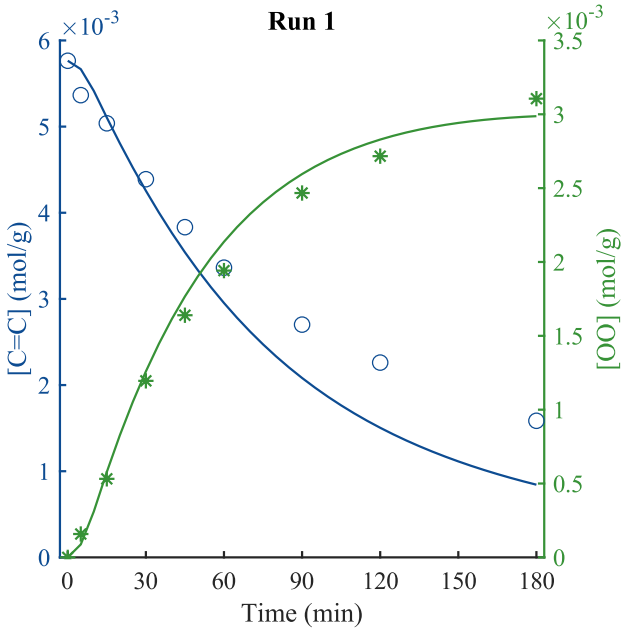

Figure D-1. Curve fitting run L1

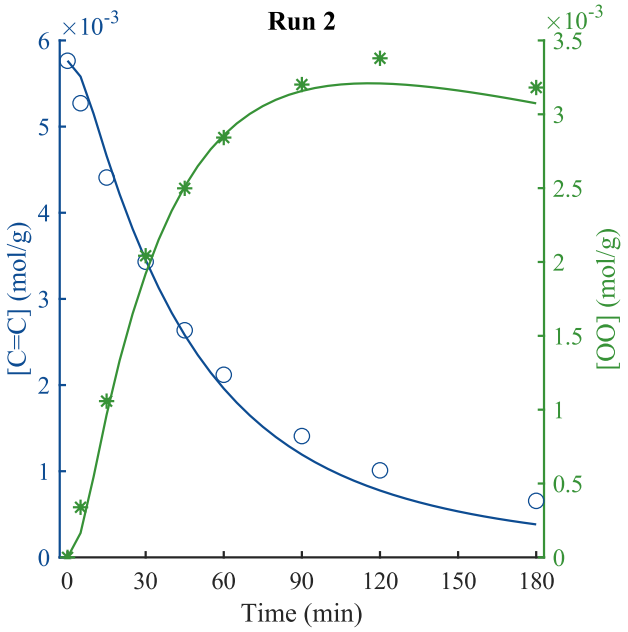

Figure D-2. Curve fitting run L2

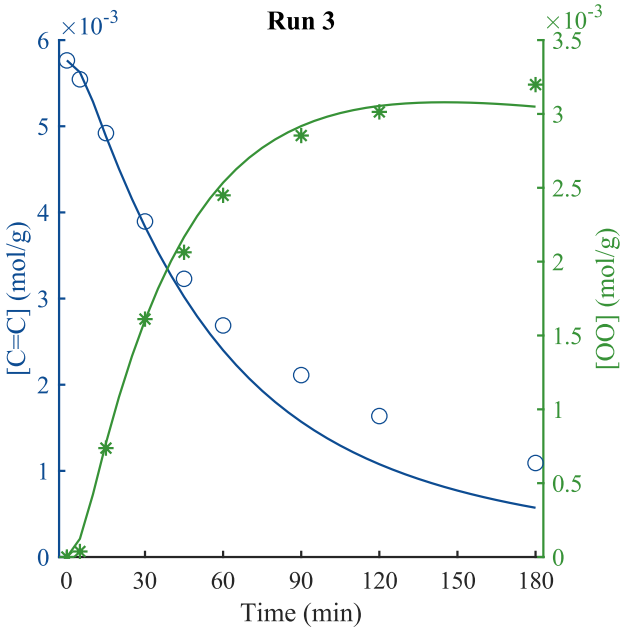

Figure D-3. Curve fitting run L3.

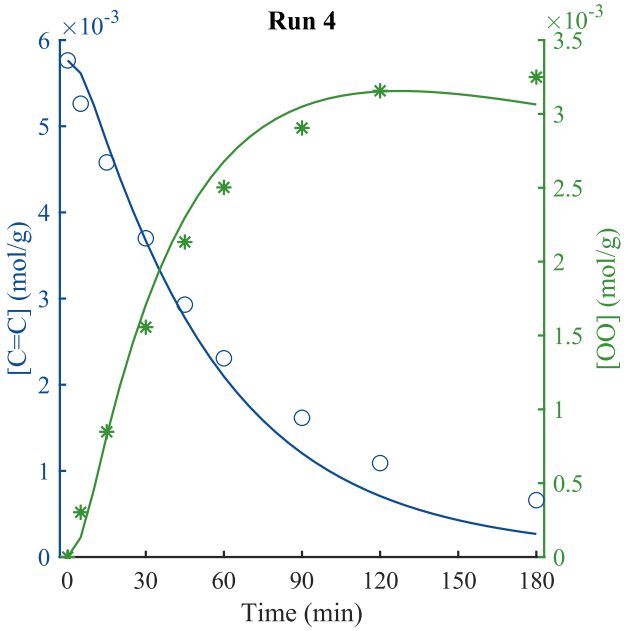

Figure D-4. Curve fitting run L4

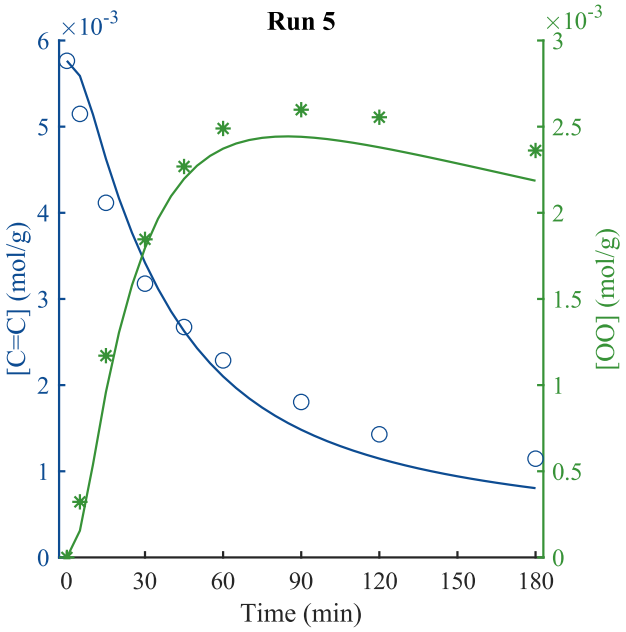

Figure D-5. Curve fitting run L5

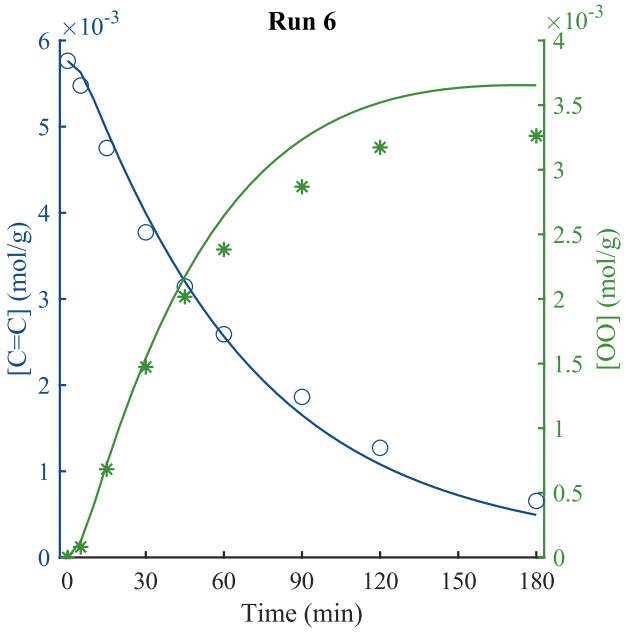

Figure D-6. Curve fitting run L6

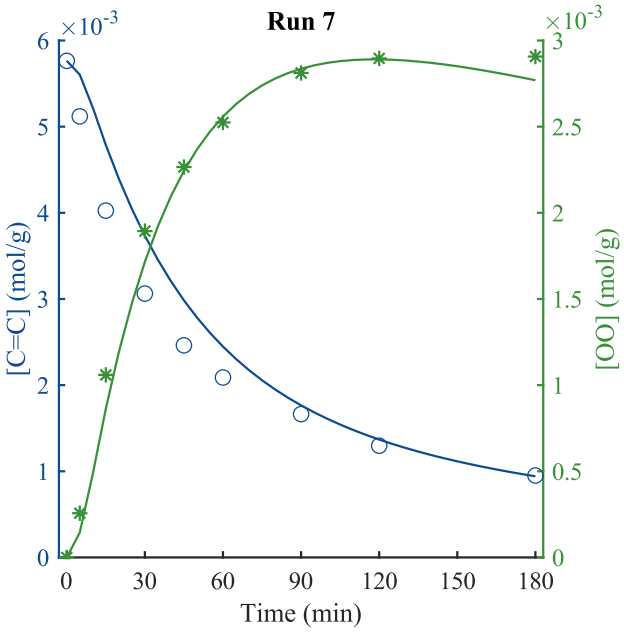

Figure D-7. Curve fitting run L7

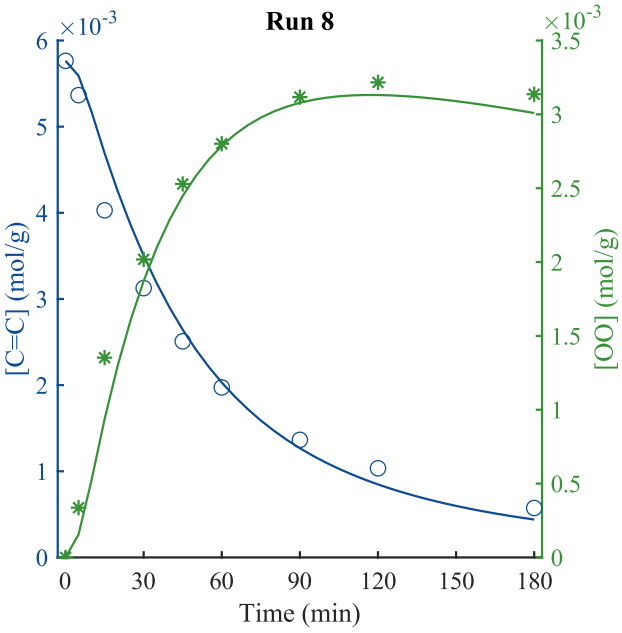

Figure D-8. Curve fitting run L8

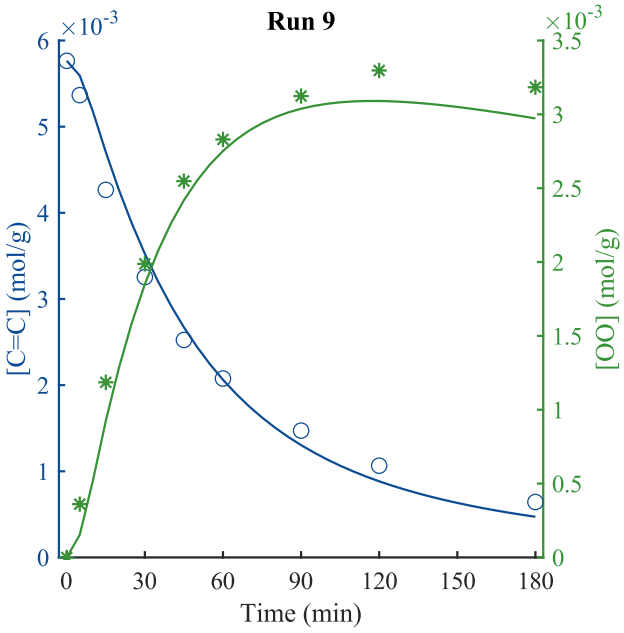

Figure D-9. Curve fitting run L9

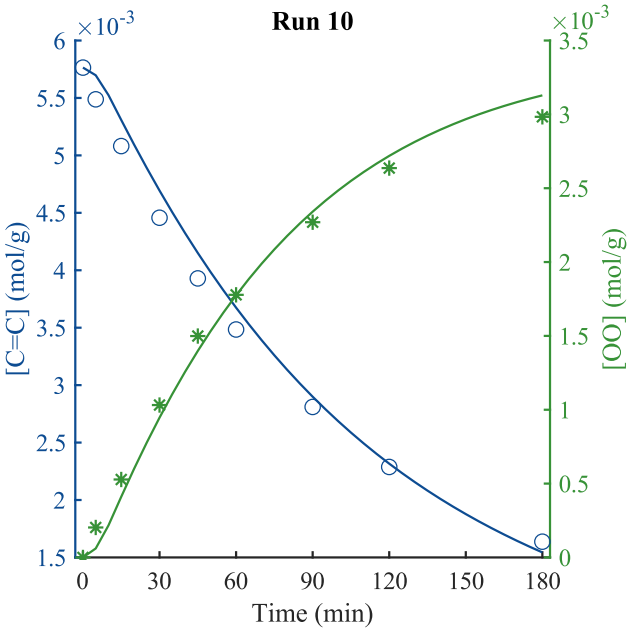

Figure D-10. Curve fitting run L10

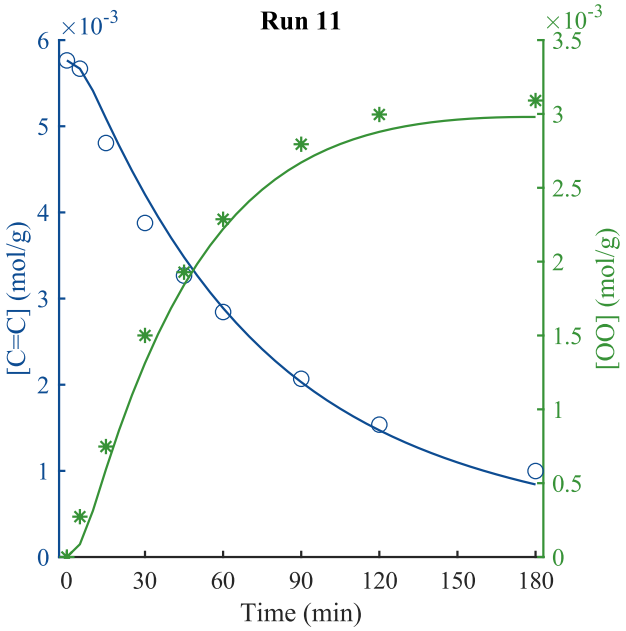

Figure D-11. Curve fitting run L11

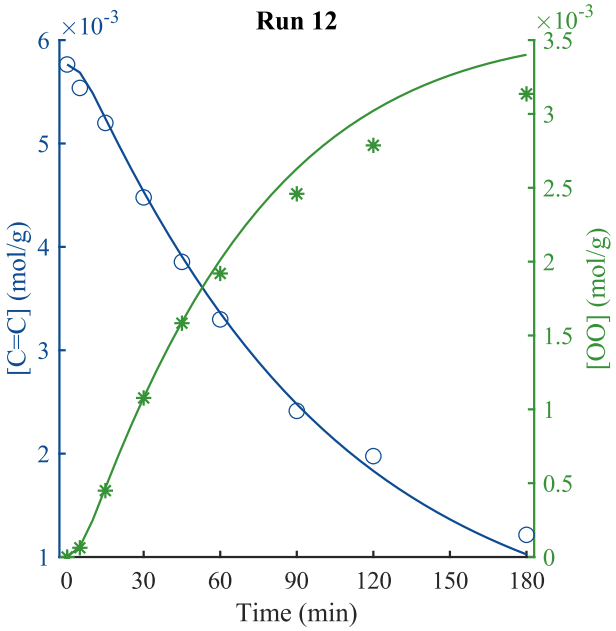

Figure D-12. Curve fitting run L12

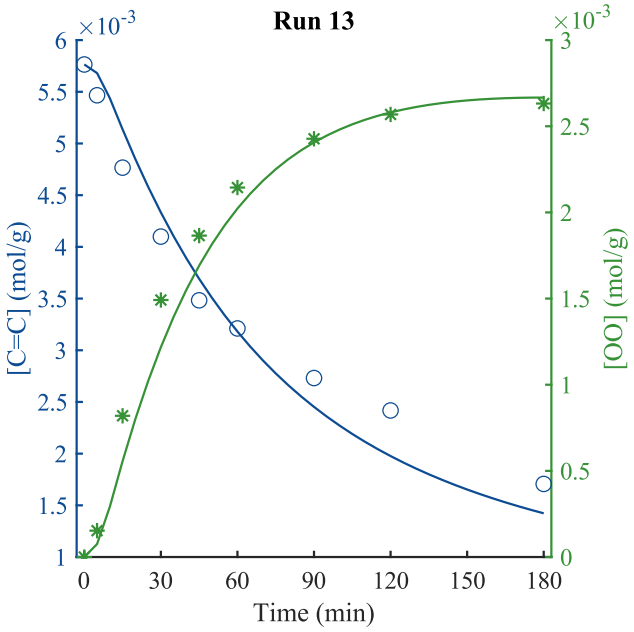

Figure D-13. Curve fitting run L13

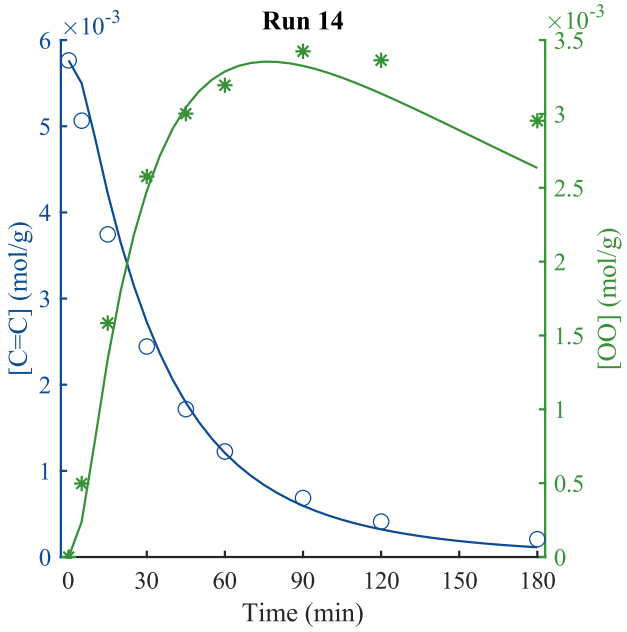

Figure D-14. Curve fitting run L14

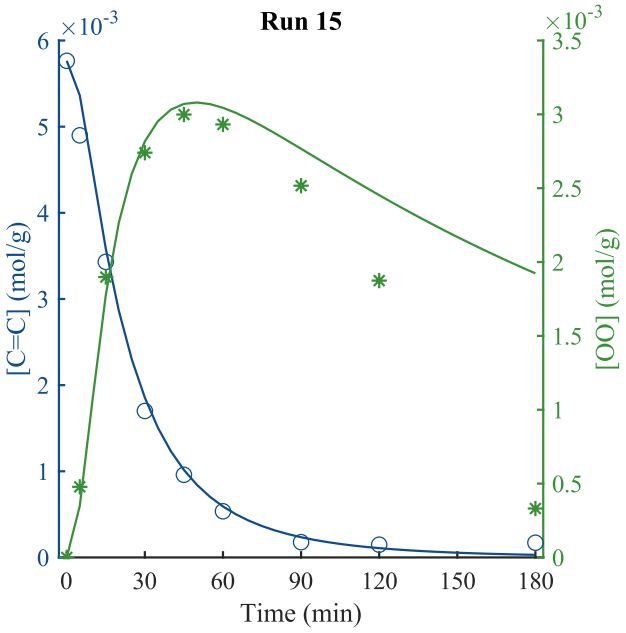

Figure D-15. Curve fitting run L15

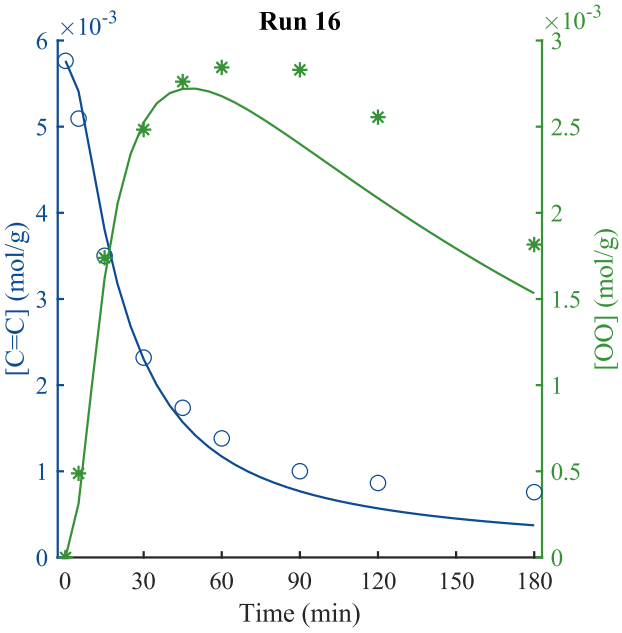

Figure D-16. Curve fitting run L16

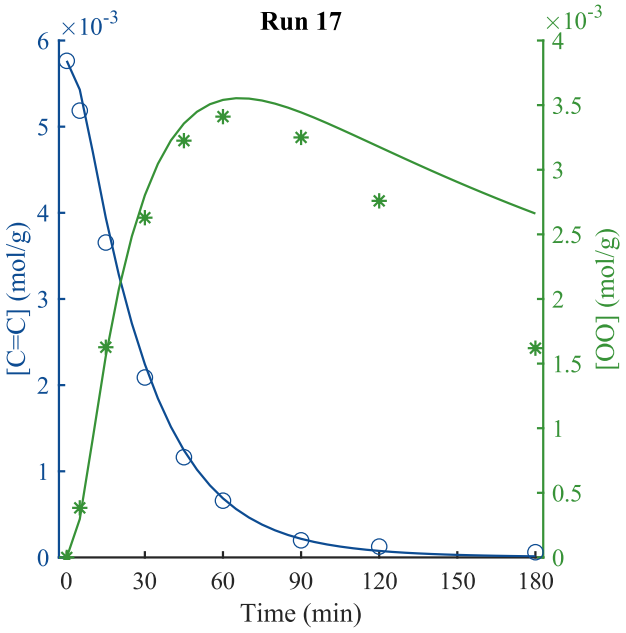

Figure D-17. Curve fitting run L17

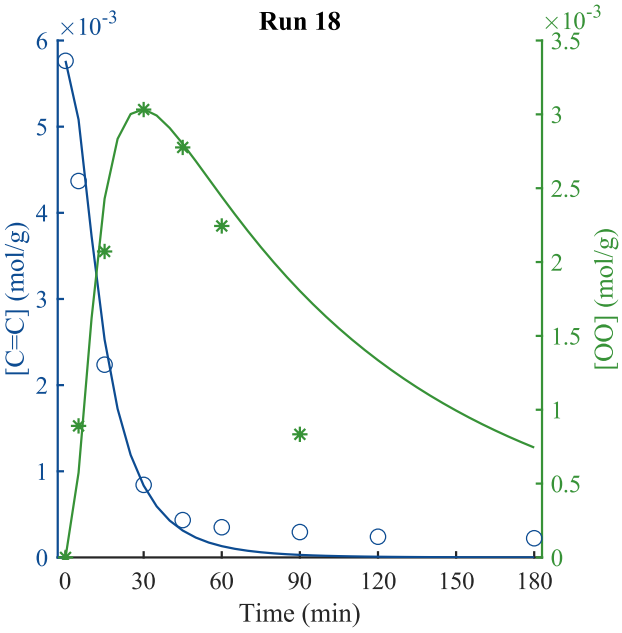

Figure D-18. Curve fitting run L18

References

[1] A. D. Godwin, “PLASTICIZERS,” in *Applied Polymer Science: 21st Century*, C. D. Craver and C. E. B. T.-A. P. S. 21st C. Carraher, Eds. Oxford: Pergamon, 2000, pp. 157–175.

[2] E. Langer, K. Bortel, S. Waskiewicz, and M. Lenartowicz-Klik, “Research Trends in Plasticizer Production,” *Plast. Deriv. from Post-Consumer PET*, pp. 101–126, 2020, doi: 10.1016/b978-0-323-46200-6.00004-0.

[3] S. G. Patrick, *Practical Guide to Polyvinyl Chloride*. United Kingdom: Rapra Technology Limited, 2005.

[4] T. Zheng *et al.*, “Structural modification of waste cooking oil methyl esters as cleaner plasticizer to substitute toxic dioctyl phthalate,” *J. Clean. Prod.*, vol. 186, pp. 1021–1030, 2018, doi: https://doi.org/10.1016/j.jclepro.2018.03.175.

[5] Fedepalma, “Anuario Estadístico 2019 - Principales cifras de la agroindustria de la palma de aceite en Colombia,” 2019.

[6] S. Madbouly, C. Zhang, and M. Kessler, *Bio-Based Plant oil polymers and composites*. Miami USA: Matthew Deans, 2016.

[7] C. Echim, R. Verhé, W. Greyt, and C. Stevens, “Production of biodiesel from side-stream refining products,” *Energy Environ. Sci. - ENERGY Env. SCI*, vol. 2, Nov. 2009, doi: 10.1039/b905925c.

[8] L. A. Rincón, J. G. Cadavid, and A. Orjuela, “Used cooking oils as potential oleochemical feedstock for urban biorefineries – Study case in Bogota, Colombia,” *Waste Manag.*, vol. 88, pp. 200–210, 2019, doi: https://doi.org/10.1016/j.wasman.2019.03.042.

[9] J. Van Gerpen, “Biodiesel processing and production,” *Fuel Process. Technol.*, vol. 86, no. 10, pp. 1097–1107, 2005, doi: https://doi.org/10.1016/j.fuproc.2004.11.005.

[10] I. M. Atadashi, M. K. Aroua, A. R. Abdul Aziz, and N. M. N. Sulaiman, “The effects of catalysts in biodiesel production: A review,” *J. Ind. Eng. Chem.*, vol. 19, no. 1, pp. 14–26, 2013, doi: https://doi.org/10.1016/j.jiec.2012.07.009.

[11] J. M. Marchetti and A. F. Errazu, “Esterification of free fatty acids using sulfuric acid as catalyst in the presence of triglycerides,” *Biomass and Bioenergy*, vol. 32, no. 9, pp. 892–895, 2008, doi: https://doi.org/10.1016/j.biombioe.2008.01.001.

[12] Y. Watanabe *et al.*, “Conversion of acid oil by-produced in vegetable oil refining to biodiesel fuel by immobilized Candida antarctica lipase,” *J. Mol. Catal. B Enzym.*, vol. 44, no. 3, pp. 99–105, 2007, doi: https://doi.org/10.1016/j.molcatb.2006.09.007.

[13] S. Gunawan and Y. Ju, “Vegetable Oil Deodorizer Distillate: Characterization, Utilization and Analysis,” *Sep. Purif. Rev.*, vol. 38, no. 3, pp. 207–241, Jul. 2009, doi: 10.1080/15422110903095151.

[14] H. K. Woodfield and J. L. Harwood, “Oilseed Crops: Linseed, Rapeseed, Soybean, and Sunflower,” B. Thomas, B. G. Murray, and D. J. B. T.-E. of A. P. S. (Second E.

Murphy, Eds. Oxford: Academic Press, 2017, pp. 34–38.
[15] E. Alencar, L. Faroni, L. Peternelli, M. Silva, and A. Costa, “Influence of soybean storage conditions on crude oil quality,” *Rev. Bras. Eng. Agrícola e Ambient.*, vol. 14, pp. 303–308, Mar. 2010, doi: 10.1590/S1415-43662010000300010.
[16] S. Khatoon, R. G. Raja Rajan, and A. G. Gopala Krishna, “Physicochemical Characteristics and Composition of Indian Soybean Oil Deodorizer Distillate and the Recovery of Phytosterols,” *J. Am. Oil Chem. Soc.*, vol. 87, no. 3, pp. 321–326, 2010, doi: 10.1007/s11746-009-1499-8.
[17] C. Benites, V. O. Concha, S. Reis, and A. Oliveira, *Physiochemical Characterization of Soybean Oil Deodorizer Distillate*, vol. 17. 2009.
[18] J. Summers and C. Daniels, “Plasticizers,” in *PVC HandBook*, Hanser, 2005, pp. 173–193.
[19] R. Wilcox, “Outlook 17: US plasticizers face shortages, new capacity,” 2016. [Online]. Available: https://www.icis.com/explore/resources/news/2016/12/28/10064206/outlook-17-us-plasticizers-face-shortages-new-capacity/.
[20] M. G. A. Vieira, M. A. da Silva, L. O. dos Santos, and M. M. Beppu, “Natural-based plasticizers and biopolymer films: A review,” *Eur. Polym. J.*, vol. 47, no. 3, pp. 254–263, 2011, doi: https://doi.org/10.1016/j.eurpolymj.2010.12.011.
[21] Cefic group, “European Plasticisers,” Bruselas, Bélgica, 2017.
[22] The European Chemical Industry Council, “Plasticisers - Information Center.” https://www.plasticisers.org/plasticisers/ (accessed Aug. 30, 2020).
[23] J. Murphy, *Additives for Plastics Handbook*, Second edi. New York: Elsevier, 2003.
[24] H. Benecke, B. Vijaydendran, and J. Elhard, “US 2002/0013396 A1,” 2002.
[25] R. Lundsgaard, “Migration of plasticisers from PVC and other polymers,” 2010.
[26] L. Bernard, R. Cueff, C. Breysse, B. Décaudin, and V. Sautou, “Migrability of PVC plasticizers from medical devices into a simulant of infused solutions,” *Int. J. Pharm.*, vol. 485, no. 1, pp. 341–347, 2015, doi: https://doi.org/10.1016/j.ijpharm.2015.03.030.
[27] M. Rahman and C. S. Brazel, “The plasticizer market: an assessment of traditional plasticizers and research trends to meet new challenges,” *Prog. Polym. Sci.*, vol. 29, no. 12, pp. 1223–1248, 2004, doi: https://doi.org/10.1016/j.progpolymsci.2004.10.001.
[28] A. H. Suzuki, B. G. Botelho, L. S. Oliveira, and A. S. Franca, “Sustainable synthesis of epoxidized waste cooking oil and its application as a plasticizer for polyvinyl chloride films,” *Eur. Polym. J.*, vol. 99, pp. 142–149, 2018, doi: https://doi.org/10.1016/j.eurpolymj.2017.12.014.
[29] LII (Legal Information Institute), “16 CFR § 1307.3 - Prohibition of children’s toys and child care articles containing specified phthalates.,” 2018. https://www.law.cornell.edu/cfr/text/16/1307.3.
[30] SGS, “Accessing the Market: European Union Phthalate Regulations | SGS,” Apr. 09, 2019. https://www.sgs.com/en/news/2019/04/accessing-the-market-european-union-phthalate-regulations (accessed Jun. 16, 2020).
[31] IHS Markit Customer Care, *Chemical Economics Handbook*. 2018.
[32] S&P Global, “Plasticizers - Chemical Economics Handbook,” *Commodity Insights*, 2020. https://www.spglobal.com/commodityinsights/en/ci/products/plasticizers-chemical-economics-handbook.html.
[33] P. Jia, H. Xia, K. Tang, and Y. Zhou, “Plasticizers derived from biomass resources: A short review,” *Polymers (Basel).*, vol. 10, no. 12, 2018, doi: 10.3390/polym10121303.
[34] The Business ResearchCompany, “Plasticizers Market 2022 - By Product Type

(Phthalates Plasticizers, Non-Phthalates Plasticizers)," 2020. https://www.thebusinessresearchcompany.com/report/plasticizers-market-global-market.

[35] ResearchAndMarkets, "Global Bio Plasticizers Market Opportunity Report 2020-2030 Featuring DuPont, DOW Chemical, PolyOne, Evonik Among Others," 2020. https://www.globenewswire.com/news-release/2020/12/03/2139125/0/en/Global-Bio-Plasticizers-Market-Opportunity-Report-2020-2030-Featuring-DuPont-DOW-Chemical-PolyOne-Evonik-Among-Others.html.

[36] V. Thakur, M. Thakur, and M. Kessler, *Handbook of Composites from Renewable Materials*. Miami USA, 2017.

[37] K. Dutta, S. Das, and P. P. Kundu, "Epoxidized Esters of Palm Kernel Oil as an Effective Plasticizer for PVC: A Study of Mechanical Properties and Effect of Processing Conditions," *Int. Polym. Process.*, vol. 29, no. 4, pp. 495–506, Aug. 2014, doi: 10.3139/217.2922.

[38] Grand View Research, "Bio Plasticizers Market Analysis By Product Type (Citrates, Castor Oil, ESBO, Succinic Acid), By Application (Packaging, Consumer Goods, Automotive, Construction, Textiles), And Segment Forecasts, 2020 - 2025," 2020. [Online]. Available: https://www.grandviewresearch.com/industry-analysis/bio-plasticizers-market.

[39] B. I. Chaudhary, C. L. Liotta, J. M. Cogen, and M. B. T.-R. M. in M. S. and M. E. Gilbert, "Plasticized PVC," Elsevier, 2016.

[40] M. Bocqué, C. Voirin, V. Lapinte, S. Caillol, and J.-J. Robin, "Petro-based and bio-based plasticizers: Chemical structures to plasticizing properties," *J. Polym. Sci. Part A Polym. Chem.*, vol. 54, no. 1, pp. 11–33, Jan. 2016, doi: 10.1002/pola.27917.

[41] O. Suárez, "Producción y Modelamiento de Gliceril ésteres como plastificantes para el PVC," Universidad Nacional de Colombia, 2011.

[42] P. Jia, M. Zhang, L. Hu, and Y. Zhou, "Green plasticizers derived from soybean oil for poly(vinyl chloride) as a renewable resource material," *Korean J. Chem. Eng.*, vol. 33, no. 3, pp. 1080–1087, 2016, doi: 10.1007/s11814-015-0213-9.

[43] Y. Yang, Z. Xiong, L. Zhang, Z. Tang, R. Zhang, and J. Zhu, "Isosorbide dioctoate as a 'green' plasticizer for poly(lactic acid)," *Mater. Des.*, vol. 91, pp. 262–268, 2016, doi: https://doi.org/10.1016/j.matdes.2015.11.065.

[44] B. Yin and M. Hakkarainen, "Oligomeric isosorbide esters as alternative renewable resource plasticizers for PVC," *J. Appl. Polym. Sci.*, vol. 119, no. 4, pp. 2400–2407, Feb. 2011, doi: 10.1002/app.32913.

[45] D.-L. Cai, X. Yue, B. Hao, and P.-C. Ma, "A sustainable poly(vinyl chloride) plasticizer derivated from waste cooking oil," *J. Clean. Prod.*, vol. 274, p. 122781, 2020, doi: https://doi.org/10.1016/j.jclepro.2020.122781.

[46] S. Kandula, L. Stolp, M. Grass, B. Woldt, and D. Kodali, "Functionalization of Soy Fatty Acid Alkyl Esters as Bioplasticizers," Saint Paul, Minnesota, 2004.

[47] P. Frenkel and S. Mckeown, "US9321901B2," 2016.

[48] G. Feng, Y. Ma, M. Zhang, P. Jia, C. Liu, and Y. Zhou, "Synthesis of Bio-base Plasticizer Using Waste Cooking Oil and Its Performance Testing in Soft Poly(vinyl chloride) Films," *J. Bioresour. Bioprod.*, vol. 4, no. 2, pp. 99–110, 2019, doi: https://doi.org/10.21967/jbb.v4i2.214.

[49] P. Jia, M. Zhang, L. Hu, F. Song, G. Feng, and Y. Zhou, "A Strategy for Nonmigrating Plasticized PVC Modified with Mannich base of Waste Cooking Oil Methyl Ester," *Sci. Rep.*, vol. 8, no. 1, p. 1589, 2018, doi: 10.1038/s41598-018-19958-y.

[50] J. Spekreijse, T. Lammens, C. Parisi, T. Ronzon, and M. Vis, *Insights into the European market for bio-based chemicals*, vol. 19, no. October. 2019.

[51] Index Mundi, "Soybean Oil Futures End of Day Settlement Price," 2020.

https://www.indexmundi.com/commodities/?commodity=soybean-oil&months=12 (accessed Mar. 03, 2020).
[52] Echemi, “Epoxidized Soybean Oil Price Analysis.” .
[53] Greenea, “Greenea Market Analysis,” 2020. https://www.greenea.com/en/market-analysis/.
[54] USDA, “Oilseeds: World Markets and Trade,” EEUU, 2020.
[55] ICIS, “Plasticizers prices, markets & analysis,” 2019. https://www.icis.com/explore/commodities/chemicals/plasticizers/ (accessed Jan. 20, 2021).
[56] Alibaba, “Soybean deodorizer distillate oil FOB Reference Price.” https://www.alibaba.com/product-detail/Soybean-deodorizer-distillate-oil_1600078593352.html?spm=a2700.7724857.normal_offer.d_image.79965073IJgoEB (accessed Jun. 07, 2021).
[57] L. A. Rincón, “Reutilzación de aceites de cocina usados en la producción de aceites epoxidados,” Universidad Nacional de Colombia, 2018.
[58] Michel Biron, *Industrial Applications of Renewable Plastics*. .
[59] Y. Wei, G. Li, Q. Lv, C. Cheng, and H. Guo, “Epoxidation of Methyl Oleate and Unsaturated Fatty Acid Methyl Esters Obtained from Vegetable Source over Ti-Containing Silica Catalysts,” *Ind. Eng. Chem. Res.*, vol. 57, no. 48, pp. 16284–16294, Dec. 2018, doi: 10.1021/acs.iecr.8b04155.
[60] L. Ramírez, “Modelo Cinético para la reacción de epoxidación aceite vegetal usado,” Universidad Nacional de colombia, 2020.
[61] DANE - Departamento Administrativo Nacional de Estadística, “Encuesta Anual Manufacturera (EAM).”
[62] D. Alperstein, D. Knani, A. Goichman, and M. Narkis, “Determination of plasticizers efficiency for nylon by molecular modeling,” *Polym. Bull.*, vol. 68, no. 7, pp. 1977–1988, 2012, doi: 10.1007/s00289-012-0705-2.
[63] Specialchem, “Adhesives Ingredients,” *Selecting Plasticizers for Adhesives and Sealants*. https://adhesives.specialchem.com/selection-guide/plasticizers-selection-for-adhesives-and-sealants.
[64] A. A. Hassan, A. Abbas, T. Rasheed, M. Bilal, H. M. N. Iqbal, and S. Wang, “Development, influencing parameters and interactions of bioplasticizers: An environmentally friendlier alternative to petro industry-based sources,” *Sci. Total Environ.*, vol. 682, pp. 394–404, 2019, doi: https://doi.org/10.1016/j.scitotenv.2019.05.140.
[65] F. D. Martínez, “Producción de ésteres de poliglicerol y evaluación de diferentes formulaciones como plastificante de PVC,” Universidad Nacional de Colombia, 2010.
[66] G. Wypych, *Handbook of Plasticizers*, 3rd ed. ChemTec Publishing, 2017.
[67] D. Krevelen and K. Nijenhuis, “Chapter 7- Cohesive properties and and solubility,” in *Properties of Polymers*, 4th editio., Elsevier, 2009.
[68] Y.-H. Ju, N. N. F. Sari, A. W. Go, M.-J. Wang, R. C. Agapay, and A. Ayucitra, “Preparation of Epoxidized Fatty Acid Ethyl Ester from Tung Oil as a Bio-lubricant Base-Stock,” *Waste and Biomass Valorization*, vol. 11, no. 8, pp. 4145–4155, 2020, doi: 10.1007/s12649-019-00749-z.
[69] D. A. G. Aranda, R. T. P. Santos, N. C. O. Tapanes, A. L. D. Ramos, and O. A. C. Antunes, “Acid-Catalyzed Homogeneous Esterification Reaction for Biodiesel Production from Palm Fatty Acids,” *Catal. Letters*, vol. 122, no. 1, pp. 20–25, 2008, doi: 10.1007/s10562-007-9318-z.
[70] P. Kuester, F; Rhodes, “High Oxirane Fatty Esters,” 3377304, 1968.
[71] M. Canakci and J. Gerpen, “Biodiesel production from oils and fats with high FFAs,” *Trans. ASAE*, vol. 44, Jan. 2001, doi: 10.13031/2013.7010.

[72] V. B. Borugadda and V. V Goud, “Improved thermo-oxidative stability of structurally modified waste cooking oil methyl esters for bio-lubricant application,” *J. Clean. Prod.*, vol. 112, pp. 4515–4524, 2016, doi: https://doi.org/10.1016/j.jclepro.2015.06.046.

[73] J. Brinks, K. Malins, V. Kampars, J. Prilucka, and L. Apseniece, “Optimization of rapeseed oil fatty acid esterification with methanol in the presence of sulfuric acid,” *Polish J. Chem. Technol.*, vol. 15, no. 4, pp. 54–59, doi: https://doi.org/10.2478/pjct-2013-0068.

[74] H. Lu, Y. Liu, H. Zhou, Y. Yang, M. Chen, and B. Liang, “Production of biodiesel from Jatropha curcas L. oil,” *Comput. Chem. Eng.*, vol. 33, no. 5, pp. 1091–1096, 2009, doi: https://doi.org/10.1016/j.compchemeng.2008.09.012.

[75] J. Cárdenas, A. Orjuela, D. L. Sánchez, P. C. Narváez, B. Katryniok, and J. Clark, “Pre-treatment of used cooking oils for the production of green chemicals: A review,” *J. Clean. Prod.*, vol. 289, p. 125129, 2021, doi: https://doi.org/10.1016/j.jclepro.2020.125129.

[76] F. Galli, S. Nucci, C. Pirola, and C. L. Bianchi, “Epoxy methyl soyate as bio-plasticizer: Two different preparation strategies,” *Chem. Eng. Trans.*, vol. 37, pp. 601–606, 2014, doi: 10.3303/CET1437101.

[77] V. V Goud, N. C. Pradhan, and A. V Patwardhan, “Epoxidation of karanja (Pongamia glabra) oil by H2O2,” *J. Am. Oil Chem. Soc.*, vol. 83, no. 7, pp. 635–640, 2006, doi: 10.1007/s11746-006-1250-7.

[78] M. Kurańska and M. Niemiec, “Cleaner Production of Epoxidized Cooking Oil Using A Heterogeneous Catalyst,” *Catalysts*, vol. 10, Oct. 2020, doi: 10.3390/catal10111261.

[79] A. Campanella, C. Fontanini, and M. Baltanas, “High yield epoxidation of fatty acid methyl esters with performic acid generated in situ,” *Chem. Eng. J.*, vol. 144, pp. 466–475, Nov. 2008, doi: 10.1016/j.cej.2008.07.016.

[80] V. B. Borugadda and V. V Goud, “Epoxidation of Castor Oil Fatty Acid Methyl Esters (COFAME) as a Lubricant base Stock Using Heterogeneous Ion-exchange Resin (IR-120) as a Catalyst,” *Energy Procedia*, vol. 54, pp. 75–84, 2014, doi: https://doi.org/10.1016/j.egypro.2014.07.249.

[81] Z. S. Petrović, A. Zlatanić, C. C. Lava, and S. Sinadinović-Fišer, “Epoxidation of soybean oil in toluene with peroxoacetic and peroxoformic acids — kinetics and side reactions,” *Eur. J. Lipid Sci. Technol.*, vol. 104, no. 5, pp. 293–299, May 2002, doi: https://doi.org/10.1002/1438-9312(200205)104:5<293::AID-EJLT293>3.0.CO;2-W.

[82] T. Vlček and Z. S. Petrović, “Optimization of the chemoenzymatic epoxidation of soybean oil,” *J. Am. Oil Chem. Soc.*, vol. 83, no. 3, pp. 247–252, 2006, doi: 10.1007/s11746-006-1200-4.

[83] R. Turco, C. Pischetola, R. Tesser, S. Andini, and M. Di Serio, “New findings on soybean and methylester epoxidation with alumina as the catalyst,” *RSC Adv.*, vol. 6, no. 38, pp. 31647–31652, 2016, doi: 10.1039/C6RA01780K.

[84] B. Rangarajan, A. Havey, E. A. Grulke, and P. D. Culnan, “Kinetic parameters of a two-phase model forin situ epoxidation of soybean oil,” *J. Am. Oil Chem. Soc.*, vol. 72, no. 10, pp. 1161–1169, 1995, doi: 10.1007/BF02540983.

[85] S. Dinda, A. V Patwardhan, V. V Goud, and N. C. Pradhan, “Epoxidation of cottonseed oil by aqueous hydrogen peroxide catalysed by liquid inorganic acids,” *Bioresour. Technol.*, vol. 99, no. 9, pp. 3737–3744, 2008, doi: https://doi.org/10.1016/j.biortech.2007.07.015.

[86] A. Campanella and M. A. Baltanás, “Degradation of the oxirane ring of epoxidized vegetable oils with solvated acetic acid using cation-exchange resins,” *Eur. J. Lipid Sci. Technol.*, vol. 106, no. 8, pp. 524–530, Aug. 2004, doi:

https://doi.org/10.1002/ejlt.200400965.
[87] Z. Wu *et al.*, “Mass transfer and reaction kinetics of soybean oil epoxidation in a formic acid-autocatalyzed reaction system,” *Can. J. Chem. Eng.*, vol. 94, no. 8, pp. 1576–1582, Aug. 2016, doi: https://doi.org/10.1002/cjce.22526.
[88] P. G. Nihul, S. T. Mhaske, and V. V Shertukde, “Epoxidized rice bran oil (ERBO) as a plasticizer for poly(vinyl chloride) (PVC),” *Iran. Polym. J.*, vol. 23, no. 8, pp. 599–608, 2014, doi: 10.1007/s13726-014-0254-7.
[89] A. Campanella and M. A. Baltanás, “Degradation of the oxirane ring of epoxidized vegetable oils in liquid-liquid systems: II. Reactivity with solvated acetic and peracetic acids,” *Lat. Am. Appl. Res.*, vol. 35, pp. 211–216, Jul. 2005.
[90] X. Zhao, T. Zhang, Y. Zhou, and D. Liu, “Preparation of peracetic acid from hydrogen peroxide: Part I: Kinetics for peracetic acid synthesis and hydrolysis,” *J. Mol. Catal. A Chem.*, vol. 271, no. 1, pp. 246–252, 2007, doi: https://doi.org/10.1016/j.molcata.2007.03.012.
[91] P. T. Wai, P. Jiang, Y. Shen, P. Zhang, Q. Gu, and Y. Leng, “Catalytic developments in the epoxidation of vegetable oils and the analysis methods of epoxidized products,” *RSC Adv.*, vol. 9, no. 65, pp. 38119–38136, 2019, doi: 10.1039/C9RA05943A.
[92] M. Mushtaq *et al.*, “Epoxidation of methyl esters derived from Jatropha oil: An optimization study,” *Grasas y Aceites*, vol. 64, pp. 103–114, Mar. 2013, doi: 10.3989/gya.084612.
[93] R. J. Gall and F. P. Greenspan, “A Modified Peracid Process for Making Epoxy Compounds from Unsaturated Fatty Acid Esters,” *Ind. Eng. Chem.*, vol. 47, no. 1, pp. 147–148, Jan. 1955, doi: 10.1021/ie50541a045.
[94] M. Kurańska, H. Beneš, A. Prociak, O. Trhlíková, Z. Walterová, and W. Stochlińska, “Investigation of epoxidation of used cooking oils with homogeneous and heterogeneous catalysts,” *J. Clean. Prod.*, vol. 236, p. 117615, Jul. 2019, doi: 10.1016/j.jclepro.2019.117615.
[95] Y. Bai, J. Wang, D. Liu, and X. Zhao, “Conversion of fatty acid methyl ester to epoxy plasticizer by auto-catalyzed in situ formation of performic acid: Kinetic modeling and application of the model,” *J. Clean. Prod.*, vol. 259, p. 120791, Mar. 2020, doi: 10.1016/j.jclepro.2020.120791.
[96] A. Ghosh-Dastidar, S. Kaujalgikar, and B. Chaudhary, “US 9499681 B2,” 2016.
[97] M. Mushtaq, I. Tan, C. Devi, S. Majidaie, M. Nadeem, and S. Lee, “Epoxidation of Fatty Acid Methyl Esters derived from Jatropha oil,” *2011 Natl. Postgrad. Conf. - Energy Sustain. Explor. Innov. Minds, NPC 2011*, Sep. 2011, doi: 10.1109/NatPC.2011.6136253.
[98] E. Milchert, A. Smagowicz, and G. Lewandowski, “Optimization of the reaction parameters of epoxidation of rapeseed oil with peracetic acid,” *J. Chem. Technol. Biotechnol.*, vol. 85, no. 8, pp. 1099–1107, Aug. 2010, doi: https://doi.org/10.1002/jctb.2405.
[99] Á. Osuna and A. Boyaca, “Two-phase kinetic model for epoxidation of soybean oil,” *Ing. e Investig.*, vol. 30, pp. 188–196, Aug. 2010.
[100] L. H. Gan, S. H. Goh, and K. S. Ooi, “Kinetic studies of epoxidation and oxirane cleavage of palm olein methyl esters,” *J. Am. Oil Chem. Soc.*, vol. 69, no. 4, pp. 347–351, 1992, doi: 10.1007/BF02636065.
[101] Icontec, “NTC 2366. Plasticos. Aceites Vegetales Epoxidados de Soya y Linaza,” 2019.
[102] Arkema, “Arkema Products.” https://www.arkema.com/global/en/search/?qc=search&q=vikoflex.
[103] PETROM, “plsgreen.” https://plsgreen.com.br/en/specifications/.

[104] IEA Bioenergy, “Bio-Based Chemicals,” 2020.
[105] IEA Bioenergy, “Bio-based Chemicals, Value Added Products from Biorefineries,” 2013.
[106] A. Liquide, “Biopropilenglicol, Tecnología alternativa para la producción de propilenglicol,” 2021. https://www.engineering-airliquide.com/es/biopropilenglicol.
[107] Arkema, “Oleris® Bio-Based 2-Octanol,” 2020. https://www.arkema.com/global/en/products/product-finder/product/technicalpolymers/oleris/oleris-2-Octanol/.
[108] R. Jamarani, H. Erythropel, J. Nicell, R. Leask, and M. Maric, “How Green is Your Plasticizer?,” *Polymers (Basel).*, vol. 10, p. 834, Jul. 2018, doi: 10.3390/polym10080834.
[109] P. Walters, D. F. Cadogan, and C. J. Howick, *Plasticizers*. 2020.
[110] E. Stefanis and C. Panayiotou, “Prediction of Hansen Solubility Parameters with a New Group-Contribution Method,” *Int. J. Thermophys.*, vol. 29, no. 2, pp. 568–585, 2008, doi: 10.1007/s10765-008-0415-z.
[111] B. E. Poling, J. M. Prausnitz, and J. P. O’Connell, *Properties of Gases and Liquids, Fifth Edition*. New York: McGraw-Hill Education, 2001.
[112] Charles M.Hansen, *Hansen Solubility Parameters Second edition: A User’s Handbook*, no. October 2013. 2007.
[113] D. W. Krevelen and K. Nijenhuis, “Cohesive Properties and Solubility,” in *Properties of Polymers*, 2009, pp. 189–227.
[114] Polymer Properties Database, “Hansen Solubility Sphere,” 2015. http://polymerdatabase.com/polymer physics/Hansen Solubility Sphere.html (accessed Feb. 23, 2021).
[115] J. Burke, “Part 6 - Three Component Parameters,” 1984. https://cool.culturalheritage.org/byauth/burke/solpar/solpar6.html (accessed May 23, 2021).
[116] L. Mascia, Y. Kouparitsas, D. Nocita, and X. Bao, “Antiplasticization of Polymer Materials: Structural Aspects and Effects on Mechanical and Diffusion-Controlled Properties,” *Polymers* , vol. 12, no. 4. 2020, doi: 10.3390/polym12040769.
[117] ExxonMobil Petroleum Chemical B.V.B.A, “Submission of information on DIDP CAS#68515-49-1, EC#271-091-4 as an alternative to DEHP,” 2014.
[118] Roderick Parkes, *JRC Technical Reports: Practical guidelines on the application of migration modelling for the estimation of specific migration*, no. 10. 2015.
[119] D. Schowope and R. Goydan, *Methods for Estimating the Migration of Aditives and Impurities from Polymeric Materials*. Washington D.C: U.S Environmental Protection Agency, 1990.
[120] E. H. Immergut and H. F. Mark, “Principles of Plasticization,” in *<bold>Plasticization</bold> and Plasticizer Processes*, vol. 48, AMERICAN CHEMICAL SOCIETY, 1965, p. 1.
[121] J. Bicerano, *Prediction of polymer properties*, 3rd Editio., vol. 31, no. 02. EEUU: Marcel Dekker, Inc, 2002.
[122] C. Camacho-Zuñiga and F. A. Ruiz-Treviño, “A New Group Contribution Scheme To Estimate the Glass Transition Temperature for Polymers and Diluents,” *Ind. Eng. Chem. Res.*, vol. 42, no. 7, pp. 1530–1534, Apr. 2003, doi: 10.1021/ie0205389.
[123] C. L. Ihemaguba and K. Marossy, “Combined thermal analysis of fluid plasticizers,” *J. Therm. Anal. Calorim.*, vol. 147, no. 1, pp. 195–201, 2022, doi: 10.1007/s10973-020-10315-8.
[124] C. A. Angell, J. M. Sare, and E. J. Sare, “Glass transition temperatures for simple molecular liquids and their binary solutions,” *J. Phys. Chem.*, vol. 82, no. 24, pp. 2622–2629, Nov. 1978, doi: 10.1021/j100513a016.

[125] W. A. Lee, “Calculation of the glass transition temperatures of polymers. Part I. Homopolymers and copolymers with alkyl side chains,” *J. Polym. Sci. Part A-2 Polym. Phys.*, vol. 8, no. 4, pp. 555–570, Apr. 1970, doi: https://doi.org/10.1002/pol.1970.160080407.
[126] E. Gustafsson, T. M. Bowden, and A. R. Rennie, “Interactions of amphiphiles with plasticisers used in polymers: Understanding the basis of health and environmental challenges,” *Adv. Colloid Interface Sci.*, vol. 277, p. 102109, 2020, doi: https://doi.org/10.1016/j.cis.2020.102109.
[127] US EPA - United States Environmental Protection Agency, “EPI Suite TM v4.11 - Estimation Program Interface.” Washington D.C, 2021.
[128] I. Cousins and D. Mackay, “Correlating the physical–chemical properties of phthalate esters using the `three solubility’ approach,” *Chemosphere*, vol. 41, no. 9, pp. 1389–1399, 2000, doi: https://doi.org/10.1016/S0045-6535(00)00005-9.
[129] A. Wypch, *Databook of Plasticizers*. Elsevier, 2017.
[130] CAS, “Sci Finder,” 2022. https://scifinder-n.cas.org.
[131] N. RAO, S. KAUJALGIKAR, B. CHAUD-HARY, S. BHIDE, S. MORYE, and S. AGASHE, “WO 2014/061026 Al,” 2014.
[132] A. Ghosh-Dastidar, R. Eaton, A. ADAM-CZYK, B. Bell, and R. Campabell, “WO2013/003225 A2,” 2013.
[133] L. G. Krauskopf, “Plasticizer structure/performance relationships,” *J. Vinyl Technol.*, vol. 15, no. 3, pp. 140–147, Sep. 1993, doi: https://doi.org/10.1002/vnl.730150306.
[134] ISO, “ISO 660 Animal and vegetable fats and oils — Determination of acid value and acidity,” 2020.
[135] ISO, “ISO 3961 Animal and vegetable fats and oils — Determination of iodine value,” p. 12, 2018.
[136] ISO, “ISO 3657 Animal and vegetable fats and oils — Determination of saponification value,” p. 10, 2020.
[137] ISO, “ISO 3960 Animal and vegetable fats and oils — Determination of peroxide value — Iodometric (visual) endpoint determination,” p. 10, 2017.
[138] ISO, “ISO 3596 Animal and vegetable fats and oils — Determination of unsaponifiable matter — Method using diethyl ether extraction,” p. 8, 2000.
[139] ASTM, “ASTM D2500 Standard Test Method for Cloud Point of Petroleum Products and Liquid Fuels,” p. 10, 2000.
[140] AMD OIL SALES, “Soybean oil, RBD (organic).” https://www.amdoilsales.com/products/soybean-oil-organic-rbd/ (accessed Nov. 15, 2022).
[141] H. Ngo, R. Latona, K. M. Wagner, A. Nuñez, R. Ashby, and R. O. Dunn, “Synthesis and low temperature characterization of iso-oleic ester derivatives,” *Eur. J. Lipid Sci. Technol.*, vol. 118, no. 12, pp. 1915–1925, Dec. 2016, doi: https://doi.org/10.1002/ejlt.201500468.
[142] L. A. García-Zapateiro, J. M. Franco, C. Valencia, M. A. Delgado, and C. Gallegos, “Viscous, thermal and tribological characterization of oleic and ricinoleic acids-derived estolides and their blends with vegetable oils,” *J. Ind. Eng. Chem.*, vol. 19, no. 4, pp. 1289–1298, 2013, doi: https://doi.org/10.1016/j.jiec.2012.12.030.
[143] International Union of Pure and Applied Chemistry, *Solubility data series - Alcohols with water*. 1984.
[144] V. R. Dhanuka, V. C. Malshe, and S. B. Chandalia, “Kinetics of the liquid phase esterification of carboxylic acids with alcohols in the presence of acid catalysts: Re-interpretation of published data,” *Chem. Eng. Sci.*, vol. 32, no. 5, pp. 551–556, 1977, doi: https://doi.org/10.1016/0009-2509(77)87013-9.
[145] S. Goto, T. Tagawa, and Y. Fukuta, “Kinetics of the reaction of sulfuric acid with

isobutyl alcohol," *Int. J. Chem. Kinet.*, vol. 21, no. 8, pp. 729–732, Aug. 1989, doi: https://doi.org/10.1002/kin.550210811.

[146] F. A. Zaher and H. M. Soliman, "Biodiesel production by direct esterification of fatty acids with propyl and butyl alcohols," *Egypt. J. Pet.*, vol. 24, no. 4, pp. 439–443, 2015, doi: https://doi.org/10.1016/j.ejpe.2015.10.007.

[147] W. Waskitoaji, E. Triwulandari, and A. Haryono, "Synthesis of Plasticizers Derived from Palm Oil and Their Application in Polyvinyl Chloride," *Procedia Chem.*, vol. 4, pp. 313–321, 2012, doi: https://doi.org/10.1016/j.proche.2012.06.044.

[148] S. Silviana, D. Anggoro, and A. Kumoro, "Kinetics study of waste cooking oil epoxidation with peroxyacetic acid using acid catalysts," *Rasayan J. Chem.*, vol. 12, pp. 1369–1374, Jan. 2019, doi: 10.31788/RJC.2019.1235190.

[149] W. F. Bohórquez, A. Orjuela, P. C. N. Rincón, J. G. Cadavid, and J. A. García-Nunez, "Experimental optimization during epoxidation of a high-oleic palm oil using a simplex algorithm," *Ind. Crops Prod.*, vol. 187, p. 115321, 2022, doi: https://doi.org/10.1016/j.indcrop.2022.115321.

[150] M. Jankovic, S. Sinadinovic-Fiser, O. Govedarica, J. Pavličević, and J. Budinski-Simendic, "Kinetics of soybean oil epoxidation with peracetic acid formed In Situ in the presence of an ion exchange resin: Pseudo-homogeneous model," *Chem. Ind. Chem. Eng. Q.*, vol. 23, pp. 97–111, Apr. 2017, doi: 10.2298/CICEQ150702014J.

[151] G. V Olivieri, J. V. J. de Quadros, and R. Giudici, "Epoxidation Reaction of Soybean Oil: Experimental Study and Comprehensive Kinetic Modeling," *Ind. Eng. Chem. Res.*, vol. 59, no. 42, pp. 18808–18823, Oct. 2020, doi: 10.1021/acs.iecr.0c03847.

[152] S. Leveneur, J. Zheng, B. Taouk, F. Burel, J. Wärnå, and T. Salmi, "Interaction of thermal and kinetic parameters for a liquid–liquid reaction system: Application to vegetable oils epoxidation by peroxycarboxylic acid," *J. Taiwan Inst. Chem. Eng.*, vol. 45, no. 4, pp. 1449–1458, 2014, doi: https://doi.org/10.1016/j.jtice.2014.01.015.

[153] M. Schwaab, L. Livia, and J. Pinto, "Optimum reference temperature for reparameterization of the Arrhenius equation. Part 2: Problems involving multiple reparameterizations," *Chem. Eng. Sci.*, 2008.

[154] K. Bakthavatchalam, S. Beyene, B. Ayalew, and S. Pilla, "Epoxidation Kinetics of High-Linolenic Triglyceride Catalyzed by Solid Acidic-Ion Exchange Resin," *Sci. Rep.*, vol. 9, Jun. 2019, doi: 10.1038/s41598-019-45458-8.

[155] J. La Scala and R. P. Wool, "Effect of FA composition on epoxidation kinetics of TAG," *J. Am. Oil Chem. Soc.*, vol. 79, no. 4, pp. 373–378, 2002, doi: 10.1007/s11746-002-0491-9.

[156] L. M. Ramírez, J. G. Cadavid, A. Orjuela, M. F. Gutiérrez, and W. F. Bohórquez, "Epoxidation of used cooking oils: Kinetic modeling and reaction optimization," *Chem. Eng. Process. - Process Intensif.*, vol. 176, p. 108963, 2022, doi: https://doi.org/10.1016/j.cep.2022.108963.

[157] LG-VINA Chem, "DOP Plasticizer Data sheet." http://aytaco.ir/wp-content/uploads/2019/01/DOP-LG.pdf.

[158] V. Borugadda and V. Goud, "Synthesis of Waste Cooking Oil Epoxide as a Bio-Lubricant Base Stock: Characterization and Optimization Study," *J. Bioprocess Eng. Biorefinery*, vol. 3, pp. 57–72, Mar. 2014, doi: 10.1166/jbeb.2014.1077.

[159] V. B. Borugadda and V. V Goud, "Response surface methodology for optimization of bio-lubricant basestock synthesis from high free fatty acids castor oil," *Energy Sci. Eng.*, vol. 3, no. 4, pp. 371–383, Jul. 2015, doi: https://doi.org/10.1002/ese3.77.

[160] S. Satapathy and A. Palanisamy, "Mechanical and barrier properties of polyvinyl chloride plasticized with dioctyl phthalate, epoxidized soybean oil, and epoxidized cardanol," *J. Vinyl Addit. Technol.*, vol. 27, no. 3, pp. 599–611, Aug. 2021, doi: https://doi.org/10.1002/vnl.21831.

[161] M. Gilbert, “8 - Poly(vinyl chloride)(PVC)-based nanocomposites,” in *Woodhead Publishing Series in Composites Science and Engineering*, F. B. T.-A. in P. N. Gao, Ed. Woodhead Publishing, 2012, pp. 216–237.
[162] A. Lindström and M. Hakkarainen, “Environmentally friendly plasticizers for poly(vinyl chloride)—Improved mechanical properties and compatibility by using branched poly(butylene adipate) as a polymeric plasticizer,” *J. Appl. Polym. Sci.*, vol. 100, no. 3, pp. 2180–2188, May 2006, doi: https://doi.org/10.1002/app.23633.
[163] ASTM, “ASTM D882-18 Standard Test Method for Tensile Properties of Thin Plastic Sheeting,” p. 12, 2018.
[164] ISO, “ISO 2528 Sheet materials — Determination of water vapour transmission rate (WVTR) — Gravimetric (dish) method,” p. 15, 2017.
[165] ASTM, “ASTM D1239 Standard Test Method for Resistance of Plastic Films to Extraction by Chemicals,” 2017.
[166] ISO, “ISO 176 Plastics - Determination of loss of plasticizers - Activated carbon method,” p. 4, 2005.
[167] M. Altenhofen da Silva, M. G. Adeodato Vieira, A. C. Gomes Maçumoto, and M. M. Beppu, “Polyvinylchloride (PVC) and natural rubber films plasticized with a natural polymeric plasticizer obtained through polyesterification of rice fatty acid,” *Polym. Test.*, vol. 30, no. 5, pp. 478–484, 2011, doi: https://doi.org/10.1016/j.polymertesting.2011.03.008.
[168] W. V. Titow, *PVC Plastics Properties, Processing and Applications*. Essex, England: ElsevierApplied Science, 1990.
[169] O. Fenollar Gimeno, “Utilización de plastificantes naturales para la obtención de PVC flexible de bajo impacto medioambiental,” Universidad Politecnica de Valencia, 2011.
[170] A. Carbonell-Verdu, M. D. Samper, D. Garcia-Garcia, L. Sanchez-Nacher, and R. Balart, “Plasticization effect of epoxidized cottonseed oil (ECSO) on poly(lactic acid),” *Ind. Crops Prod.*, vol. 104, pp. 278–286, 2017, doi: https://doi.org/10.1016/j.indcrop.2017.04.050.
[171] A. Carbonell-Verdu, D. Garcia-Sanoguera, A. Jordá-Vilaplana, L. Sanchez-Nacher, and R. Balart, “A new biobased plasticizer for poly(vinyl chloride) based on epoxidized cottonseed oil,” *J. Appl. Polym. Sci.*, vol. 133, no. 27, Jul. 2016, doi: https://doi.org/10.1002/app.43642.
[172] V. K. Haugaard and G. Mortensen, “11 - Biobased food packaging,” in *Woodhead Publishing Series in Food Science, Technology and Nutrition*, B. Mattsson and U. B. T.-E.-F. F. P. Sonesson, Eds. Woodhead Publishing, 2003, pp. 180–204.
[173] Y. Wang *et al.*, “Antibacterial poly(butylene succinate-co-terephthalate)/titanium dioxide/copper oxide nanocomposites films for food packaging applications,” *Food Packag. Shelf Life*, vol. 34, p. 101004, 2022, doi: https://doi.org/10.1016/j.fpsl.2022.101004.
[174] K. Subramanian, K. S. Vadivu, L. Subramaniyam, and M. D. Kumar, “Synthesis, characterization, and analysis of bioplasticizer derived from Hibiscus rosa-sinensis leaves and cinnamon bark for poly (vinyl chloride) films,” *Ind. Crops Prod.*, vol. 182, p. 114933, 2022, doi: https://doi.org/10.1016/j.indcrop.2022.114933.
[175] SHIMADZU, “Spectrophotometric Analysis No. A421,” Tokyo, Japan, 2021.
[176] M. Pandey, G. Joshi, A. Mukherjee, and P. Thomas, “Electrical properties and thermal degradation of poly(vinyl chloride)/polyvinylidene fluoride/ZnO polymer nanocomposites,” *Polym. Int.*, Jun. 2016.
[177] Alibaba, “DIDP diisodecyl phthalate.” https://www.alibaba.com/showroom/didp-diisodecyl-phthalate.html (accessed Jan. 21, 2021).
[178] Alibaba, “DBP dibutyl phthalate.” https://www.alibaba.com/showroom/dibutyl-

phthalate-price.html (accessed Jan. 20, 2021).
[179] ICIS, “ICIS Chemical Prices-B.” https://www.icis.com/explore/resources/news/2000/12/11/128127/chemical-prices-b/ (accessed Jan. 20, 2021).
[180] ICIS, “Asia methanol higher on potential Saudi Arabia supply issues,” 2019. https://www.icis.com/explore/resources/news/2019/09/17/10418063/asia-methanol-higher-on-potential-saudi-arabia-supply-issues (accessed Jan. 20, 2021).
[181] ICIS, “US spot fuel ethanol prices mixed amid varying demand,” 2020. https://www.icis.com/explore/resources/news/2020/07/15/10530504/us-spot-fuel-ethanol-prices-mixed-amid-varying-demand (accessed Jan. 20, 2021).
[182] Alibaba, “Propyl alcohol price.” https://www.alibaba.com/showroom/propyl-alcohol.html (accessed Jan. 20, 2021).
[183] ICIS, “Southeast Asia IPA prices hit six-year high, market warns of peak,” 2020. https://www.icis.com/explore/resources/news/2020/04/06/10493861/southeast-asia-ipa-prices-hit-six-year-high-market-warns-of-peak (accessed Jan. 20, 2021).
[184] ICIS, “Asia oxo-alcohols face weak demand; deep-sea cargo influx,” 2019. https://www.icis.com/explore/resources/news/2019/12/09/10451591/asia-oxo-alcohols-face-weak-demand-deep-sea-cargo-influx (accessed Jan. 20, 2021).
[185] ECHEMI, “Isobutyl Alcohol Price Analysis,” 2020. https://www.echemi.com/productsInformation/pd1804281021-isobutyl-alcohol.html (accessed Jan. 20, 2021).
[186] Alibaba, “Isoamyl Alcohol price.” https://www.alibaba.com/product-detail/Best-selling-chemicals-Isoamyl-Alcohol-Cas_1600110577919.html?spm=a2700.7724857.normal_offer.d_title.dbc874a8QIsZfQ (accessed Jan. 20, 2021).
[187] Made in China, “High Pure Capryl Alcohol C8h18o Octanol.” https://hailijia888.en.made-in-china.com/product/oKIxSrkvZcUH/China-CAS-111-87-5-High-Pure-Capryl-Alcohol-C8h18o-Octanol.html (accessed Jan. 20, 2021).
[188] ICIS, “Asia MEG nears six-month highs on regional output cuts, US shutdowns,” 2020. Asia MEG nears six-month highs on regional output cuts, US shutdowns (accessed Jan. 20, 2021).
[189] Alibaba, “Propylene glycol price.” https://www.alibaba.com/product-detail/Propylene-Glycol-Propylene-Glycol-Price_62329752387.html?spm=a2700.7735675.normal_offer.d_image.4a384f2aFpeMcy&s=p (accessed Jan. 20, 2021).
[190] ICIS, “Asia BDO market faces year-end lull, weak downstream PBT demand,” 2019. https://www.icis.com/explore/resources/news/2019/11/07/10440781/asia-bdo-market-faces-year-end-lull-weak-downstream-pbt-demand (accessed Jan. 20, 2021).